Time Equivalent for Protected Steel and Reinforced Concrete Structures

By

Arthur Ting Kung Kii

Supervised by

Professor Andrew Hamilton Buchanan

A research project report presented as a partial fulfilment of the requirements for the degree of Master of Engineering in Fire Engineering.

30th August 1999

Department of Civil Engineering,
University of Canterbury,
Private Bag 4800
Christchurch, New Zealand.

Table of Contents

Acknowledgments

I would like to thank the following people for their assistance and supports which make the completion of this report possible.

First of all, my supervisor, Professor Andy Buchanan who has provided me with precious guidance and ideas.

My family who has all the way supported me, especially my parents.

Finally, the New Zealand Fire Service Commission for the financial support of the fire engineering program.

Abstract

This report aims to evaluate the reliability of the formulae commonly used to determine the severity of a compartment fire. It briefly explains the concept behind fire resistance rating for structural elements, describing how the severity of a 'real' compartment fire is equated to that of the 'standard' fire used in laboratories for fire resistance testing. This is followed by a discussion of the computer method used in this report in dissecting those formulae and the development of some computer techniques for calculating fire severity.

Apart from that, various physical parameters of a compartment such as the opening sizes are looked at to determine the significance of their influence on the fire severity. This report also goes beyond the works carried out in the past and examines the validity of the formulae for scenarios that have not previously been considered and explores the validity of the calculation methods intended for steel member for reinforced concrete structure. Finally some discussions and conclusions are made from the findings.

List of Figures

1 Introduction

1.1 Objectives

The objectives of this study are:

- To summarise briefly the time equivalent concept that lies behind the fire severity rating for compartment fires.
- To develop a computer technique for calculating time equivalent for steel members.
- To study the effect of various physical parameters of a compartment fire on time equivalent.
- To investigate the possibility of calculating the time equivalent for concrete structures using the spreadsheet method developed.
- To examine the validity of the Eurocode time equivalent formula for reinforced concrete structure.

1.2 Time Equivalent

The time equivalent concept is a method of correlating the severity of a 'real' compartment fire to the standard fire, ISO 834 (Buchanan 1999). According to Drysdale (1985), in the past, fire resistance of an element was considered the time to failure of that element exposed to the standard ISO 834 fire used in laboratory testing.

However, in the 1920s, it was realised that the 'real' fire that a structural element may be exposed to during its service life is almost always nothing similar to the standard fire used to determine its fire resistance rating. Since it is impossible to have a fire resistance rating that considers all possible 'real' fire situations, structural elements are tested only with the standard fire in laboratories. Fire resistance for a structural element is therefore only available and expressed in term of Standard fire resistance duration. In designing fire protection for a building, fire engineers have to convert the expected 'real' fire to its equivalent standard fire severity and thus determine the required fire resistance for the building elements. This is the concept of time equivalent. Various attempts have been made to design the most reliable way of correlating real fire severity to the standard fire. They are briefly discussed in the following sections.

1.2.1 The Equal Area Concept

Ingberg (1928) came up with an 'equal area' hypothesis, which assumes two fires having the same area under their temperature-time curves to have the same fire severity. Therefore, according to Ingberg's theory, the required fire resistance is the time at which the area under the temperature-time of the standard fire curve is equal to the entire area under the 'real' fire curve. Figure 1.1 helps explain this concept more

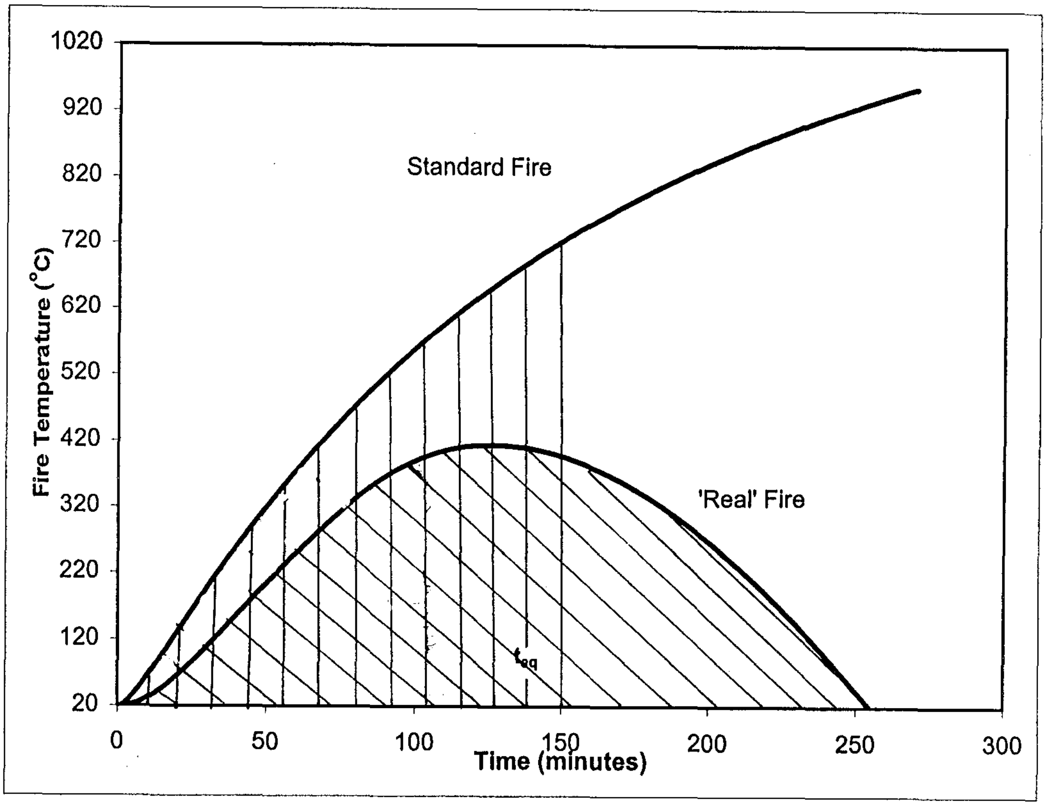

Figure 1.1: The Equal Area Concept

Figure 1.1 shows two temperature-time curves of the standard and 'real' fire respectively. It is found that at 150 minutes, the area under the standard curve is equal to the entire area under the real curve. Thus, according to Ingberg's method, an element must be designed not to fail before 150 minutes of exposure to the standard fire in order to survive that particular 'real' fire.

This method although was a useful way of comparing fire severity, is inadequate in the way that it does not include the difference between a long cool fire and a hot short one. As explained by Buchanan (1999), a hot short fire although may have the same area under the temperature-time curve as the long cool fire, is actually a more severe fire. The reason simply being that the heat transfer from a fire is mainly by radiation which effectiveness is directly proportional to the fourth power of the fire temperature. Therefore, the heat transfer from a short but much hotter and luminous fire would be much higher than that from a long, cool fire with the same area under the temperature-time curve.

1.2.2 Maximum Temperature or Minimum Load Bearing Capacity Concept

Margaret Law (1971) developed the current time equivalent concept, which is studied in this report. According to Law, time equivalent is defined as the time of exposure of a protected steel member to the standard fire that would produce the same maximum temperature or same minimum load bearing capacity in the member exposed to a real fire.

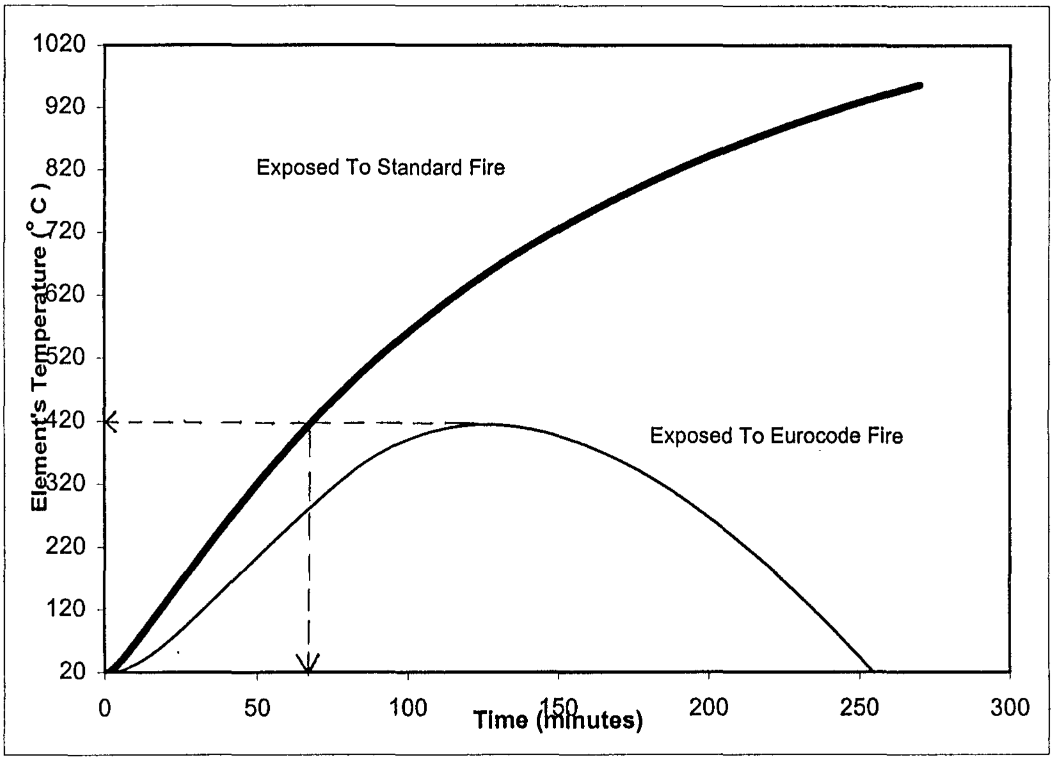

Figure 1.2(a): Temperature-time curve of protected steel member exposed to fires

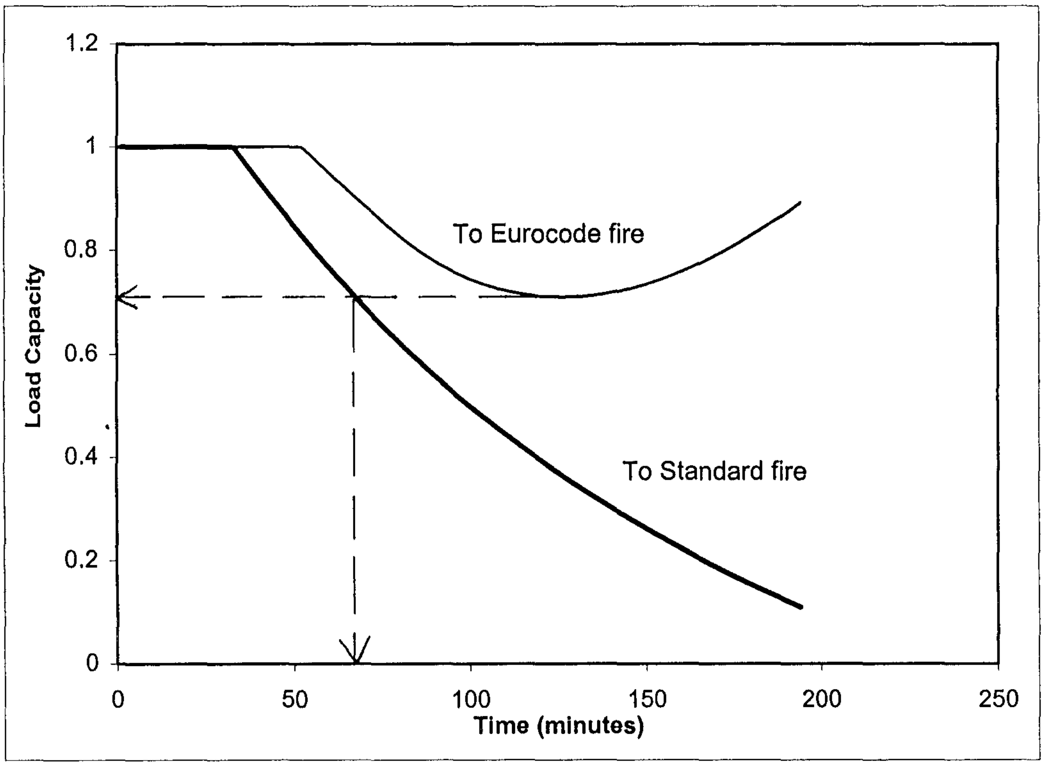

Figure 1.2(b): Load bearing capacity-time curve of protected steel member exposed to fires

Figure 1.2(a) shows the time-temperature curves for steel beam exposed to the standard and Eurocode parametric fires (real fire) while figure 1.2(b) shows the change in the load bearing capacity of a steel beam with the time of exposure to fires.

As shown in the graph, the steel beam exposed to the real fire reaches its maximum temperature of 420 ^{O}C and minimum load bearing capacity of 0.72 or 72% at 127 minutes. It can been seen that the load bearing capacity of the steel decreases when it is heated up but returns to its original value after the fire 'cools' down. This indicates the regain of the steel strength after it is cooled down. According to Law, the time equivalent would be the time at which the standard fire would yield the same temperature as the maximum temperature of the real fire, which is 67 minutes in this case. Thus, an exposure of 67 minutes to the standard fire in the laboratory would produce the same heating effect to the structural element by this particular compartment 'real' fire.

However, according to Cooke (1999), the required fire resistance is also dependent on its load ratio. The general idea is simply that, the higher the load ratio is, the lower its fire resistance would be.

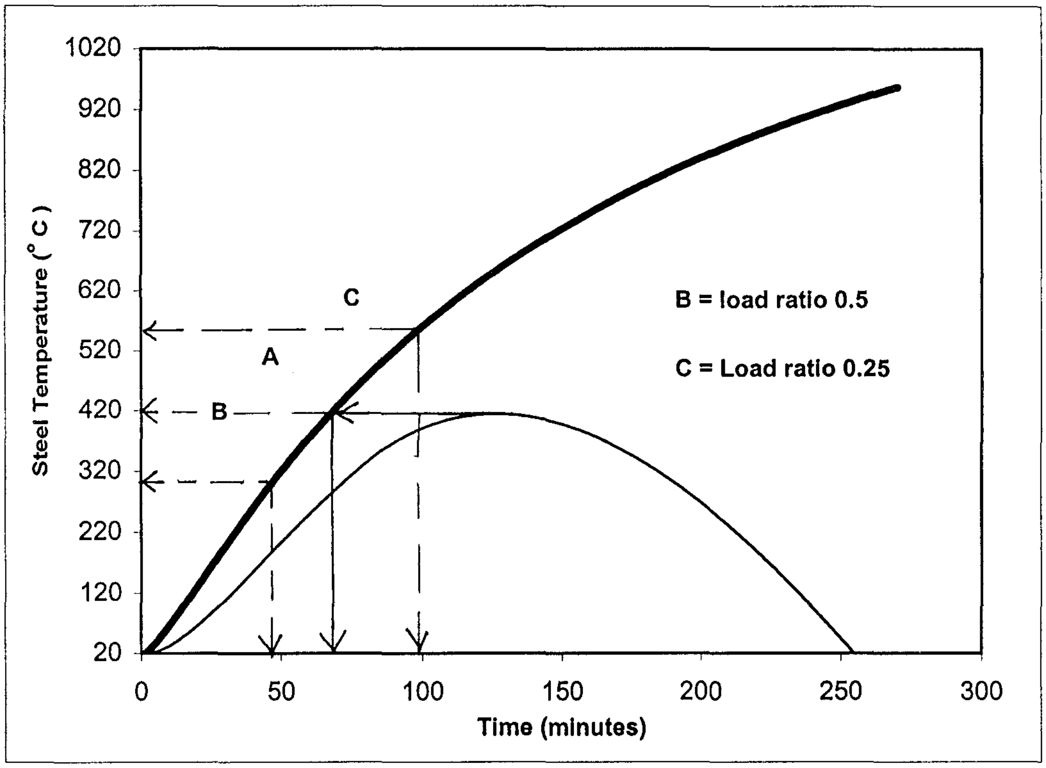

Figure 1.3: Time Equivalent for different load ratio (Cooke 1999)

Figure 1.3 shows that the same column in previous example would buckle at a temperature of 550° C if it only holds a load ratio of 0.25 and at a much lower temperature of 300 °C at a load ratio of 0.5 due to the extra load that it holds. Therefore, it can be concluded that the fire resistance for the same column is different for different load ratios.

1.3 The Time Equivalent formulae

1.3.1 Introduction

Time equivalent formulae are used by the fire engineer in determining the fire severity of a compartment with designated fuel load and physical characteristics. They are derived empirically (Thomas 1997), based on a set of experimental data produced from numerous laboratory testings. The formulae are developed by regression analysis using the results of a selected number of tests or calculations. Thus, the time equivalent formulae may not be suitable for all fire scenarios and the aim of this report is to look at the validity of the formulae for fire situations that have not been considered before.

The commonly used Eurocode, CIB and Law formulae are studied in this report. Although time equivalent formulae are originally intended for protected steel member, they have also been widely used for unprotected steel and non-steel member such as concrete. Therefore, this report also evaluates the validity of the formulae for reinforced concrete.

1.3.2 The CIB Formula

The CIB formula is based on experimental data produced from the exposure of insulated steel members to fires in concrete lined compartment (Thomas,1997). According to Buchanan (1999), the formula is derived by Petterson (1973) based on ventilation parameters of the compartment and fuel load.

The CIB formula for the equivalent exposure time to the standard ISO 834 fire is:

$$t_{eq,CIB} = k_c \, w \, Q_f \quad ....(1.1)$$

where k_c = correction factor to account for different compartment linings (Table 1.1)

Formula	Term	Units	$(k \rho c_p)^{0.5}$			
			high >2500	medium 720 - 2500	low < 720	General
CIB W 14	kc	min $m^{2.25}$ / MJ	0.05	0.07	0.09	0.1
Eurocode	kb	min m^2 / MJ	0.04	0.055	0.07	0.07
k = Thermal conductivity (W/mK) ρ = density (kg/m^3) c_p =Specific heat (J/kg K)						

Table 1.1 Values of k_c and k_b (Buchanan 1999)

Q_f = fuel load per floor area (MJ/m^2)

w = ventilation factor

$= A_f / (A_v A_t H_v^{1/2})^{1/2}$

and

A_f = Floor area (m^2)

H_v = Height of ventilation (m)

A_v = Total window area (m^2)

A_t = Total area of the bounding surfaces (m^2) of the compartment.

Obviously, the formula only allows the calculation of time equivalent for compartment with vertical openings.

1.3.3 The Eurocode Formula

The Eurocode time equivalent formula is a modification of the CIB formula to include the effect of horizontal openings. It is used in the structural Eurocodes and also in the German Standard DIN 18230 (Feeney 1998). The formula is based on the result of simulations of steel exposure to fire using a German computational program called the "Multi Room Fire Code" (MRFC). Unlike the CIB formula, the ventilation factor of Eurocode formula is dependent on the ceiling height of the compartment, H_r instead of the opening height, H_v. The Eurocode time equivalent formula is:

$$\mathbf{t_{eq,Eurocode} = k_b\, w\, Q_f} \quad \textbf{.....(1.2)}$$

where k_b is a correction factor from table 1.1

Q_f = Fuel load per floor area (MJ / m^2)

w = ventilation factor

$= (6/H_r)^{0.3}\,[\,0.62 + 90(\,0.4 - \alpha_v\,)^4 / (1 + b_v\,\alpha_h)] > 0.5$ ....(1.2.1)

where H_r =compartment height (m)

$\alpha_v = A_v / A_f$ $\quad 0.05 < \alpha_v < 0.25$ .....(1.2.2)

$\alpha_h = A_h / A_f$ $\quad \alpha_h > 0.2$ .....(1.2.3)

$b_v = 12.5\,(\,1 + 10\alpha_v - \alpha_v^{\,2}\,)$ .....(1.2.4)

where A_v, A_h being the area (m^2) of vertical and horizontal opening respectively.

1.3.4 The Law Formula

The Law time equivalent formula is a modification of Kawagoe and his colleagues' time equivalent formula which was :

$$t_{eq,\,Kawagoe} = k_2\, L''\, (A_t / A_v\, h^{½})^{\,0.23}$$

for $\quad 5 < A_t / A_v\, h^{½} < 30\ m^{-½}$

where A_v = ventilation area (m^2)

A_t = Total area of the bounding surfaces (m^2)

h = height of the opening (m).

L" = Fuel load mass per floor area (kg / m^2)

and the factor, k_2 =1.06

From there, Law (1997) developed a time equivalent formula incorporating the results from CIB experimental research program of wood crib fires. The experiment results showed that the time equivalent is independent of the opening height, therefore Kawagoe's formula was modified to:

$$t_{eq,Law1} = k_3 L'' A_F / [A_v (A_t - A_F - A_v)]^{1/2}$$

Where A_F = floor area (m^2)

k_3 = 1.0

Note that the expression in the bracket ( ) represents the area of the solid surface of the compartment, that is, the 'net' internal surface area which excludes the ventilation area. The equation however also excludes the floor area in calculating this net solid surface due to the fact that the floors were thermally well insulated in the experiment. When further research shows that the floor area should be included in the solid surface, the formula was further modified to its final form, which is:

$$\mathbf{t_{eq,Law} = k_4 L'' A_F / [A_v (A_t - A_v)]^{1/2}} \quad \textbf{....(1.3)} \qquad \text{where} \qquad k_4 = 1.0$$

1.4 Overview of Methodologies in This Study

A spreadsheet has been formulated for this report to simulate the development of standard and 'real' fires in compartment using equations discussed in chapter 2. It can also calculate the corresponding increase in temperature of a steel beam due to fires. With the temperature of the steel and fire known, the time equivalent can be calculated by the spreadsheet based on the time equivalent concept discussed previously and shown in figure 1.2(a). The spreadsheet is used to check against the time equivalents calculated by the formulae.

As the spreadsheet is used as the 'tool' to check against the reliability of time equivalent formulae, its accuracy is of great concern. Therefore, a computer program, SAFIR that simulates the exposure of steel beams to fires is used to verify this by comparing the response of steel beam to fire predicted by the program to that predicted by the spreadsheet. As shown in chapter 3, results from the spreadsheet and SAFIR agree well. Therefore, the spreadsheet method is used throughout the report in dissecting the time equivalent formulae.

Area of study in this report includes the physical parameters of the fire compartment such as the size of openings, size of compartment, fuel load density and beam sizes. Time equivalents calculated by the formulae for the variation in these parameters are compared to those calculated by the spreadsheet method.

1.5 Computer Simulation Models

As mentioned previously, a few computer programs for heat transfer are involved in this report. The following sections give a brief description of all the computational tools used:

1.5.1 The SAFIR program

SAFIR program (Gilvery and Dexter 1997) is a specialised fire simulation software developed by Dr. Jean-Marc Franssen from the University of Liege, co-operated by ARBED. The program simulates the heat transfer through steel and concrete structures using the finite element theory.

In a report prepared by the National Institute of Standards and Technology (NIST) to speculate the possibility of using computational method as an alternative to the furnace test in determining fire resistance ratings for structures, SAFIR program is rated as the best among several other computational methods (Gilvery and Dexter 1997). The investigation shows that the simulation of the exposure of loaded steel columns and concrete filled tubes to the ASTM-E119 fire using SAFIR program yields similar response in steel as those exposed to real ASTM-E119 furnace fire tests.

Therefore, SAFIR is recommended by NIST to serve as an alternative to the ASTM-E119 furnace test method for determining fire resistance ratings. This important achievement would lead to a significant decrease in the cost of evaluating fire resistance of structures, increase in fire safety, a more economical building construction and more advanced use of construction materials. Apart from that, it is also a user-friendly program.

SAFIR consists of three modules, which are the Wizard, Safire98 and Diamond98. Each module is discussed briefly below:

a) Wizard-- Pre processor

The Wizard allows the user to select the type and size of beam with or without protection. The four commonly used beam types, the BHP, IPE, HE and American are available for selection in the Wizard. It also allows the users to create own beam by specifying the dimension of flange and web. Users can also choose the type of fire that their beam is to be exposed to. The fire curves that are available are FISO (ISO 834 or the standard fire), ASTME 119 and F1000THPS.

Output files from this module are then processed by the SAFIR 98, discussed below.

b) SAFIR 98

This program does the actual simulation of the exposure of the beam to the fire specified by the user. At the end of each simulation, SAFIR 98 produces an output file that is to be analysed by Diamond 98 program.

c) Diamond 98--Post processor

Diamond 98 analyses the result of simulations and presents the results in graphical form. It shows the variation of the steel beam temperature with time. The user can choose to view the distribution of the temperature across the cross section of the beam or the temperature-time curve of any nodal point within the beam section.

1.5.2 Spreadsheet Method

The spreadsheet method developed in this study basically comprises of equations or formulae that calculate the:

a) Temperature rise of a compartment fire with time.
b) Corresponding temperature rise in element exposed to the fire in (a).

This spreadsheet method is described by Buchanan (1999), based on Gamble (1989) and EC1 (1994). A detailed discussion of this spreadsheet method and the formulae involved are found in chapter 3.

As mentioned previously, this spreadsheet method is found to be accurate in predicting the response in steel beam exposed to fires and calculating the time equivalents. Therefore, it is used to check the calculated values from time equivalent formulae.

1.5.3 Finite Element Model

A one dimensional heat transfer model has also been developed to simulate the exposure of concrete structures to design fire. This model is created on the computer spreadsheet. It consists of equations that calculate the temperature rise in concrete exposed to a certain fire for a certain time of exposure at certain depth.

This model has also been used to look at the validity of the spreadsheet method for calculating time equivalent in non-steel structure such as concrete. A detailed description of the model can be found in chapter 10 of this report.

2 Mathematical Models For Post-Flashover Fires

2.1 *Post Flashover*

Time equivalent is used to determine the fire severity for a completely burnt out compartment. In another words, a compartment that reaches flashover and burns to decay without intervention.

Flashover is the start of the burning phase of a compartment fire when its temperature is high enough to cause all combustibles available to burn fiercely and reach their maximum temperature and heat release rates. A compartment fire is considered to have reached this phase when the temperature of the upper layer gases reaches 600°C and the direct radiation at floor level reaches 20 kW /m^2 (Buchanan, 1994). The size of a post flashover fire is limited by the ventilation, which is, the air supply to the fire, instead of the amount of fuel available. As the post flashover fire represents the worst possible burning situation in a compartment, it is conservative to use it in the calculation of the fire severity of a compartment.

2.2 Fires Curves — Standard ISO 834 and Eurocode Parametric Fires

The two fires used in this study are the standard fire ISO 834 and the Eurocode parametric or 'real' fires.

2.2.1 The ISO 834 standard fire

The standard fire ISO 834 (Drysdale 1985) is originally a pattern of temperature-time variation of the fire gases used in large furnace for full scale fire resistance testing of structures. The desired temperature-time curve can be achieved in furnace through the control of the fuel supply.

The standard fire curve used in the USA, which is the ASTM E119 is specified by a set of data points. A mathematical equation had later been developed to represent this fire curve. This fire curve is slightly different from the ISO 834.

The mathematical equation representing ISO 834 has the form:

$$T=345 \log_{10}(8t+1) + T_o \ (^{\circ}C) \ldots.(2.1)$$

where T_o = Ambient temperature (20 °C)

and t = time in minutes

Obviously, the standard fire is dependant solely on the time and does not take into consideration of physical parameters such as the fuel load or ventilation. A plot of the standard fire temperature against time is shown in figure 2.1:

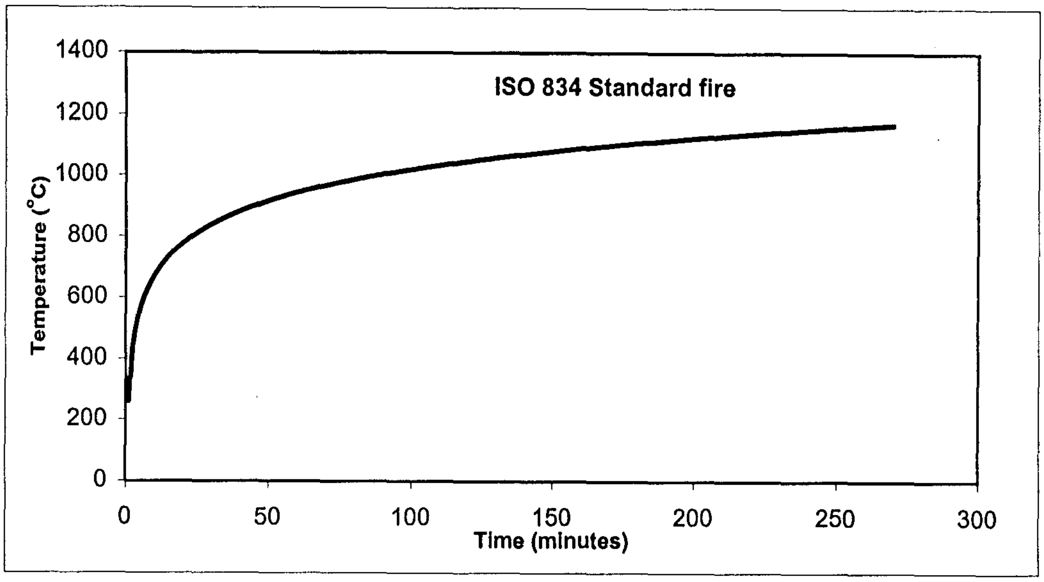

Figure 2.1: The ISO 834 standard fire

Figure 2.1 shows the variation of the standard fire temperature with time. As expected, the temperature of the fire increases infinitely with time. It follows a curve that initially increases rapidly with time but starting to slow as the time proceeds.

2.2.2 Eurocode Parametric Fire

The Eurocode fire (EC1 1994) is considered a 'realistic' fire that takes into account the fuel load available for burning, the ventilation and wall linings of compartment.

Unlike the Standard fire, Eurocode fire consists of a growth and decay phase. The increase in its temperature is limited by the fuel load and ventilation factor. The fire temperature starts to decrease with time after burning for some duration of time as shown in the figure 2.2.

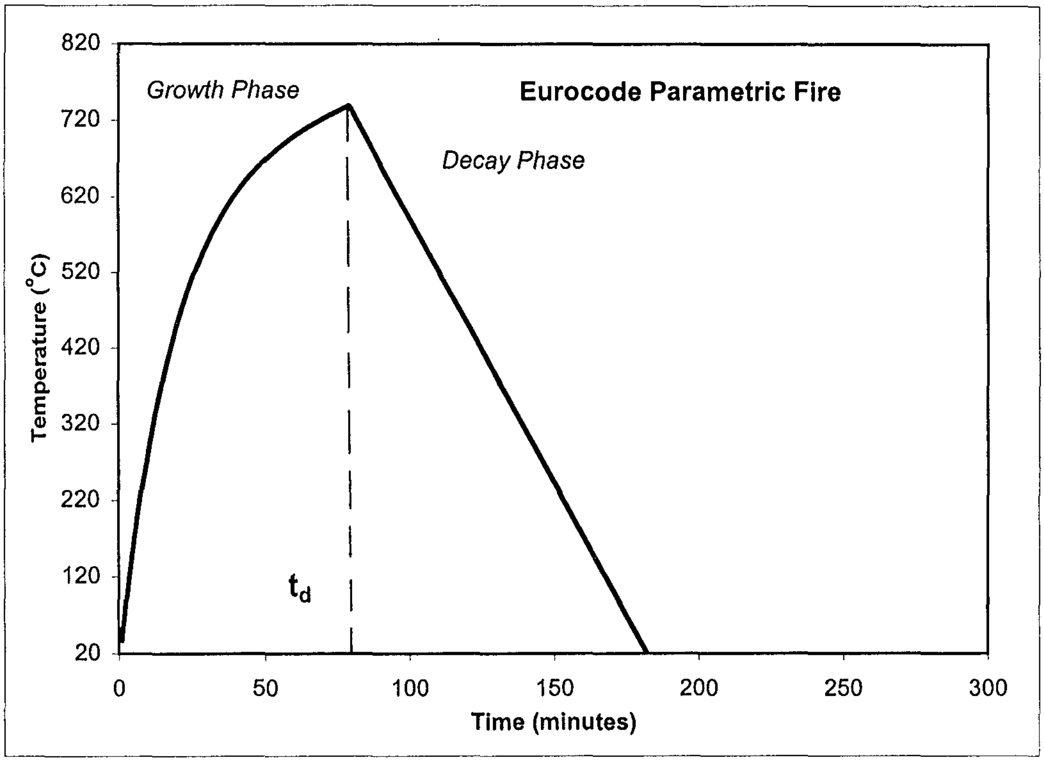

Figure 2.2: The Eurocode Parametric Fire

As shown in the figure 2.2, the three important components of an Eurocode parametric fire are the growth (heating) phase, its burning duration and decay phase. Each one is discussed below (EC 1 1994):

a) Growth (heating) Phase

The temperature-time behaviour of the Eurocode fire in its growth phase is given by the formula:

$$T=1325(1-0.324e^{-0.2t^*} - 0.204e^{-1.7t^*} - 0.472e^{-19t^*}) \quad ....(2.2)$$

Where

t^* = the fictitious time (hours)is given as

$$= t \; [F_v / 0.04]^2 \, [1160 / (k\rho c_p)^{½}]^2 \quad .....(2.2.1)$$

F_v = ventilation factor ($m^{½}$)

$$= A_v \, H_v^{½} / A_t \quad .....(2.2.2)$$

and t = real time (hours)

A_v =area of the ventilation (m^2)

A_t = total area of internal boundary surfaces (m^2)

H_v = height of ventilaion (m)

k = thermal conductivity of the compartment wall material (W/m K)

ρ = density of wall material (kg/m^3)

c_p = specific heat of wall material (J/kg K)

$[k\rho c_p]^{½}$ being the thermal inertia or thermal characteristics of the compartment boundaries. A high thermal inertia would indicate a poorly insulated compartment and vice versa.

b) Duration of Heating Phase

Duration of the heating phase for Eurocode fire , after being simplified:

$$t_d = 0.00013e_t / (A_v H_v^{½} / A_t) \qquad .....(2.3)$$

where e_t = fuel load of compartment (MJ / m ^{2} total surface area)

c) Decay phase

The decay phase occurs at the end of the heating phase. It starts at the calculated time t_d and is given by the equation:

$dT / dt = 625 [F_v / 0.04]^2 [1160 / (k\rho c_p)^{½}]^2$ ($^\circ$C / hour)

for $t^*_d < 0.5$ hours

$dT / dt = 250 (3 - t_d^*) [F_v / 0.04]^2 [1160 / (k\rho c_p)^{½}]^2$ ($^\circ$C / hour)

for $0.5 < t^*_d < 2$ hours

and

$dT / dt = 250 [F_v / 0.04]^2 [1160 /(k\rho c_p)^{½}]^2$ (^{0}C / hour)

for $t^*_d > 2$ hours

.....(2.3)

with t_d^* = burning duration in fictitious time (hours)

$= t_d \; [F_v / 0.04]^2 [1160 /(k\rho c_p)^{½}]^2$

It must be pointed out (Buchanan 1999) that the duration of heating phase given by the above equation is less than the theoretical duration for ventilation controlled burning given by the equation:

$t_b = M_f / m'$ where M_f is the mass of the fuel and m' being the burning rate. Therefore, it is reasonable to assume some continuing burning taking place in the decay phase.

3 Heat Transfer in Steel

3.1 The Spreadsheet Method for Heat Transfer in Steel

3.1.1 Introduction

The spreadsheet method used throughout this report to calculate the time equivalents for steel is based on the time equivalent concept suggested by Law (1971). As discussed previously in chapter 1, the spreadsheet method, developed by Buchanan (1999) consists of formulae that models the fires temperature variation with time and the corresponding heat transfer in steel beams.

Step by step, this section explains the spreadsheet method. This includes the formulae involved, how they are related to each another in order to simulate the exposure of a steel beam to fires and how some functions of the spreadsheet are used to simplify the task of locating the time equivalent.

3.1.2 Formulae Involved

Formulae used in the spreadsheet are:

(a) Equations for the Standard and Eurocode parametric fires, equation (2.1) and (2.2) as described in chapter 2.

(b) Equation for calculating the change in protected steel temperature in corresponding to the variation in fire temperature in (a), given by the equation :

$$\Delta T = (F/V)\ (k_i / d_i\ \rho_s\ c_s)\ \{\rho_s\ c_s / (\rho_s\ c_s + (F/V)\ 2\ d_i\ \rho_i\ c_i)\}\ (T_f - T_s)\ \Delta t \quad \text{....(3.1)}$$

Where
F = surface area per unit length of the steel beam (m^2/m)
V = Volume per unit length (m^3 / m)
k_i = thermal conductivity of the insulation (W/m°C)
d_i = thickness of the insulation (m)
ρ_s = Density of the steel (kg/m^3)
ρ_i = Density of the insulation (kg/m^3)
c_s = Specific heat of the steel (J/kg°C)
c_i = Specific heat of the insulation (J/kg°C)
Δt =Time step (seconds)
T_s = Steel temperature (°C)
T_f = Fire Temperature (°C)

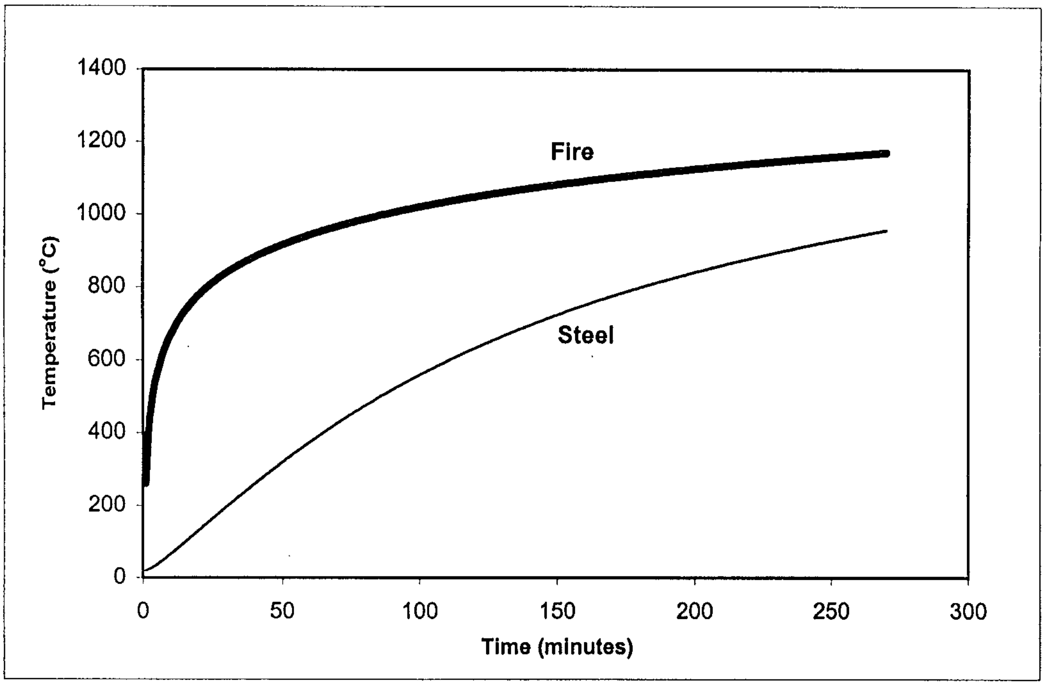

Figure 3.1(a): Fire and steel temperature (ISO 834)

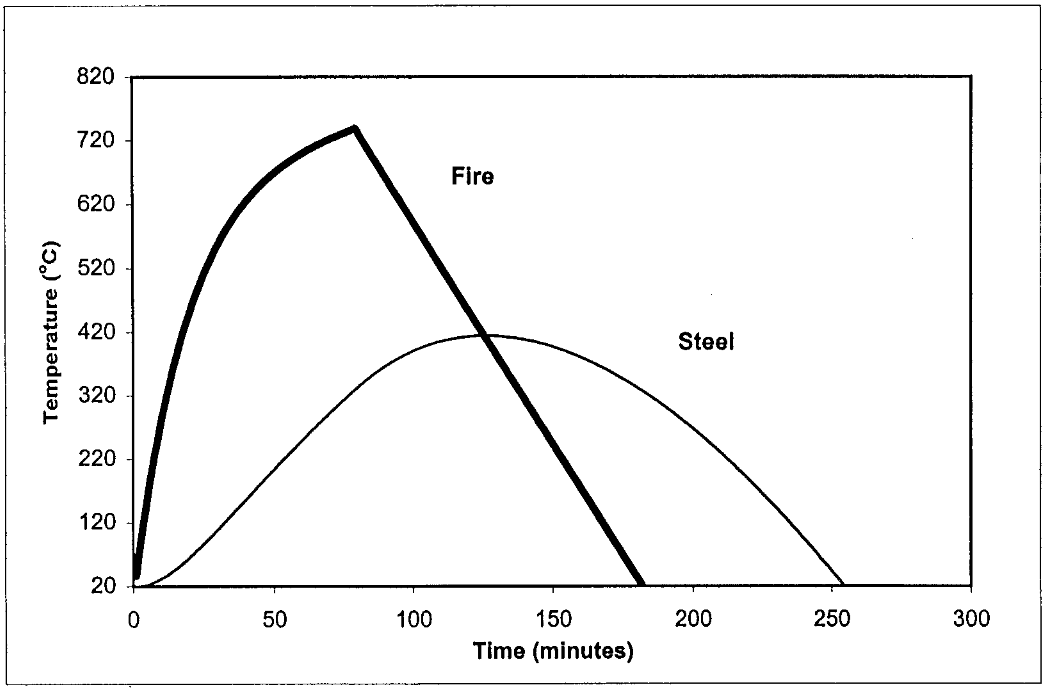

Figure 3.1(b): Fire and steel temperature (Eurocode parametric fire)

Figure 3.1(a) and 3.1(b) show the temperature-time curve of the standard ISO 834 fire and the Eurocode parametric fire as well as the corresponding temperature-time curve of the steel member exposed to them. As shown by both figures, there is a time lag between the increase in the steel temperature and the fire temperature. This is expected since the transfer of heat into the steel of certain specific heat and thermal conductivity values requires certain amount of time.

3.1.3 Method of Obtaining Time Equivalent

Figure 3.2 shows the temperature-time curves of the steel exposed to the Standard and Eurocode fires are plotted together and shown in the figure 3.2.

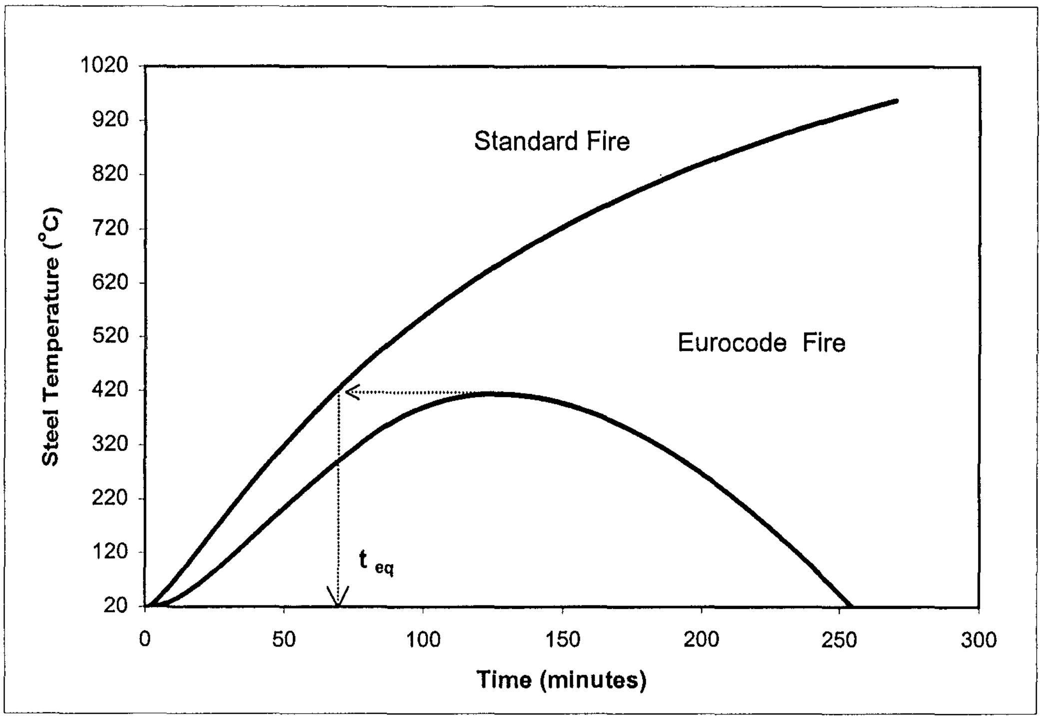

Figure 3.2: Steel temperature exposed to standard and Eurocode fires

As discussed earlier in chapter 1, the time equivalent is the time at which the Standard fire curve has the same temperature as the Eurocode fire's maximum temperature. Therefore, the time equivalent can be obtained by reading off the value from figure 3.2.

However, the author has simplify the task of having to locate the time equivalent on the temperature-time curves by using the logic functions available on the computer spreadsheet:

a) 'MAX( )' function is used to locate the maximum temperature of steel exposed to the Eurocode fire from the steel temperatures column (ie. column A of fig 3.3 (b))
b) 'Lookup( )' function which is able to locate from column B, the temperature of the steel exposed to the Standard fire which is equal or closest to the maximum temperature found in step (a).
c) 'IF( )' logical function to indicate the time at which temperature in part (b) occurs, which is also the time equivalent.

3.1.4 Layout of The Spreadsheet

Layout of the spreadsheet closely follows that suggested by Buchanan (1999), as shown in figure 3.3(a).

Time	Steel Temperature T_f	Fire TemperatureT_s	Difference $T_f - T_s$	Change in Steel Temperature
$t_l = \Delta t$	Ambient T_{so}	Fire temperature at $\Delta t/2$		Equation 3.1
$\Delta t + t_l$	$T_{so} + \Delta T_s$	Fire temperature at $(t_l + \Delta t/2)$		

Figure 3.3 (a)

Result	Fictitious Time, t* (hours)	Time (minutes)	Time , t (seconds)	Fire Temperature,T_f ISO 834 (°C)	Fire Temperature,T_f Eurocode (°C)	Steel Temperature,Ts ISO 834 (°C)	Steel Temperature,Ts Eurocode (°C)	Difference $T_f - T_s$ ISO 834 (°C)	Difference $T_f - T_s$ Eurocode (°C)	Change in steel temp. ISO 834 (°C)	Change in steel temp. Eurocode (°C)
	0.03499	0	0	261.14	322.3143	20	20	241.14	302.314	4.8613	6.09442
	0.10497	1	60	404.31	593.3823	24.861	26.0944	379.45	567.288	7.6494	11.4361
	0.17495	2	120	476.17	687.1807	32.511	37.5305	443.65	649.65	8.9437	13.0965
"t_{eq}"	0.24493	3	180	524.53	732.0208	50.8	50.627	483.07	681.394	9.7384	13.7364
	0.31491	4	240	561.03	762.0759	51.[illegible]93	45.3633	509.84	697.713	10.278	14.0654

"IF ( )" function used to indicate the time Equivalent *Column B* *A*

Figure 3.3(b)

Figure 3.3(a) is the basic set-up of the spreadsheet method and figure 3.3(b) is a sample layout of the actual spreadsheet method used in this report.

3.2 Specific Heat of Steel, C_s

3.2.1 Introduction

Thermal properties of steel vary at elevated temperature. Variations of thermal properties such as the specific heat and thermal conductivity affect the heat transfer into and within the material. Thus, indirectly affect the time equivalent calculated.

The spreadsheet method and one-dimensional heat transfer model in this report use an averaged specific heat value in their simulation of heat transfer into the steel beam. These averaged values are assumed to give results close enough to those obtained by including the variation of the thermal properties into consideration. Therefore, this section has been added to the report with the aim of verifying this assumption.

A constant value of 600 J/kg °C is usually used as the average specific heat for steel (Buchanan 1999). A mathematical equation (Purkiss 1996) has been used to model the variation of the steel specific heat value with temperature:

$$C_s = 475 + 6.010 \text{ X } 10^{-4}\, T^{2} + 9.46 \text{ X } 10^{-2}\, T \quad ....(3.2)$$

Where T = steel temperature (°C)

Figure 3.4 shows the variation of the specific heat of steel with temperature, according to equation 3.2. As implied by the formula, the increase in specific heat of steel follows a second order equation.

The variation of the steel density with temperature has not been included in this investigation since according to Purkiss (1996), " The density of steel may be taken as its ambient value of 7850 kg/m^3 over the normal experienced temperature range." Since the thermal conductivity of steel is not involved in the spreadsheet method, therefore it has not been included here as well.

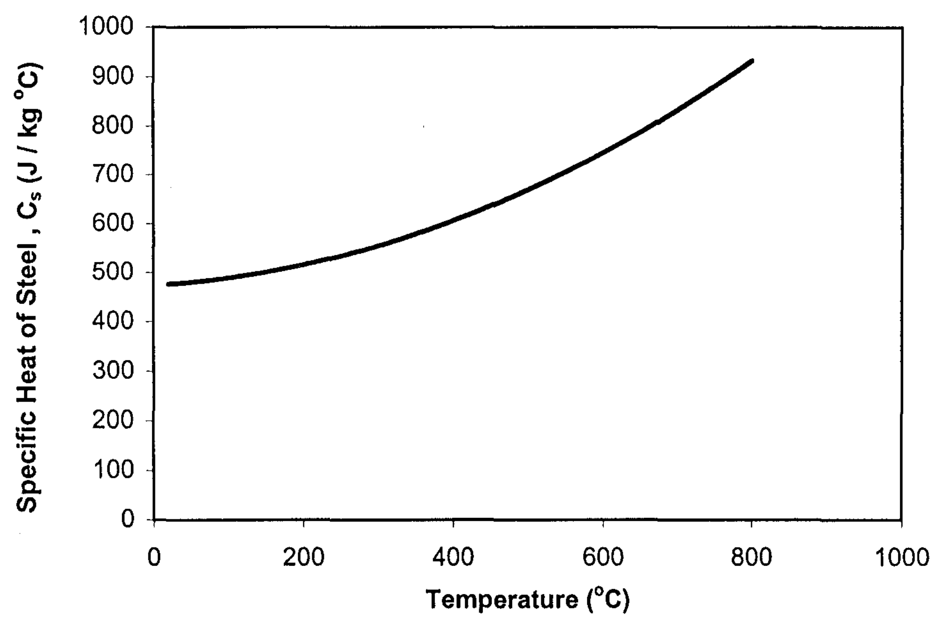

Figure 3.4: Variation of specific heat with temperature for steel

3.2.2 Methodology

Two sets of data are produced from the simulation of the exposure of steel beam to certain fire scenarios using the spreadsheet method. The first set of simulations uses averaged thermal property values while the second takes the variation of thermal properties into account. These two sets of data are compared to study any difference that exists.

Since we are only interested in the difference that exists between both sets results due to the different thermal properties used, the details of the simulations have been omitted here and only discussed in chapter 5.

3.2.3 Results

The time equivalents calculated by the spreadsheet method with and without the variation of the specific heat with temperature taken into account are plotted in figure 3.5.

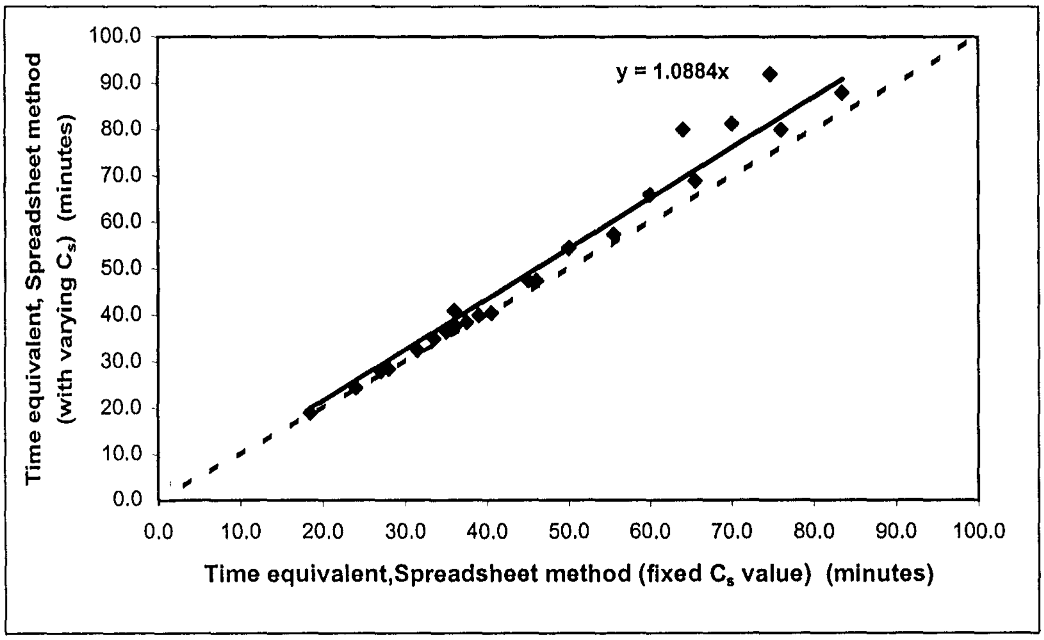

Figure 3.5: Time equivalents by spreadsheet method with and without variation of C_s

Figure 3.5 shows the comparison between the time equivalents calculated using a varying and using a fixed steel specific heat value, $C_s = 600$ J/kg °C. Almost perfect agreement between both sets of results can be seen from the figure. Both sets of results have a correlation factor of 0.99 and slope of regression line of 1.08.

It can be concluded that, for the spreadsheet method, variation of steel thermal properties need not be taken into account. An assumed average specific heat of 600 J/kg °C would yield an almost exact result.

3.3 The SAFIR Program vs Spreadsheet Method

3.3.1 Introduction

SAFIR program, as mentioned in section 1.4.1, is considered to be a very accurate, realistic heat transfer model for the simulation of beam exposure to fires. Therefore, it is used in this report to evaluate the spreadsheet method.

3.3.2 Methodology

As the time-temperature fire curves available in SAFIR does not include the Eurocode parametric fire, the author could only run simulations of steel beam with different insulation thickness and sizes exposed to the Standard ISO-834 fire. The temperature-time curves of the steel created from the SAFIR are then compared with those of from the spreadsheet method.

Simulations are run for three beam sizes, 150UB14, 250UB37 and 610UB125 and for insulation thickness: 5, 10, 20 and 50 mm.

3.3.3 Results and Comparisons

The temperature-time curves from the SAFIR and spreadsheet are plotted together in figure 3.6.

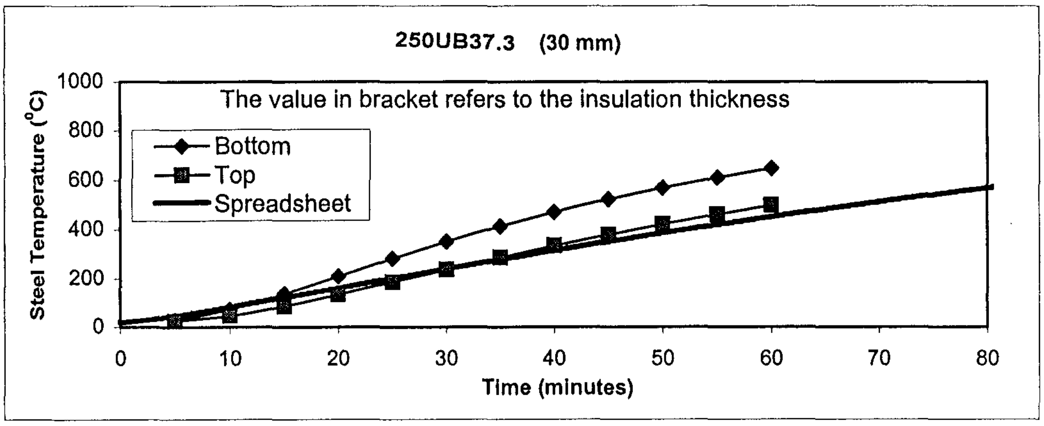

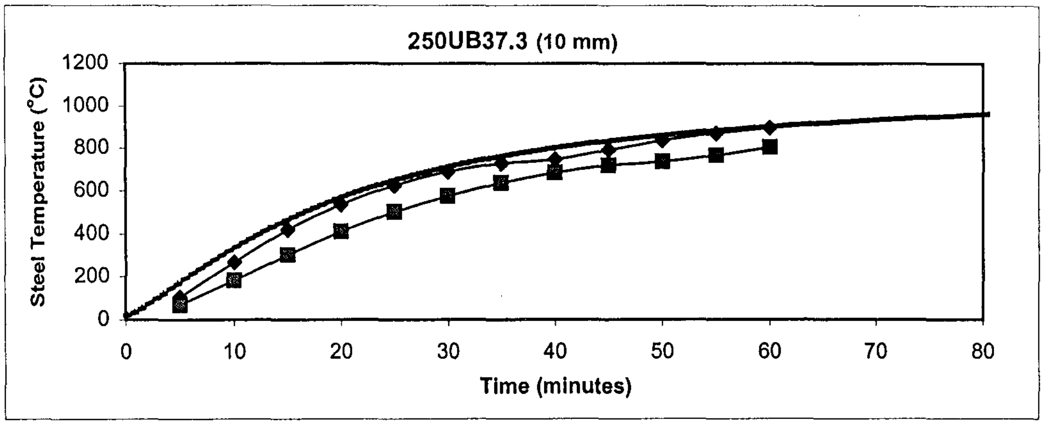

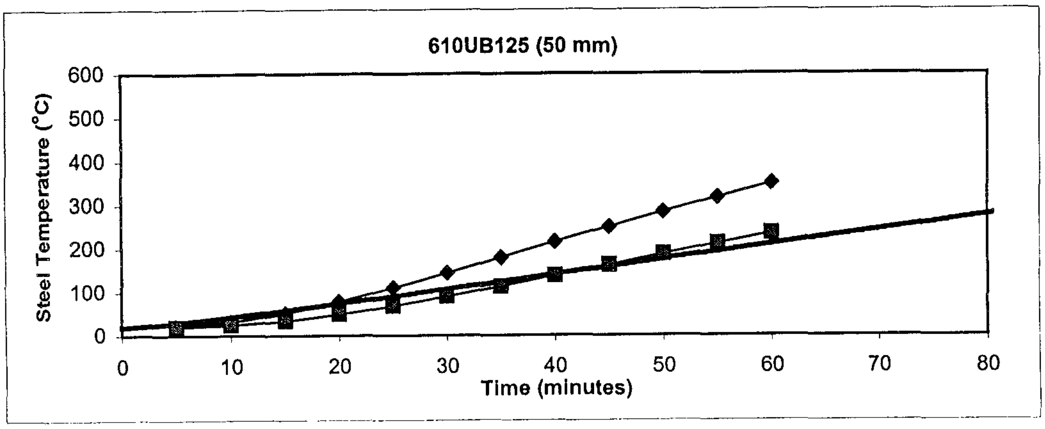

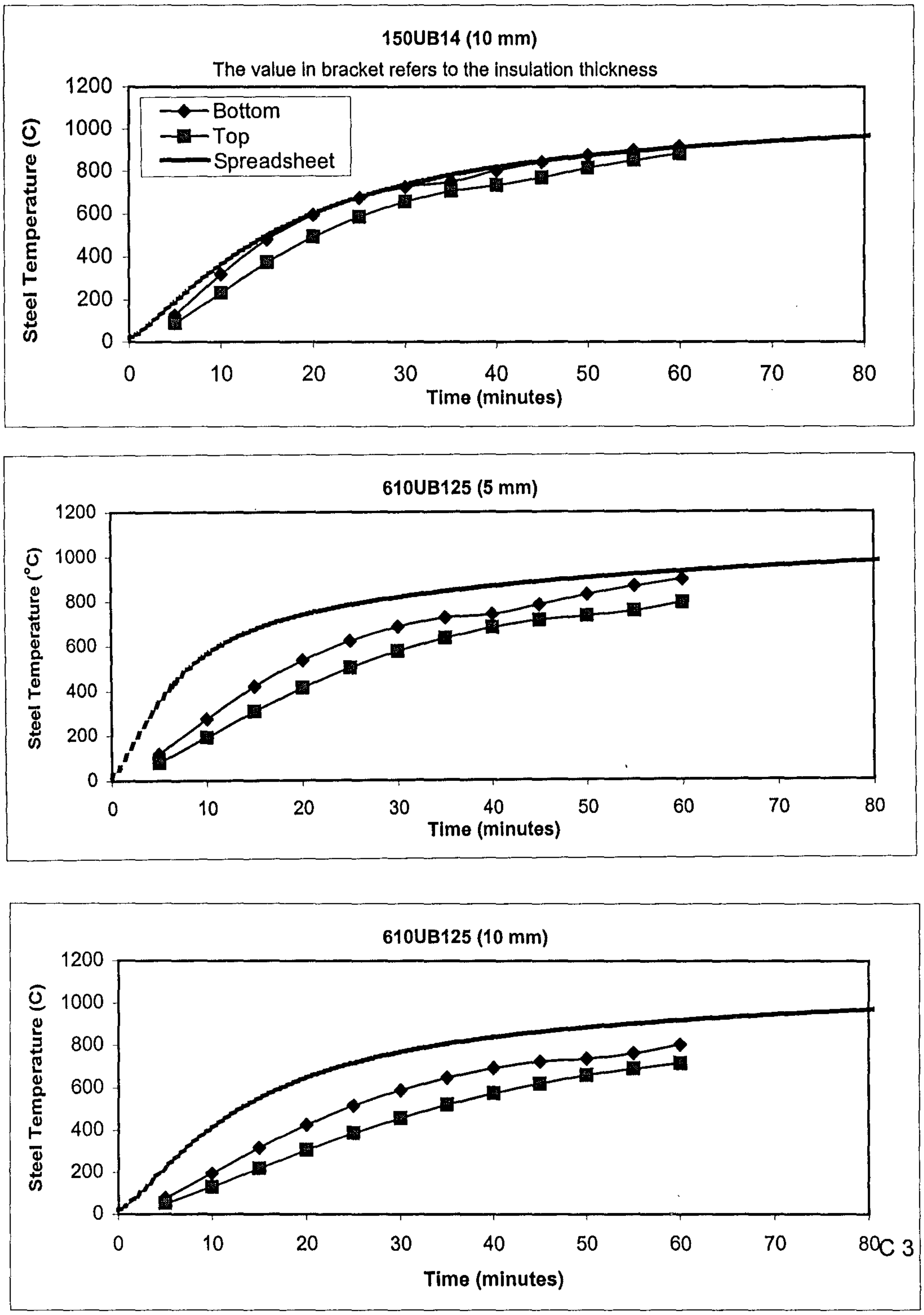

Figure 3.6: Temperature-time curves of protected steel by SAFIR and spreadsheet method

Figure 3.6 shows the temperature-time curves for protected steel beams exposed to the standard fire obtained from the SAFIR and spreadsheet method. Temperature-time curves have been plotted for the top and bottom of the steel beam. Since the steel beam is only exposed to fire on three sides, the top of the steel beam is not in direct contact with the fire.

As shown in the graphs, the behaviour of the steel beam exposed to the fire as predicted by the spreadsheet method is close to the simulation result from SAFIR, especially for small beam with thin insulation. In fact, for steel member with insulation thickness less than 20 mm, results from the spreadsheet method agrees nearly perfectly with the result obtained from SAFIR for the bottom surface of the steel beam, the side of beam that is exposed directly to fire. This implies that the spreadsheet method is conservative in predicting the steel beam temperature. However, as the insulation thickness increases, the results from the spreadsheet method becomes less conservative and tend to agree better with results obtained from SAFIR for the top of the beam, which is not exposed to fire.

Apart from that, the spreadsheet method agrees quite poorly with SAFIR in calculating the temperature for large steel beam. For the beam 610UB125, a temperature difference up to 200 °C exists between the two methods.

3.4 Conclusions

Spreadsheet method is especially accurate in calculating time equivalent for small steel member with thin protection. The variation of the steel member's specific heat need not be taken into account in the spreadsheet method. An averaged value yields an almost exact result.

4 Effects of Physical Parameters on Time Equivalent

Physical parameters of a fire compartment refer to the geometry set up of the compartment, thermal characteristics of the compartment walls, opening size and fuel load. These parameters govern the growth and duration of the fire, rise of the gas temperature in the compartment and affect the corresponding heat transfer to the steel beam. Therefore, the parameters are important in determining the resultant time equivalent of a compartment fire. However, the degree by which a certain parameter affect the time equivalent is different than the other. Finding out in what way does each parameter affects the time equivalent is the aim of this chapter.

4.1 Previous Work

The author has repeated similar work done by Franssen (1996) on examining the effect different physical parameters of a compartment fire have on time equivalent. Franssen had looked at the three main categories of physical parameters including:

- Fire load
- Geometry of compartment and
- Thermal properties of surrounding material

for three structures :

- Unprotected Steel Section
- Protected Steel Section
- Concrete Structure.

The author has only looked at the protected steel section in this part of the report.

4.1.1 Franssen's Methodology

For the protected steel section, Franssen used the SAFIR program to calculate the exposure of protected steel beam to the Eurocode fire described in Eurocode 1: Annex B. A steel beam with massivity or H_p/V of 211 m-1 was chosen. The thermal properties of the insulation are: C_p of 850 J/kgK, k of 0.15 W/m^{2}K and ρ of 300kg/m3. The scope of Franssen's investigation are as listed below with the underlined values being the standard case:

- Fuel load per floor area

  Density of the fuel load available for burning, per floor area of compartment.

Fuel loads used are 250, 500, 750, 1000, 1250, 1500, 1750, 2000 MJ/m^2

- Opening Height

  Refers to the height of the ventilation, h_v used in the ventilation factor of the CIB and Law formula.

  The H_v values used are 2.4, 2.5, 3, 3.5, 4, 4.5, 5 m

- Opening Width

  The width of ventilation is varied within the range: 0.5, 1, 2, 3, 4, 5 m

- Thermal Inertia

  Refers to the characteristics of the compartment boundary linings. As the main mean of heat transfer to the element exposed to fire is through the heat radiation by its boundary. Therefore, a low thermal inertia value for a well insulated compartment means less heat will be absorbed by the internal boundary surfaces or higher heat transfer rate to the element and vice versa.

The thermal inertia, $(k\rho C)^{1/2}$ values used are 500, 1000, 1300, 1600, 2000 $J/m^2s^{1/2}K$

- Room Height

  Height of the compartment used are 2.4, 2.5, 3, 3.5, 4, 4.5, 5 m

- Floor Area

  Floor areas of the compartment used are: 16, 25, 36, 64, 100,144, 256, 324, 400 m^2

4.2 Methodology in this Study

Time equivalent for fires with the physical parameters listed above are calculated using the spreadsheet method.

In order to study the effect of each parameter on the time equivalent, in each computer run only the value of a selected parameter is changed its certain range while the other parameters are fixed. The corresponding change in the time equivalent calculated is studied. The results are compared to Franssen's.

After successfully repeating Franssen's results, the research proceeds to go beyond his research and looks at the effect of some parameters never been looked at before in chapter 8.

4.3 Comparison of results - Repeat of Franssen's Study

Results of the repeated Franssen's investigation obtained by the spreadsheet method are plotted together with Franssen's original results in the following section for comparison.

The graphs show a successful repeat of Franssen's investigation. The results obtained from the report's spreadsheet method are almost identical to his. However, some slight difference exists in some graphs. In general, the Eurocode time equivalent formula also shows close results to the spreadsheet method's.

4.3.1 Floor Area

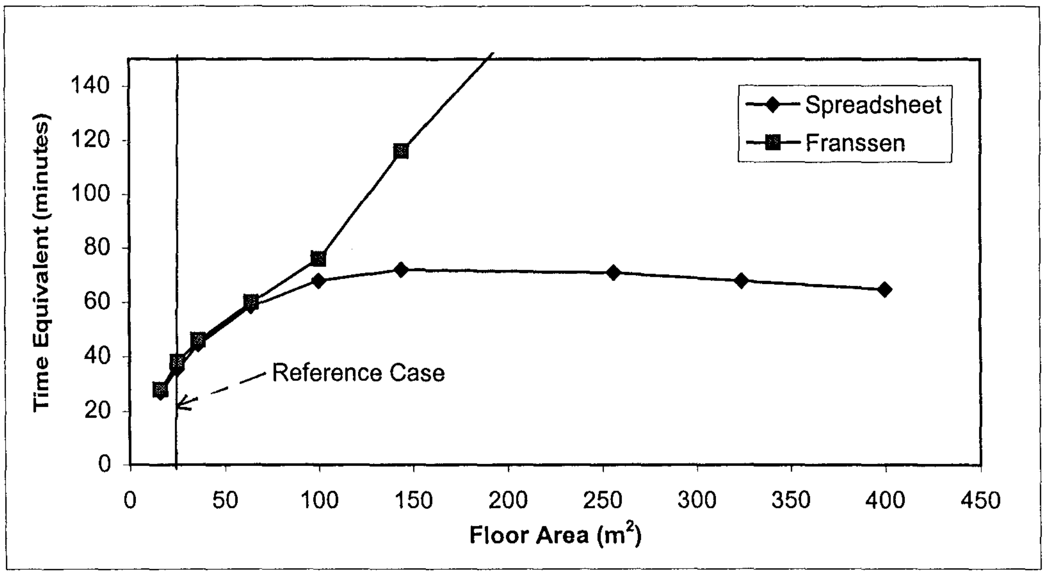

Figure 4.1(a): Time equivalent versus floor area: comparison between spreadsheet method and Franssen's results

Figure 4.1(a) shows the variation of the time equivalent with floor area calculated by the spreadsheet method and Franssen. It can be seen that the results obtained from spreadsheet agree very well with Franssen's results up to the floor area $64m^2$, the difference between them is found to be negligible. Beyond that point, the two results start to deviate from one another largely. Time equivalent from Franssen's result starts to increase rapidly up to more than 150 minutes after 144m^2.while the spreadsheet gives slowly declining time equivalent. However, it should be noted that for floor area greater than144 m^2, the data from Franssen's paper lie in the region, which he labeled as beyond the applicability limit of the method used.

It must also be pointed out that in assessing the influence of floor area, Franssen did not fix the other two related parameters, which are the ventilation factor and total fuel density to be constant. The ventilation factor is basically the ratio of the window size to the total boundary surface area, which also includes the floor area. Therefore, by varying the floor area without a reciprocal adjustment in the window size to maintain the ventilation factor, the ventilation factor simply decreases as the floor area increases. As for the total fuel load density which is dependent on the fuel density per floor area e_f (MJ / m^2), it changes as the floor area varies.

Therefore, the change in time equivalent calculated does not 'purely' reflect the effect of the variation in floor area but rather a combined effect of the variations in the ventilation factor and fuel load. After modifying the test by eliminating the effect of the ventilation and fuel load, the result that shows the 'pure' effect of the variation in floor area is shown in figure 4.1(b).

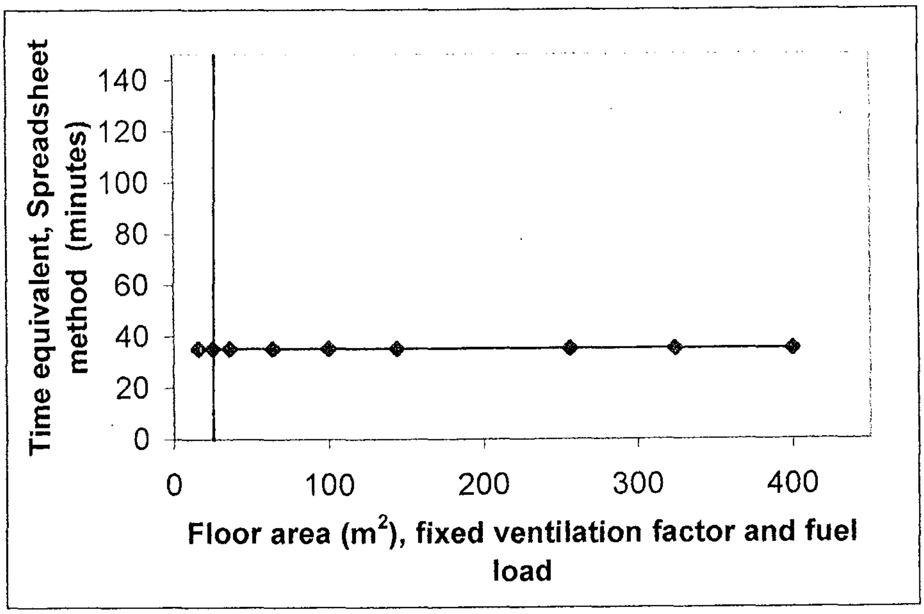

Figure 4.1(b): Time equivalent versus floor area with fixed ventilation factor and fuel load

4.3.2 Fuel Load

Figure 4.2 shows the variation in time equivalent due to the change in fuel load density per floor area, e_f (MJ/m^2). The difference between the spreadsheet and Franssen's result is negligible.

The graph shows a linear increment in the time equivalent with fuel load. The rate of increment is approximately 2.4 seconds per MJ/m^2 increase in fuel load density.

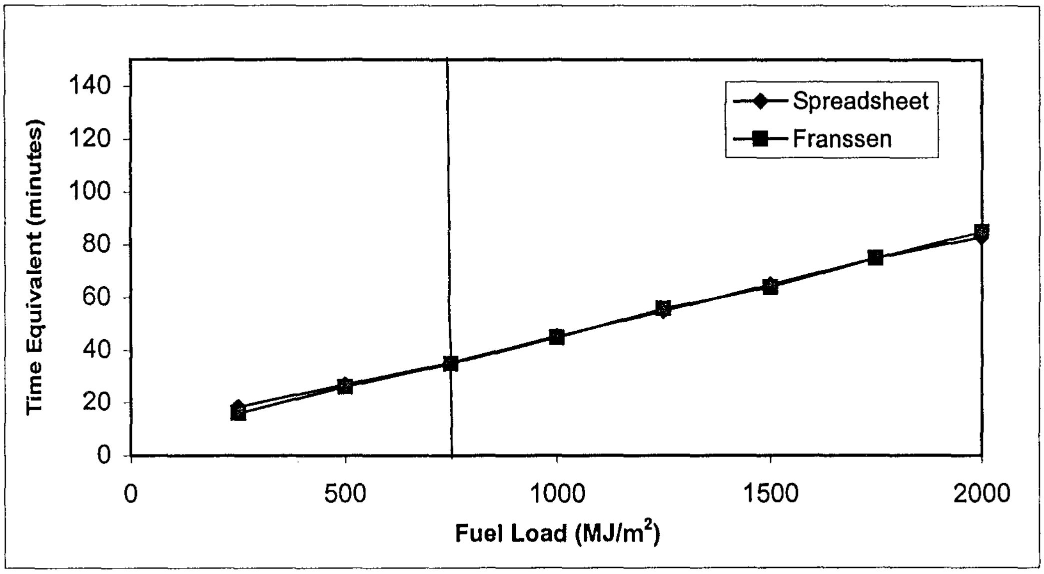

Figure 4.2: Time equivalent versus fuel load: comparison between spreadsheet method and Franssen's results

4.3.3 Room Height

Figure 4.3 is a plot of the time equivalent against the compartment height. Again, the result shows almost identical result from both studies. The variation in room height is also made without fixing the ventilation factor and the fuel density per total area, therefore the result does not entirely reflect solely the effect of the room height on time equivalent. However, the time equivalents shown in the graph remains relatively unchanged with the increment in room height, which indicates a very small change in the total fuel density and ventilation factor as a result of the increment in room height.

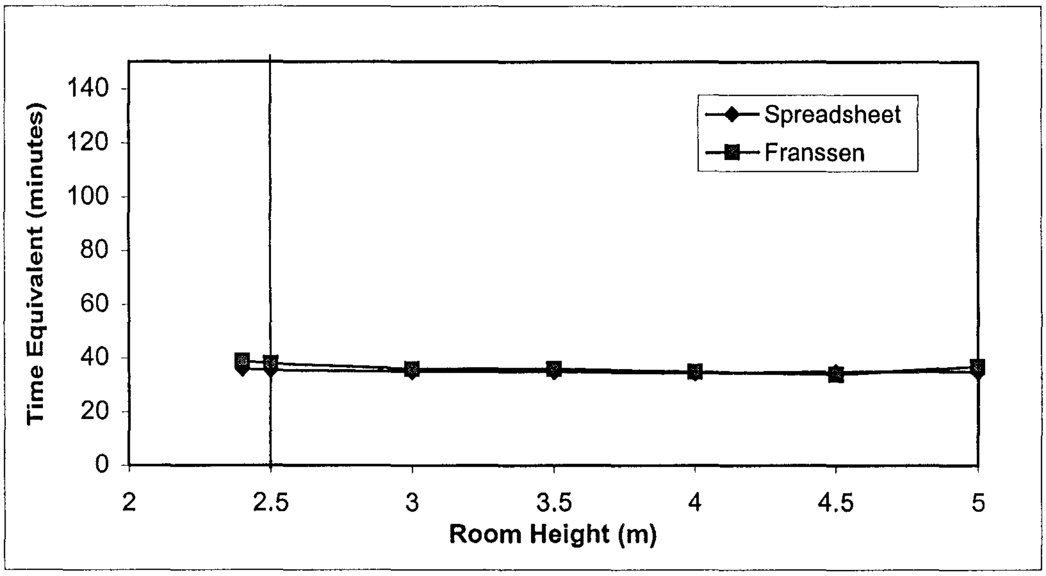

Figure 4.3: Time equivalent versus room height: comparison between spreadsheet method and Franssen's results

4.3.4 Ventilation Height and Width

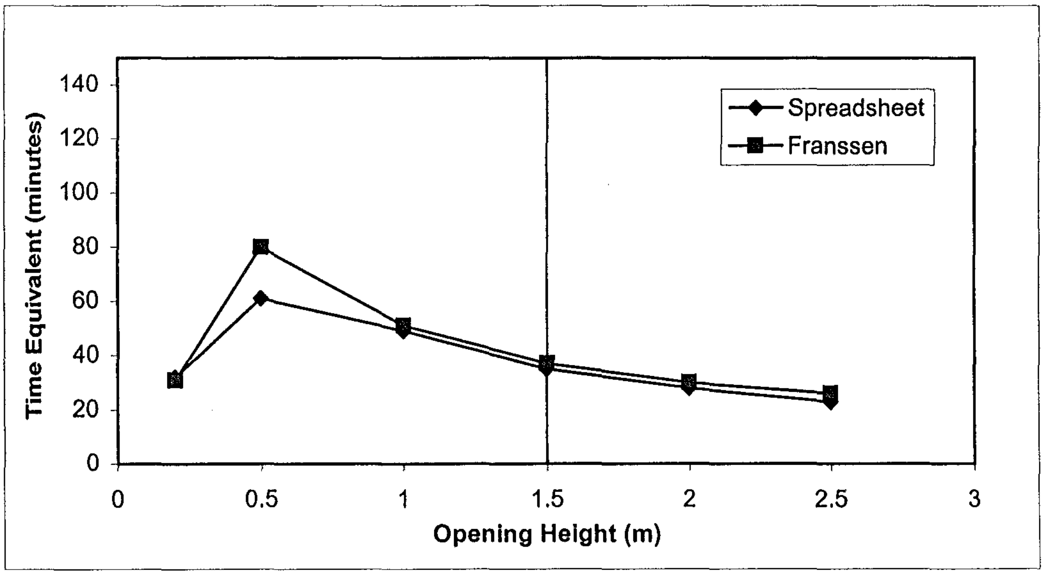

Figure 4.4: Time equivalent versus opening height: comparison between spreadsheet method and Franssen's results

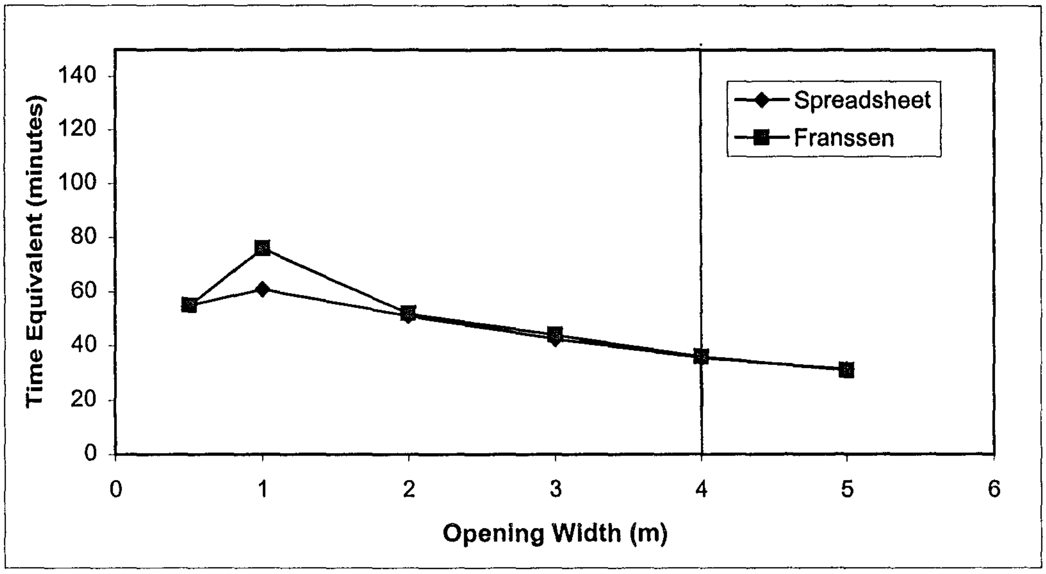

Figure 4.5: Time equivalent versus opening width: comparison between spreadsheet method and Franssen's results

Figure 4.4 and figure 4.5 show the variation in time equivalent due to the change in the ventilation height and width respectively. As the ventilation factor, F_v is directly proportional to the window area, these two graphs show basically the variation in the time equivalent with the change in ventilation factor, F_v.

It can be seen that the results from both studies are close to each other in this case. Except for opening height of 0.5m and opening width of 1m where the spreadsheet method differs from Franssen's quite substantially for some unknown reasons. However, it should be pointed out that these two points also lie in the zone described in Franssen's paper to be beyond the applicability limit of his method as mentioned before.

4.3.5 Thermal Inertia

The variation of time equivalent with the thermal inertia of the compartment walls is plotted in figure 4.6. The graph shows nearly no variation in time equivalent with thermal inertia. It also shows good agreement of the results from spreadsheet method and Franssen.

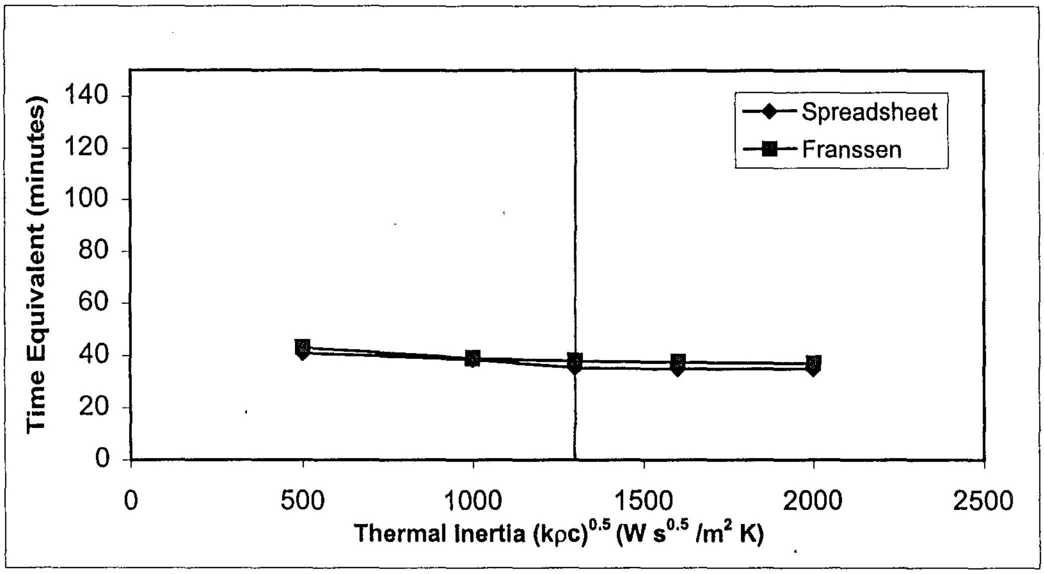

Figure 4.6: Time equivalent versus thermal inertia: comparison between spreadsheet method and Franssen's results

4.4 Conclusion

It has been shown that the spreadsheet method developed for this report has been successful in repeating the results of Franssen's paper.

Some of Franssen's results do not show the real effect of the parameter it claims to show but rather a combined effect of more than one parameter. Modification of those tests in order to investigate the 'pure' effect of those parameters yields a totally different result from those published.

5 Time Equivalent Formulae for Steel Beam

5.1 Introduction

The three commonly used time equivalent formulae, the Eurocode, CIB and Law formulae have been introduced in chapter 1. The accuracy of time equivalent formulae has always been debatable issue. Which is the best formula to use; in what way is one formula different from the other and what is the magnitude of the difference?

A great number of researches and studies on the topic can be found. According to Buchanan (1999), the CIB time equivalent formula is the most widely used formula while the Eurocode formula is used in the Eurocode for fire safety design. Law later pointed out in her study that the formulae are insufficient and thus developed her own Law formula.

However, according to a recent study carried out by Cadorin and Cajot (1999) to investigate the accuracy of the Eurocode formula by comparing the time equivalents calculated from the formula to those obtained from actual experimental tests, the Eurocode formula is found to be excellent in estimating time equivalent.

This chapter therefore aims to look at the correlation of these three formulae, how well one formula agrees with another, in what way are they different from one another and the magnitude of the difference.

5.2 Methodology in This Study

Time equivalents are calculated for a various combinations of compartment fire parameters such as the fuel load, ventilation sizes and wall thermal properties using the three formulae. The three sets of results are then plotted together in graphical form for comparison. Conclusions are then made from the comparison.

The compartment fire parameters that are included in the calculation and their ranges are as follow. In each calculation, only one of the parameters are changed while the other parameters are fixed at the standard case as underlined.

- Fuel load per floor area, e_f (MJ / m^2)
  250, 500, <u>750</u>, 1000, 1250, 1500, 1750, 2000
- Height of window, H_v (m)
  0.2, 0.5, 1, <u>1.5</u>, 2, 2.5
- Thermal Inertia of Walls, $[k\rho c]^{1/2}$ ($Ws^{1/2}/m^2K$)
  500, 1000, <u>1300</u>, 2000, 3000
- Floor area, A_f (m^2)
  16, <u>25</u>, 36, 64, 100, 144, 256, 324, 400

5.3 Results and Comparisons

The time equivalents are calculated using the three time equivalent formulae, the Eurocode formula, the CIB formula and the Law formula. Although the combination of the four different parameters can generate a total of 28 data for each formula only 17data points appear in the graphs below. The 'missing' 11 points are explained below:

(a) Four data points calculated for floor area larger than 144m^2 and one for the window height of 0.2m are eliminated because these five points result in ventilation factors that are smaller than the lower limit of the ventilation factor of Eurocode formula. This limit, beyond which the formula should not be used, has been described in chapter 1, equation 1.22.

(b) Besides that, the standard case, which has the underlined values occurs once when each parameter is varied within its range. Thus, for four parameters, four data points that have the exact same value are generated, which when plotted on the graph, appear only to be one data points.

(c) Finally, as the time equivalent formulae are independent of the thermal inertia of the compartment walls, the variation of this parameter actually causes no changes in the calculated time equivalent, therefore, generating four identical data points (one of them is standard case). Again they appear only as one data point , which is also the point for the standard case.

5.3.1 Eurocode vs CIB

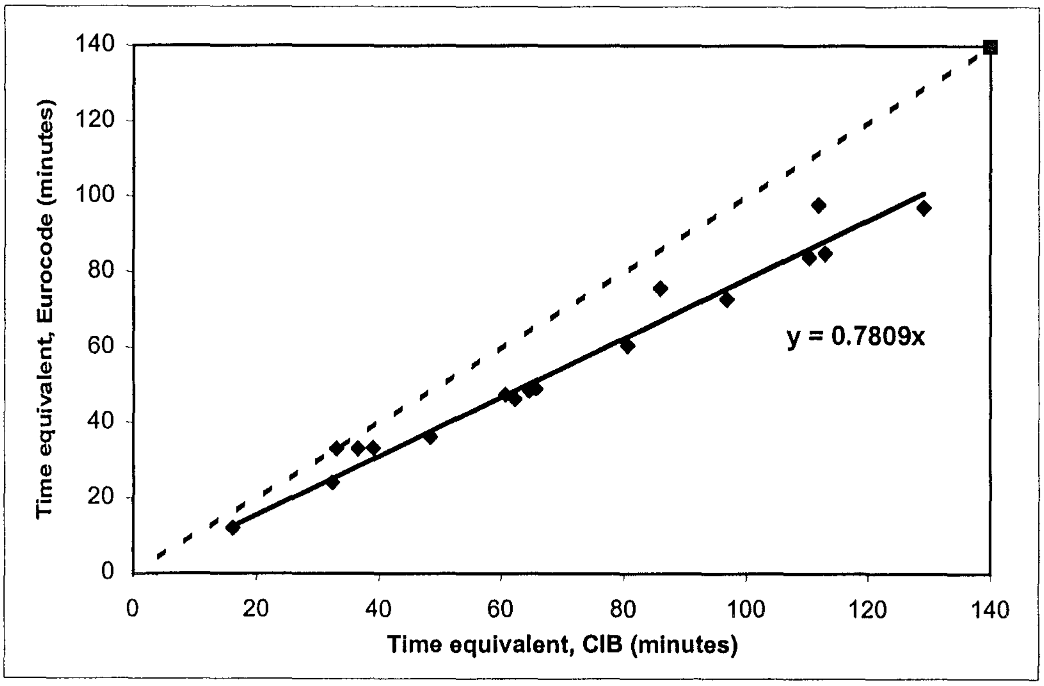

Figure 5.1: Comparison between Eurocode and CIB time equivalent formula

Figure 5.1 shows a comparison between the time equivalents calculated by the Eurocode and the CIB formulae

Summary of Results	**Eurocode vs CIB Formula**	
	Slope of Regression line through the origin	**Correlation Coefficient, R^2**
	0.78	**0.99**

On average, the CIB formula tends to give more conservative time equivalents than the Eurocode. Compared to the Eurocode formula, the CIB formula overestimates the time equivalent by 28 %.

5.3.2 Eurocode vs Law

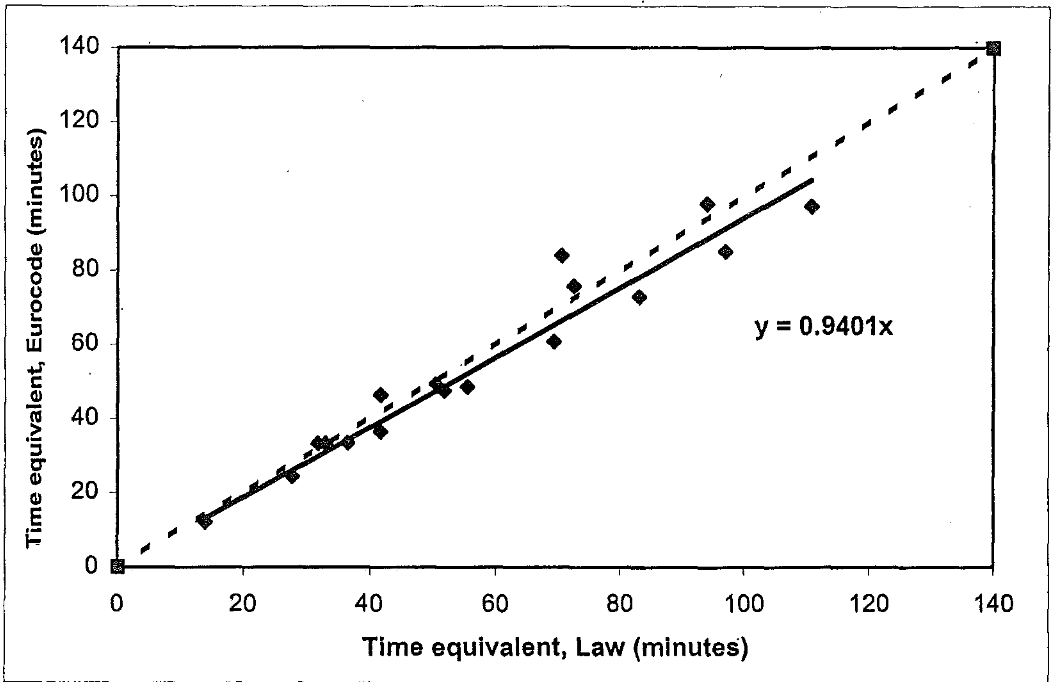

Figure 5.2: Comparison between Eurocode and Law time equivalent formula

Summary of Results	Eurocode vs Law Formula	
	Slope of Regression line through the origin	Correlation Coefficient, R^2
	0.94	0.97

Figure 5.2 shows a comparison between the Eurocode and the CIB formula. As shown in the graph, both formulae almost agree perfectly with one another. On average, the Law formula tends to give slightly more conservative time equivalents than the Eurocode

formula. Compared to the Eurocode formula, the Law formula only overestimates the time equivalent by 6 %

5.3.3 Law vs CIB

A comparison between the Law and the CIB formulae is shown in figure 5.3.

Summary of Results	**Law vs CIB Formula**	
	Slope of Regression line through the origin	**Correlation Coefficient, R^2**
	0.82	**0.98**

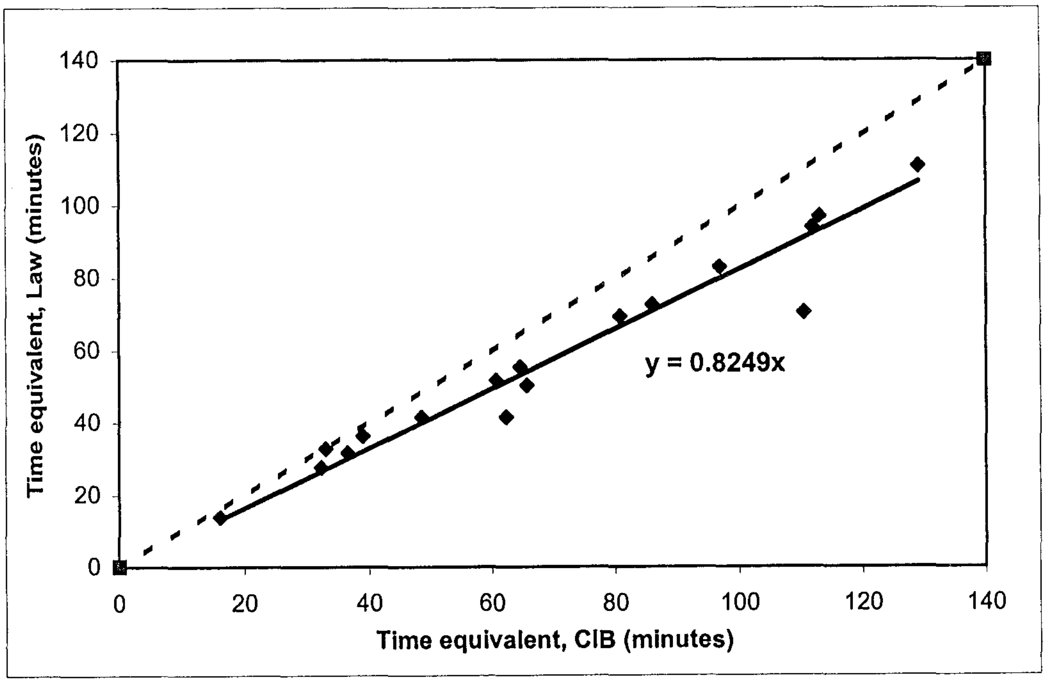

Figure 5.3: Comparison between Law and CIB time equivalent formula

On average, the CIB formula is more conservative time equivalents than the Law formula. Compared to the Law formula, the CIB formula overestimates the time equivalent by 21%.

5.4 Conclusions

The three formulae are found to be highly correlated with one another. An average correlation of 0.98 is calculated. Among the three time equivalent formulae, the CIB formula is found to be the most conservative one, followed closely by the Law formula that is 21% less conservative than the CIB. The Eurocode formula is found to be the least conservative but agrees very closely with the Law formula.

6 Spreadsheet Method versus Time Equivalent Formulae

6.1 Introduction

In the last chapter, three time equivalent formulae, the Eurocode, CIB and Law formula have been examined and discussed. These three formulae have also been compared to one another and conclusion has been derived from the comparison.

As mentioned before, the time equivalent formulae are derived empirically, based on a set of experiment data and developed by regression analysis using the results of a selected number of tests. Thus, the formulae may not be suitable for all fire scenarios.

This chapter aims to investigate, using the spreadsheet method, the accuracy and reliability of the time equivalent formulae for a range of fire scenarios.

6.2 Previous Work

Thomas (1997) evaluated the CIB and the Eurocode time equivalent formula for concrete and steel structures. He used two computer models to calculate the time equivalents for materials including steel and concrete and compared the results to those calculated by the CIB and Eurocode formulae. These two models are the COMPF-2 and TASEF.

COMPF-2 is used to develop post flashover compartment fires model with different characteristic time-temperature curves, thermal behaviour for compartment boundaries, fuel loads, opening factors and fire duration.

TASEF is a two-dimensional finite element model for modelling the heat transfer in concrete and steel structures subjected to fires developed using COMPF-2 program.

6.3 Results and Conclusions

Thomas (1997) ran the computer model for concrete floor, concrete wall, steel I-column and steel I-beam and his results are as shown below:

% time equivalent underestimated (unconservative)		
	CIB Formula	Eurocode Formula
Protected steel member	16 %	43 %
Concrete member	11 %	25 %

Thomas (1997) concluded in his report that the time equivalent formulae especially the Eurocode formula, are poor formulae for fire resistance rating. He found them to be highly unconservative, tend to underestimate the time equivalent compared to the calculation by the computer models. He suggested that a safety factor to be included in the formulae and also the formulae should be used for limited application only.

Thomas' results are strongly dependent on the type of design fire selected. He used the COMPF program to calculate design fires with temperature over 1100 °C and very rapid decay rates. Feasey (1999) has shown that COMPF when calibrated to real fire tests, produces rather different design fires. Therefore, the results of Thomas may need to be re-investigated.

6.4 Methodology

In this chapter, the spreadsheet method is used to calculate the time equivalent for range of fire scenarios discussed in chapter 5. The calculated time equivalents are then plotted together with those previously obtained from the formulae for comparison.

6.5 Results

Figure 6.1(a) shows a plot of the time equivalents obtained from the spreadsheet method against those from the Eurocode formula. It can be seen that there are four points, labelled point A,B,C,D (as indicated in the plots) which deviate a lot from the 'zone' where other data lie. These points are produced by varying the floor area of the compartment (except for point A which is produced by variation of the ventilation height). A closer investigation of these four points shows that the great deviation from the rest of the data is due to the sudden jump in the time equivalent by the spreadsheet method at ventilation factor smaller than 0.007. This is actually the range beyond which the Eurocode time equivalent formula is valid for, as discussed in chapter 5.

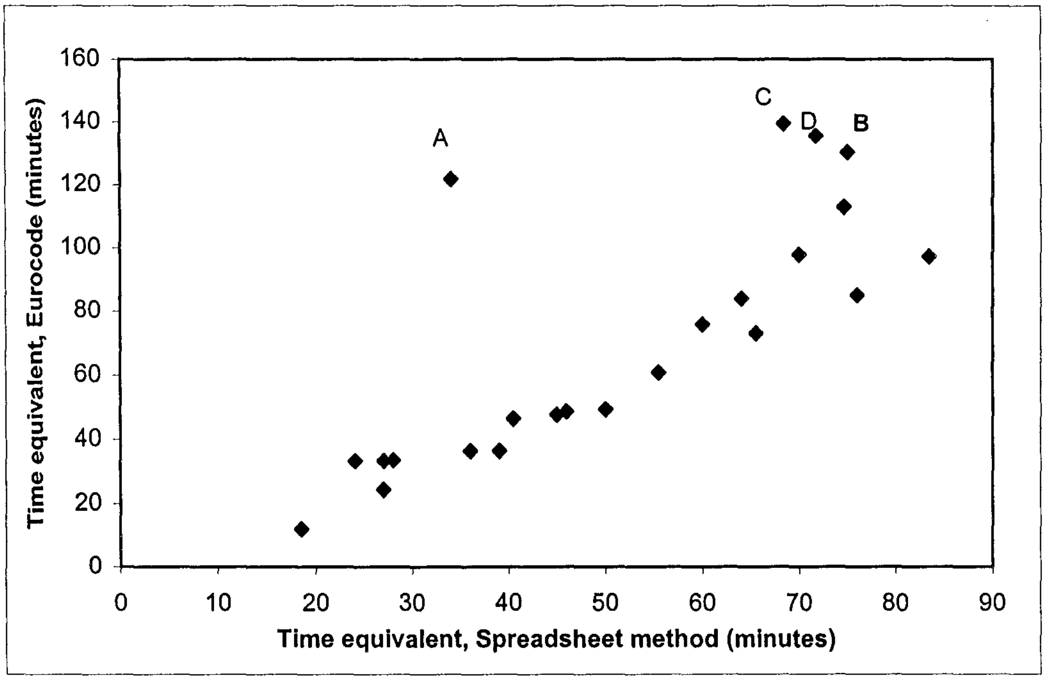

Figure 6.1: Comparison between spreadsheet method and Eurocode formula: points A,B,C,D

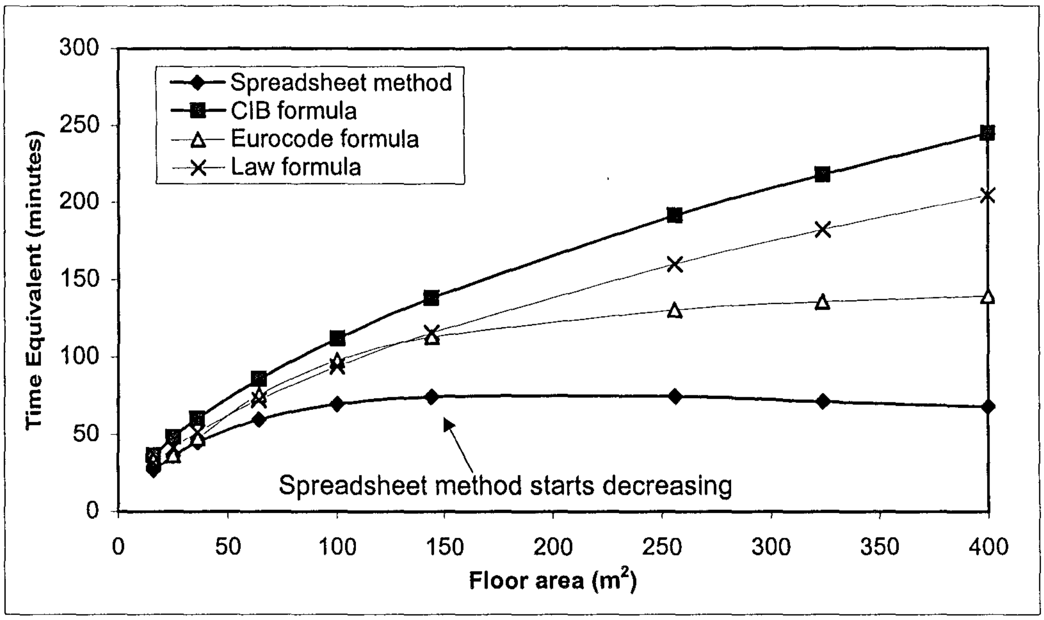

Figure 6.2: Time equivalent versus floor area: points A,B,C,D

To understand this phenomenon, a plot of the time equivalent versus the variation in floor area must be used. As shown in the plot figure 6.2(a), the time equivalent calculated by the spreadsheet method starts to decrease after the floor area 144 m^2 while that calculated by formulae continue to increase. Although the time equivalent seems to vary with the floor area, it actually changes due to the variation in the ventilation factor. This is so since the floor area is varied without fixing the compartment's ventilation factor. As the ventilation factor is a ratio of the area of ventilation to the total boundary surfaces area, which also includes the floor area, changes in the floor area would cause a corresponding change in the ventilation factor. Thus another way of presenting this data would be plotting the time equivalent against the ventilation factors that correspond to the floor areas, as shown in figure 6.2(b).

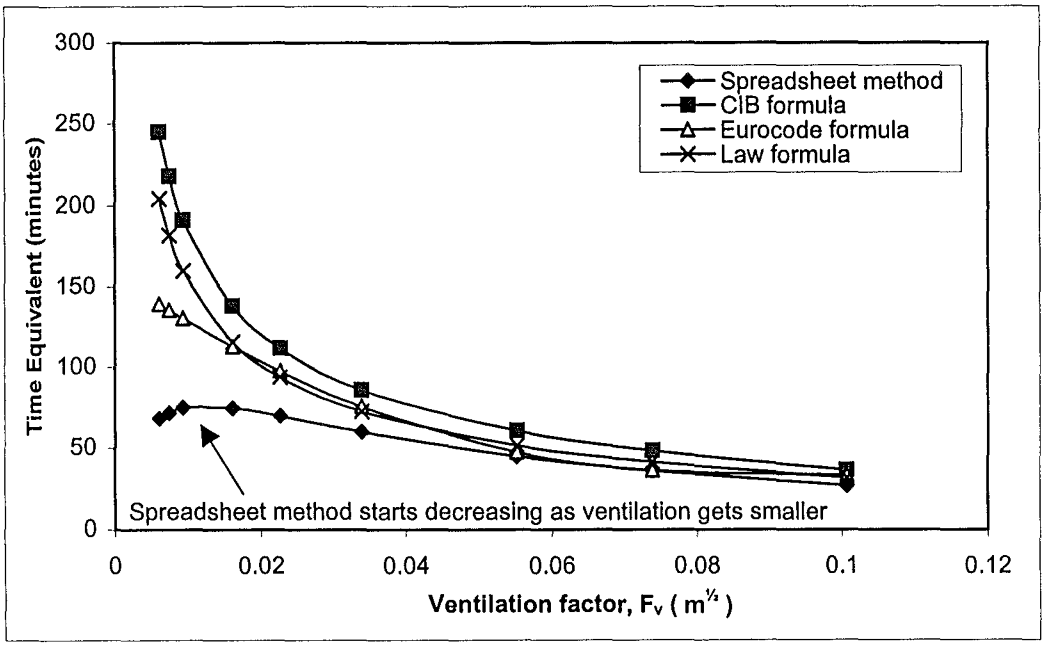

Figure 6.2(b): Time equivalent versus floor area /ventilation factor

Figure 6.2(b) shows that at ventilation factor of 0.0161 which corresponds to floor area of 144 m^2, the time equivalent from the spreadsheet method starts to decrease as the ventilation factor decreases while the time equivalent from the formulae continue to increase. This vast difference in the behaviour of time equivalent calculated by the spreadsheet method and formulae results in the points A,B,C,D.

A closer study of this phenomenon is made by examining the behaviour of the steel temperature for this range of ventilation factors. As shown in the figure 6.3, the maximum temperature reached by the steel increases as the ventilation factor decreases. In another word, the steel gets hotter as the ventilation factor gets smaller. However, as the ventilation factor reaches about 0.0093, the maximum temperature starts to decrease with the increase in ventilation factor while the time to maximum temperature continues to increase. This behaviour of the steel temperature can be more easily comprehended with the help of figure 6.4.

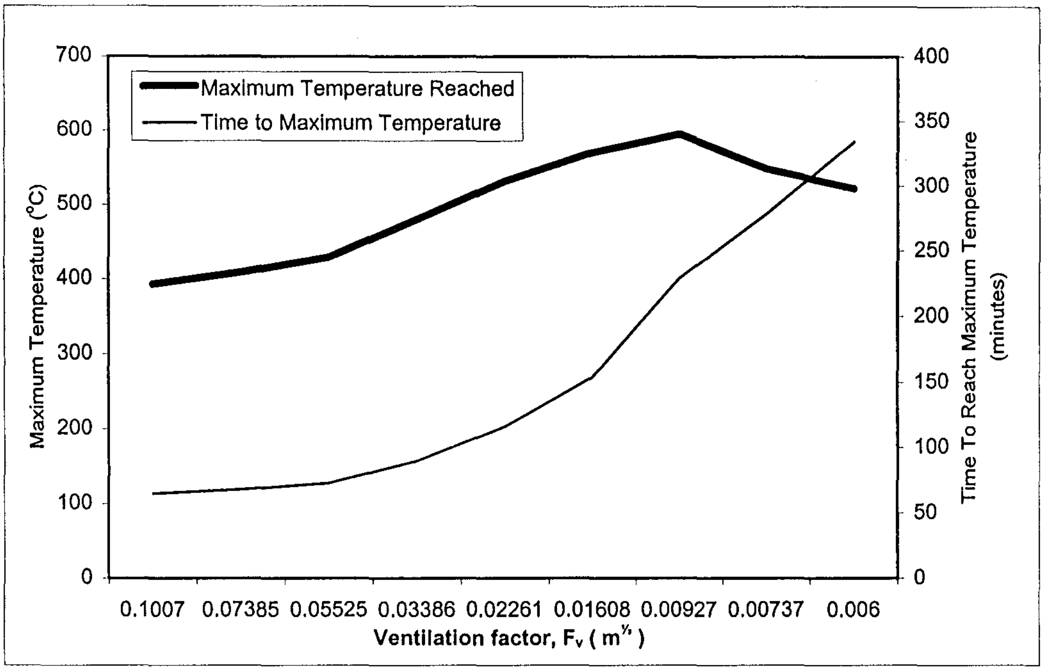

Figure 6.3: Maximum temperature reached and time to reach maximum temperature versus ventilation factor for protected steel exposed to fire

Figure 6.4 shows that, as the ventilation factor decreases from 0.1 to 0.0093 the temperature of the steel member increases as well as the corresponding time to reach the maximum temperature but at ventilation factor of 0.007, the steel is suddenly 'cooled' down. This can simply be explained by the fact that as the ventilation factor decreases from 0.1 to 0.0093, the Eurocode parametric fire changes from an extremely hot but short fire to hot but longer fire, which allows the steel to be heated up, thus producing a higher steel temperature. However, as the ventilation factor is reduced to 0.007, the temperature of the fire becomes so low that the steel temperature simply drops. The Standard fire, on the other hand remains unchanged since it is only dependent on the time. As a result, the time equivalent starts to drop at ventilation factor of 0.007.

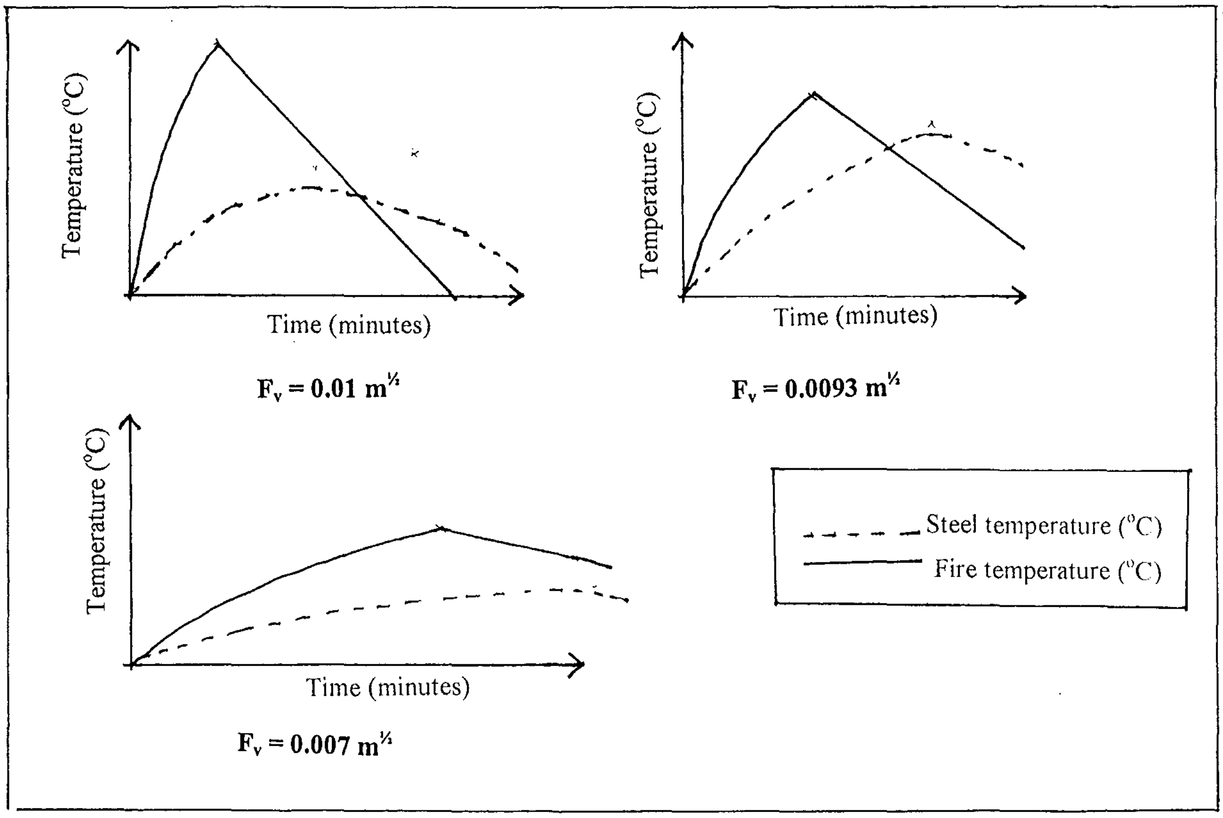

Figure 6.4: Illustration: behaviour of steel exposed to fire for different ventilation factor

This also implies that the time equivalent formulae do not take into account of this phenomenon and assume a continuously increase in the maximum steel temperature. Therefore, there is a minimum ventilation limit beyond which the formulae are not valid and the points A,B,C,D lie beyond this limit, therefore, they should really not be taken into account in the evaluation of results thus they have not been included in the following plots.

Apart from that, where there are only 17 data points in the plots shown in chapter 5, there are 19 data points in each of the following plots. The reason being that the unlike the time equivalent formulae, the spreadsheet method is dependent on the thermal inertia value of the compartment walls. Thus, generates two 'extra' data points due to the change in the thermal inertia, in addition to the 17 data points that are mentioned and discussed in chapter 5.

6.5.1 Eurocode Formula vs Spreadsheet method

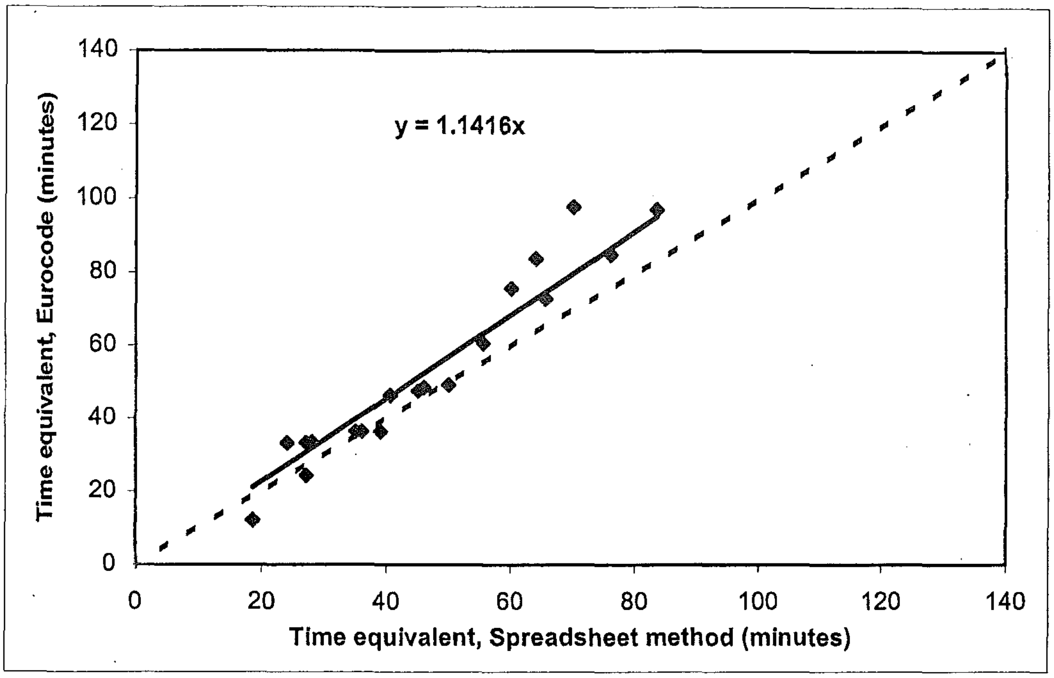

Figure 6.5: Comparison between Eurocode formula and spreadsheet method

Summary of Results	Eurocode Formula vs Spreadsheet Method	
	Slope of Regression line through the origin	Correlation Coefficient, R^2
	1.14	0.97

Figure 6.5 shows the comparison between the time equivalents from the Eurocode formula and the spreadsheet method. In contrast to the results shown by Thomas' study, the Eurocode formula is found to be conservative compared to the spreadsheet method. In general, the Eurocode formula overestimates the time equivalent by 14 %. Both methods have a high correlation factor of 0.97.

6.5.2 CIB Formula vs Spreadsheet method

Figure 6.6 shows the comparison between the spreadsheet method and the CIB formula.

Summary of Results	CIB Formula vs Spreadsheet Method	
	Slope of Regression line through the origin	Correlation Coefficient, R^2
	1.46	0.99

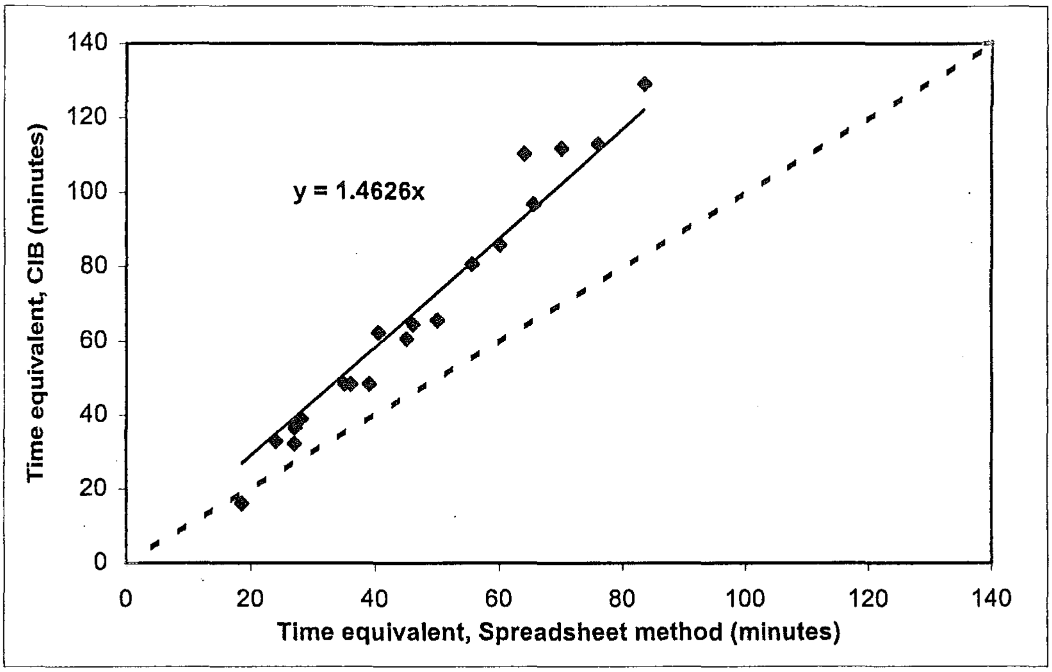

Figure 6.6: Comparison between CIB formula and spreadsheet method

Once again, the results yielded contradict to those shown in Thomas report. The CIB formula is found to be highly conservative in estimating the time equivalent. In fact, it generally overestimates the time equivalent by a significant 46 % and correlates perfectly with the spreadsheet method.

6.5.3 Law Formula vs Spreadsheet method

Summary of Results	Law Formula vs Spreadsheet Method	
	Slope of Regression line through the origin	Correlation Coefficient, R^2
	1.21	0.98

Figure 6.7 shows that the Law formula is found to be conservative and in general overestimates the time equivalent by 21 % and correlation factor of 0.98.

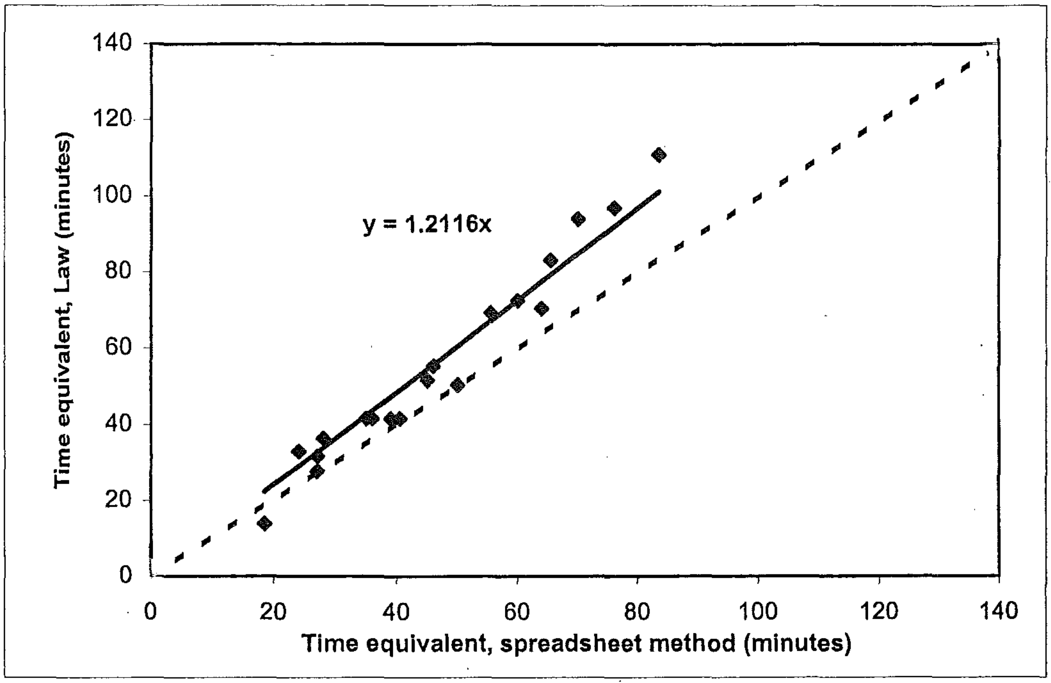

Figure 6.7: Comparison between Law formula and spreadsheet method

6.6 Conclusion

The results of this study show that all the three time equivalent formulae seem to be good formulae. They all estimate time equivalents that are conservative and highly dependent on the results obtained from the spreadsheet method. The time equivalents calculated by CIB formula differ quite significantly from those by the spreadsheet method. In general, it overestimates the time equivalents by 46%. The Eurocode and Law formulae give much closer results to the spreadsheet method.

7 Alternative Decay Rate

7.1 Introduction

So far, our studies have all been done by the spreadsheet method that follows the Eurocode decay rate (EDR) described by equation 2.3 of chapter 2. However, Buchanan (1999) pointed out that ~~te~~ the Eurocode decay rate may be incorrect in relative to a compartment's insulation property. The law of physics would tell us that for a fixed fuel load and ventilation factor, the gas temperature in an well-insulated fire compartment (ie. with low thermal inertia value) would be higher compared to that in a poorly insulated compartment. The reason being that, the heat generated by the fire is lost through conduction into the walls at a much slower rate than in a poorly insulated compartment.

The EDR on the contrary, suggest a faster decay rate for fire curve in a well-insulated compartment than that in a poorly insulated one. Two plots of fire curves using the EDR for compartment with different insulation property are shown in figure 7.1(a) and 7.1(b).

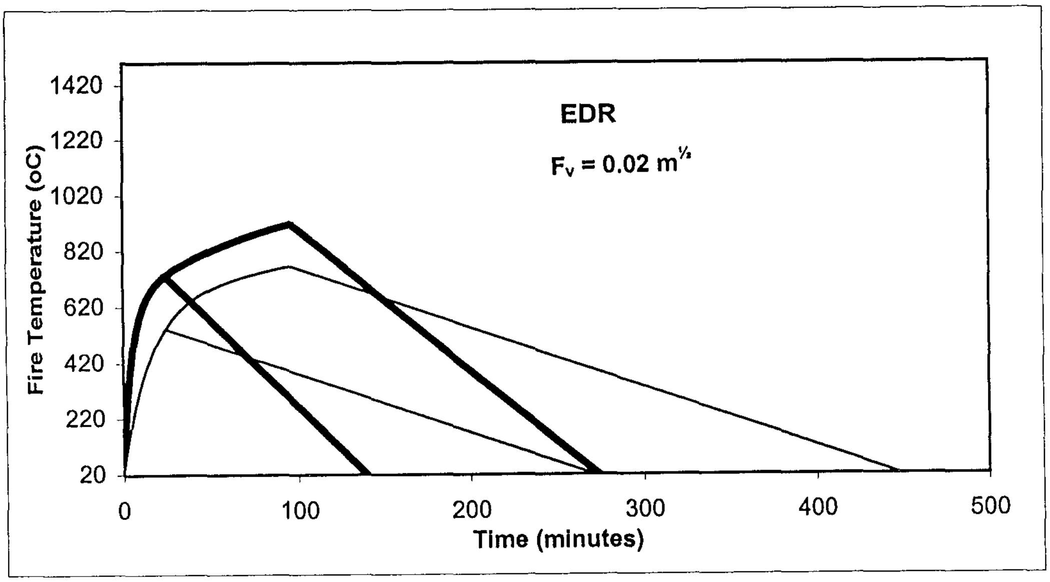

Figure 7.1(a): Eurocode parametric fire with EDR: ventilation factor, $F_v = 0.02\ m^{½}$

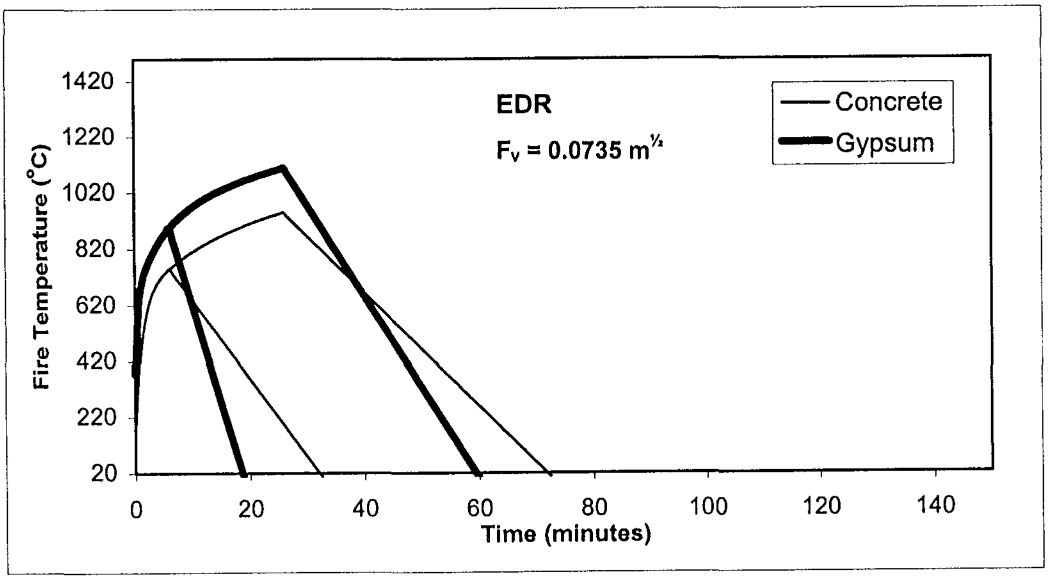

Figure 7.1(b): Eurocode parametric fire with EDR: ventilation factor, $F_v = 0.0735\ m^{½}$

Figure 7.1(a) shows the temperatures of the Eurocode parametric fire in a compartment with ventilation factor of 0.02. The thicker lines represent the temperature curves for fire in a well-insulated compartment or compartment with low thermal inertia while the thinner lines represent the fire temperatures in poorly insulated compartment. As shown in the figure, the temperature is calculated for both high and low fuel load for each case. Figure 7.1(b) shows the same information for a compartment with ventilation factor of 0.0735.

It can be seen from the figure that the decay rates are steeper for compartment with lower thermal inertia and vice versa. According to Buchanan (1999), the decay rate should be the other way around.

Therefore, Buchanan (1999) has proposed an Alternative decay rate (ADR) that has the following form:

$$dT/dt = 625\ [\ (F_v / 0.04)]\ [(k\rho c)^{½} / 1160)\ ] \qquad \text{for } t_d < 0.5 \text{ hour}$$

$$dT/dt = 250\ [\ (F_v / 0.04)]\ [(k\rho c)^{1/2} / 1160)\ ] \qquad \text{for } t_d > 2 \text{ hours}$$

and linear interpolation for the decay rate between these two fire duration. This decay rate when adapted in the plotting of the fire curves yields the results as shown in figure 7.2(a) and 7.2(b).

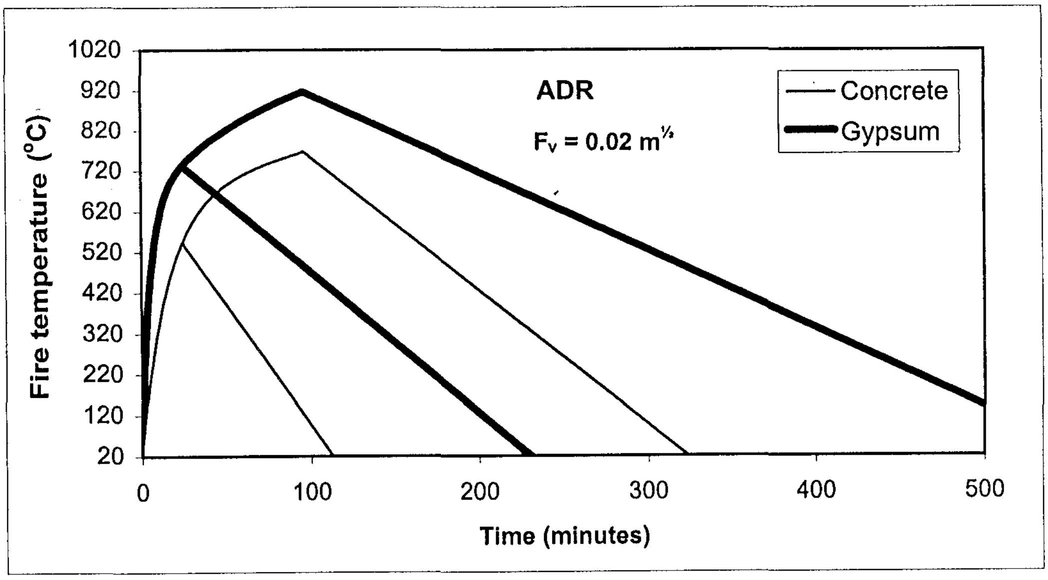

Figure 7.2(a): Eurocode parametric fire with ADR: ventilation factor, $F_v = 0.02\ m^{1/2}$

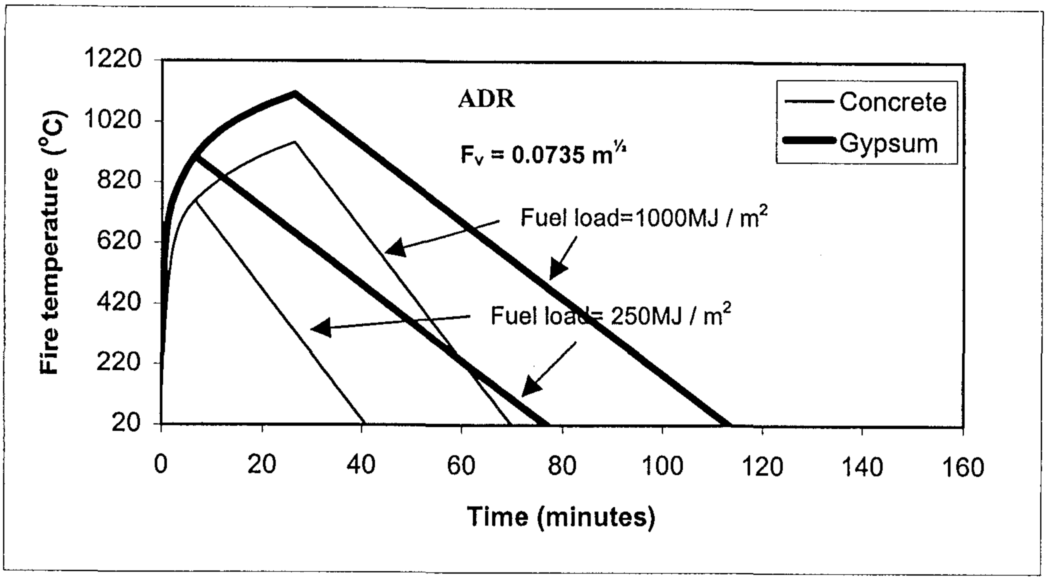

Figure 7.2(b): Eurocode parametric fire with ADR: ventilation factor, $F_v = 0.0735\ m^{1/2}$

Figure 7.2(a) and 7.2(b) show the same thing as figure 7.1(a) and 7.1(b) but for Eurocode fire using the alternative decay rate. As we can see, the decay rates are faster for poorly insulated room and vice versa, thus suggesting more logical compartment fire behaviour.

7.2 Comparison of the ADR and EDR.

The Franssen's tests discussed in chapter 4 are repeated with the spreadsheet method using the ADR. The results are compared to those obtained using EDR and shown in figures 7.3 to 7.7.

7.2.1 Floor Area

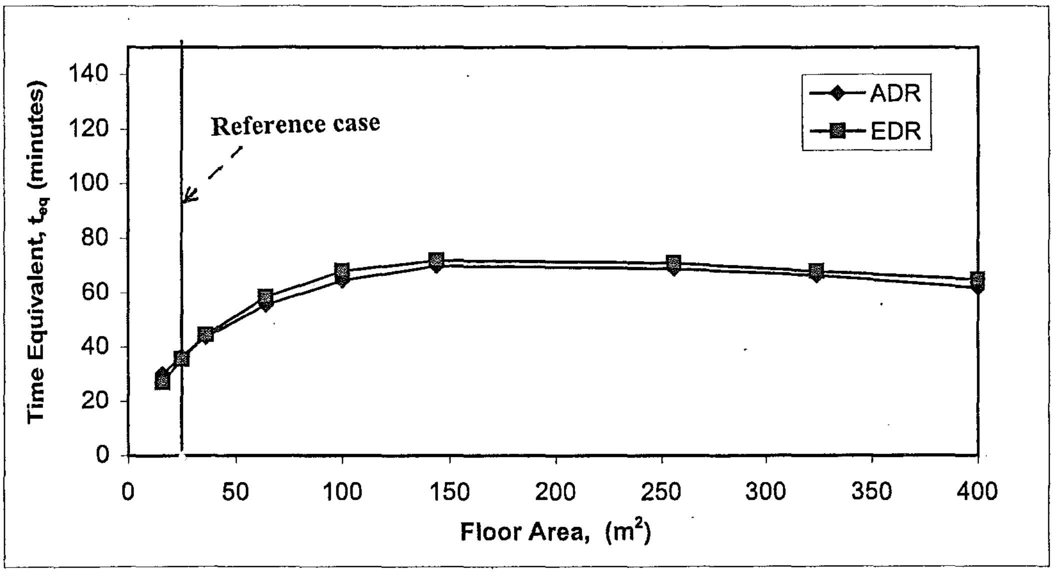

Figure 7.3: Time equivalent versus floor area: comparison of EDR and ADR

Figure 7.3 shows the variation of the time equivalent with change in floor area. It can be seen that the time equivalents calculated by the spreadsheet method using ADR are very similar to those calculated using the EDR. The average difference in the calculated time equivalents is only 2.22 minutes which is almost negligible considering the time equivalents calculated which range from 30 to 60 minutes. Both results also have an almost perfect correlation of 0.998.

7.2.2 Fuel load

Similarly, figure 7.4 shows an almost perfect agreement between the time equivalents calculated using both decay rates for different fuel load density per floor area. A correlation factor of 1.00 is found and the average difference is only 3.19 minutes for sets of data ranging from 20 to 80 minutes.

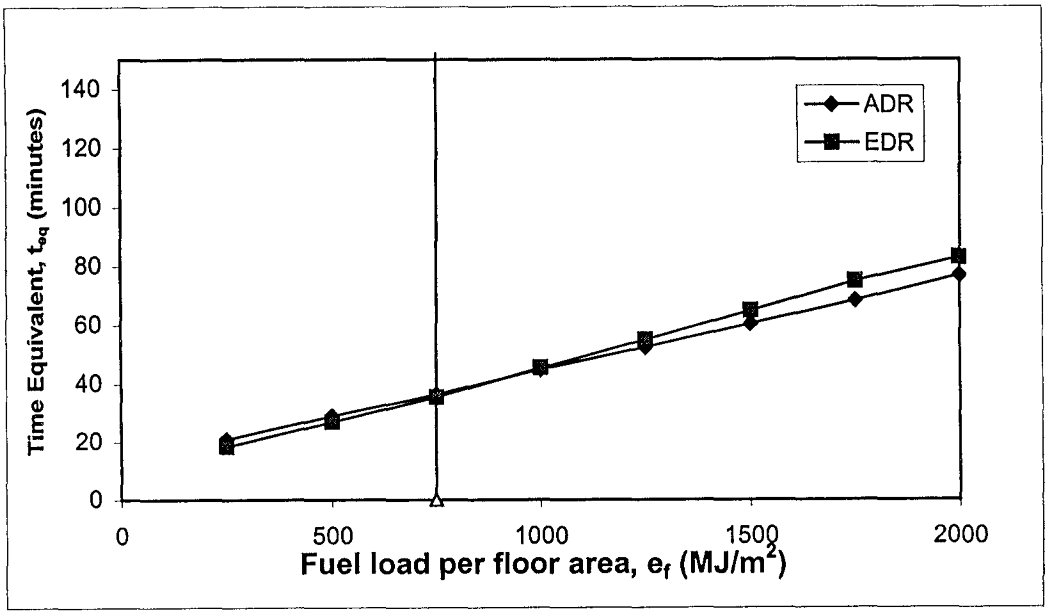

Figure 7.4: Time equivalent versus fuel load: comparison of EDR and ADR

7.2.3 Room Height

Figure 7.5(a) shows the time equivalents calculated for different room heights using both decay rates. Both sets of data do not agree with one another as well as the previous case. A correlation of only 0.72 is found. The difference between the two data however is less than a minute due to the very small change that occurs in the time equivalent with the variation in room height. A closer look at these data as shown in figure 7.5(b) reveals the poor correlation between both sets of results.

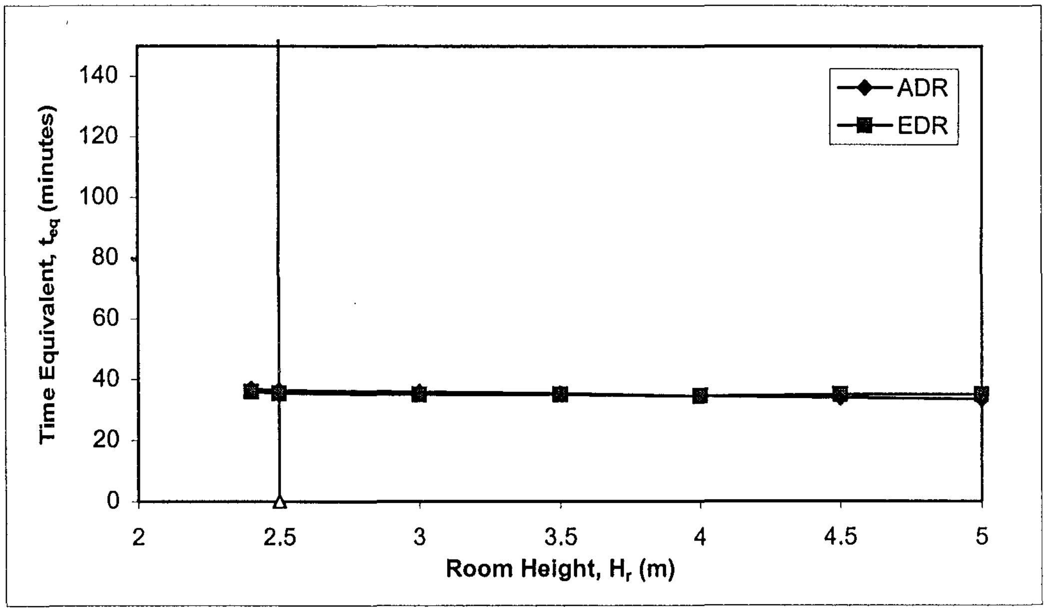

Figure 7.5(a): Time equivalent versus room height: comparison of EDR and ADR

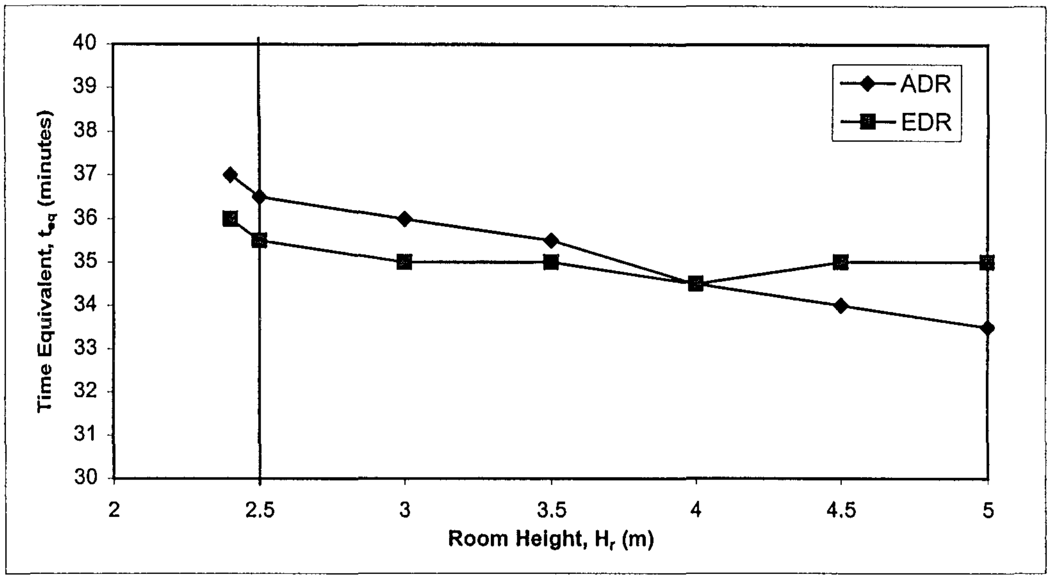

Figure 7.5(b): Time equivalent versus room height: comparison of EDR and ADR: closer study

7.2.4 Ventilation

Figure 7.6(a) and 7.6(b) show the variation of the time equivalent with the opening height and width respectively.

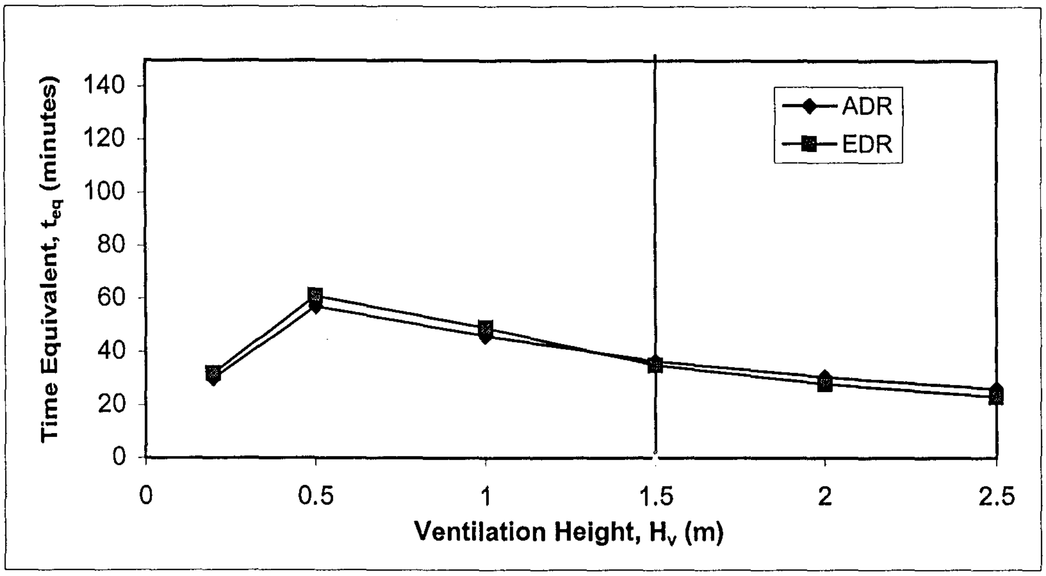

Figure 7.6(a): Time equivalent versus opening height: comparison of EDR and ADR

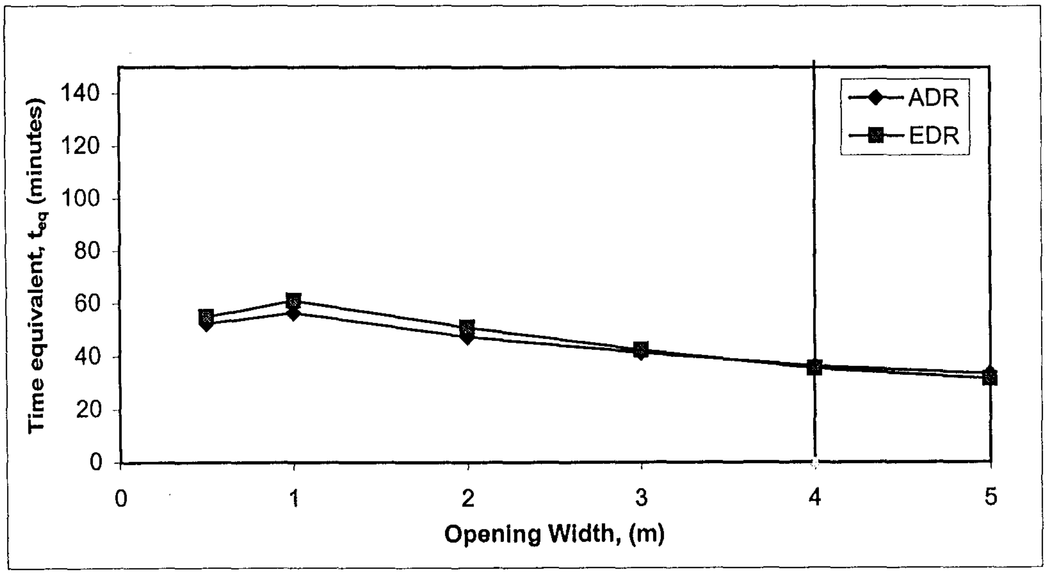

Figure 7.6(b): Time equivalent versus opening width: comparison of EDR and ADR

Again figures 7.6(a) and 7.6(b) show very similar time equivalents calculated by spreadsheet method using ADR and EDR. The correlation of the data for both cases is as high as 0.992 and 0.998. The average difference between the two decay rates in both cases is 2.67 and 2.42 minutes respectively. Compared to the magnitude of the data, which ranges from 20 to 60 minutes.

7.2.5 Thermal Inertia

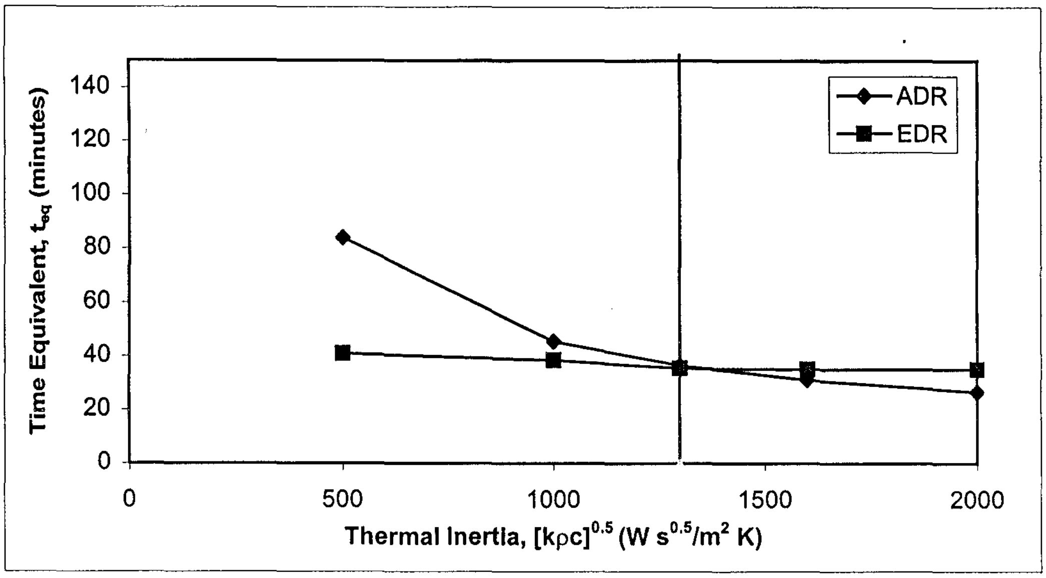

Figure 7.7: Time equivalent versus thermal inertia: comparison of EDR and ADR

Figure 7.7 shows the variation of the time equivalent with the thermal inertia of the compartment walls. Low thermal inertia value indicates a well-insulated compartment and vice versa. A thermal inertia value of 500 $J/m^2s^{½}K$ is typical for material such as gypsum plaster.

This figure best illustrate the difference between ADR and EDR. As shown in the graph, major difference in the calculated time equivalent is observed at both ends of the thermal inertia value. According to EDR results, thermal inertia has very little influence on the time equivalent. The time equivalents obtained from EDR remains relatively constant. In contrast, a significant decrease in time equivalent is observed for ADR as the thermal inertia increases.

The largest difference between both results is 43 minutes, which occurs at the thermal inertia of 500 $J/m^2\ s^{½}\ k$. A difference of 10 minutes is observed at thermal inertia of 2000 $J/m^2\ s^{½}\ k$. The difference is caused by the very different behaviour for both decay rates mentioned at the beginning of this chapter. As EDR suggests a more rapid decay rate for fire in highly insulated compartment (that is, a lower thermal properties value) and lower decay rate for poorly insulated compartment. Therefore at low thermal inertia, although the fire reaches a higher temperature, the rapid decay rate causes it to cool down so fast that the steel beam simply does not have sufficient time to get heated up to a high temperature. Whereas at high thermal inertia, the very slow decay rate causes the fire temperature to cool down much slower. Thus, giving the steel beam sufficient time to reach a temperature that is similar to that achieved in a well insulated compartment, despite the significant difference in the maximum fire temperature reached in both cases. This explains the consistency of the time equivalent obtained throughout the different thermal inertia values for EDR.

On contrary, ADR gives a slower decay rate for well-insulated compartment fire and a more rapid one for poorer insulated compartment fire. Therefore, the steel beam in a well insulated compartment (low thermal inertia value and higher maximum fire temperature) reaches a much higher temperature than that in a poorer insulated compartment, resulting in a much higher time equivalent.

7.3 Conclusion

When the thermal inertia value of an compartment lies in the region where the EDR and ADR happen to agree well with one another, such as in the region of $1000\ J\ /\ m^2\ s^{½}\ K < (k\rho c)^{½} < 1600\ J\ /\ m^2\ s^{½}\ K$, the time equivalent calculated from spreadsheet using either decay rates would be similar.

This explains the almost perfect agreement in the time equivalents calculated from both decay rates shown in figures 7.3 to 7.6 of this chapter. In all these cases, the thermal inertia used is 1300 J/m^2 s^{½} K, a value, as shown in figure 7.7 happens to be the point where the result from EDR and ADR coincide. This also implies that very small change in result would be expected if the tests of chapter 6 are repeated using the ADR since for most of the time the thermal inertia value used in the test is 1300 J/m^2 s^{½} K.

Therefore, the good agreement of the results as shown in this chapter should not be misinterpreted as the good agreement between the two decay rates. In fact, if a different thermal inertia value had been used, say 500 J/m^{2}s^{½} K, huge different in the calculated time equivalents would be expected.

8 Beyond Franssen's Study

It has been shown in chapter 4 that the spreadsheet method developed for this study is able to repeat Franssen's results. The study is followed by investigation on parameters not included in Franssen's study.

8.1 Characteristics of Beam

Cooke (1999) states that since time equivalent is a measure of the fire severity, it should be independent of the response of the member in the compartment fire. The time equivalents calculated therefore should be the same for all different structural members, regardless of the difference in their sizes.

This is true with the time equivalent formulae. The variables taken into account in the formulae only include the fuel load, ventilation factor and the thermal characteristic of the boundary walls of the compartment. Therefore, the time equivalent formulae assume all structural elements in a post-flashover fire compartment to experience the same fire severity.

However, as discussed in chapter 3, the spreadsheet method is also dependent on the characteristics of the structural element besides the physical parameters of the compartment. It is therefore, interesting to find out the difference in the calculated time equivalent caused by the variation in the characteristics of the structural element used.

8.2 Methodology

The investigation carried out in chapter 6 is repeated using two different beam sizes for the spreadsheet method and observations are made about the resultant changes. The two different beam dimensions, besides the 250UB37.3 used in chapter 5 are:

- Beam dimension

  150UB14 with $H_p/A = 280\ m^{-1}$ (small beam) and 610UB125 with $H_p/A = 116m^{-1}$ (large beam)

Apart from that, the thickness of the insulation is also changed to study the effect on the time equivalent.

- Insulation thickness, d_i (mm)

5, 15, 30

and the insulation material has the following properties: specific heat, $C_p = 850$ J/kg K; thermal conductivity, $k = 0.15$ W/m^{2}K; density, $\rho_p = 300$kg/m^3

8.3 Results and Comparison

The results obtained for the different beam sizes and insulation thickness are only plotted with the Eurocode's for comparison instead of with all three formulae. This will be enough to give us an idea of how well the other two formulae would agree with the spreadsheet method since they have already been compared to the Eurocode formula earlier on. As discussed in chapter 6, there are 19 data points in each result.

Summary of Results	**Eurocode Formula vs Spreadsheet Method**	
	Slope of Regression line through the origin	**Correlation Coefficient, R^2**
For beam 150UB14	**1.21**	**0.94**
For beam 250UB37.3	**1.14**	**0.97**
For beam 610UB125	**1.04**	**0.96**

Figures 8.1(a) to 8.1(c) are plots of the time equivalents obtained from the Eurocode formula against those from the spreadsheet method for three beam sizes as indicated. As shown by the results, all three graphs show reasonably good agreement between the spreadsheet method and the Eurocode formula. A correlation factor of more than 0.9 exists in all three cases.

In coherent to the result obtained in chapter 6, the Eurocode formula is found to be more conservative in estimating the time equivalent. Calculation of time equivalents using bigger beam yields better agreement between the spreadsheet method and Eurocode formula. It also implies that the type of beam chosen affects the spreadsheet method; the bigger the beam size is the longer the calculated time equivalent tends to be. To further investigate this, the calculated time equivalents for each beam type have been plotted against one another in figures 8.2(a) to 8.2(c).

8.3.1 Beam Sizes

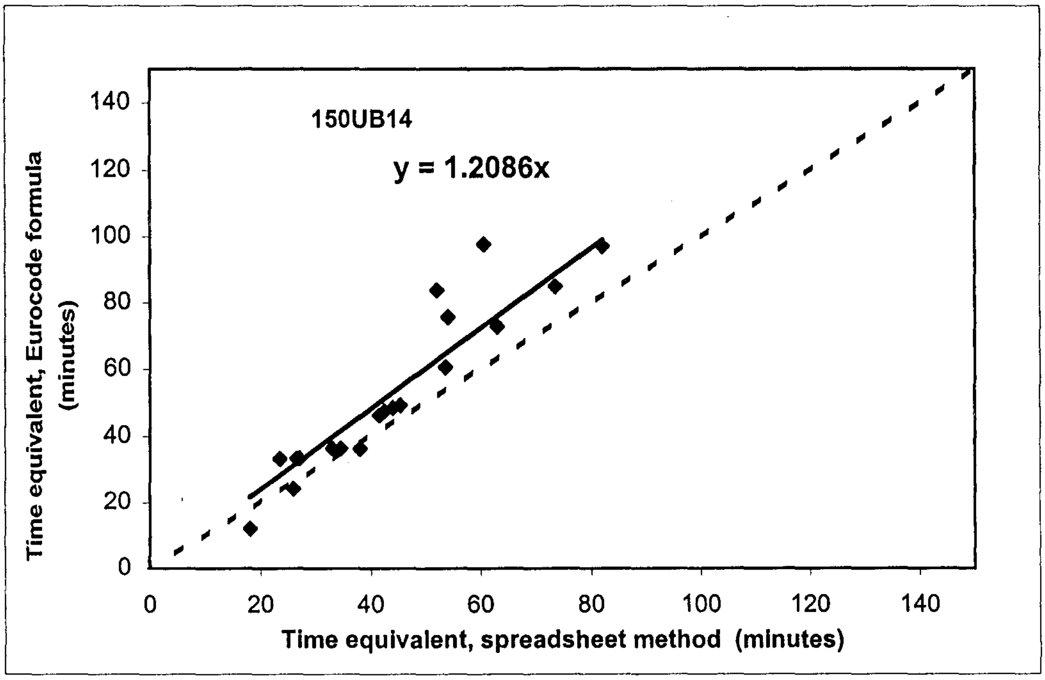

Figure 8.1(a): Comparison between Eurocode formula and spreadsheet method for 150UB14

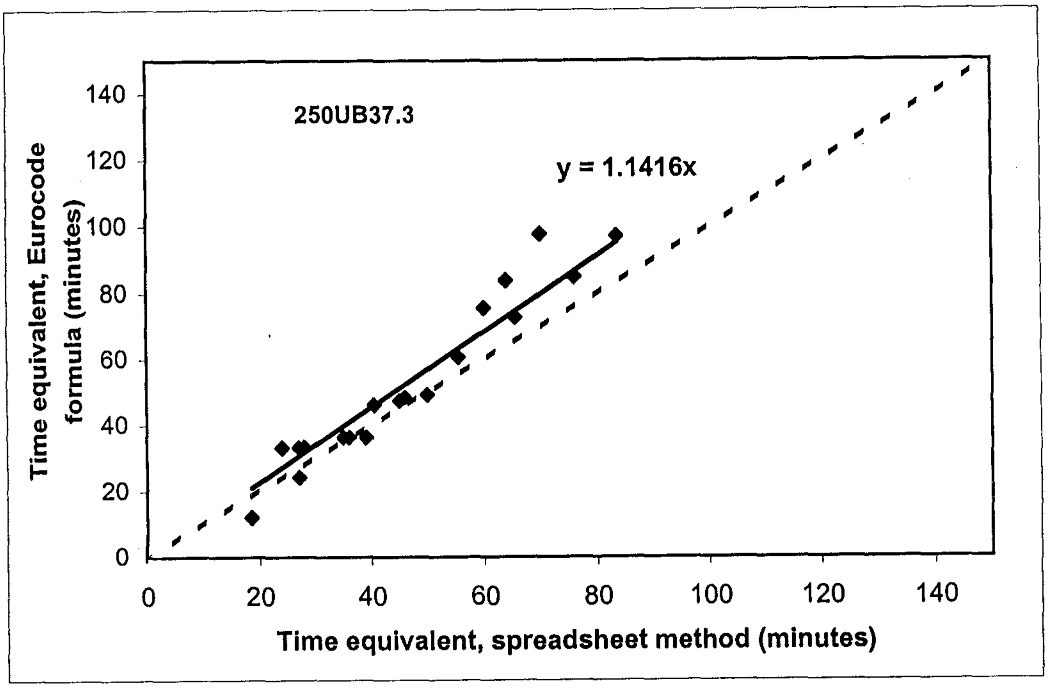

Figure 8.1(b): Comparison between Eurocode formula and spreadsheet method for 250UB37.3

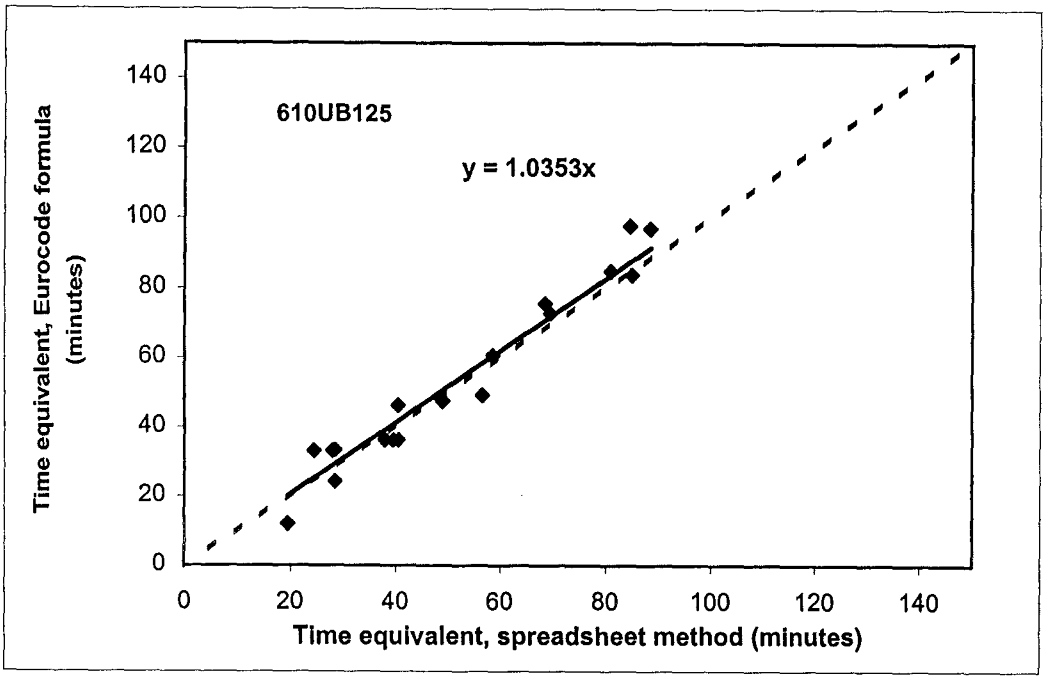

Figure 8.1(c): Comparison between Eurocode formula and spreadsheet method for 610UB125

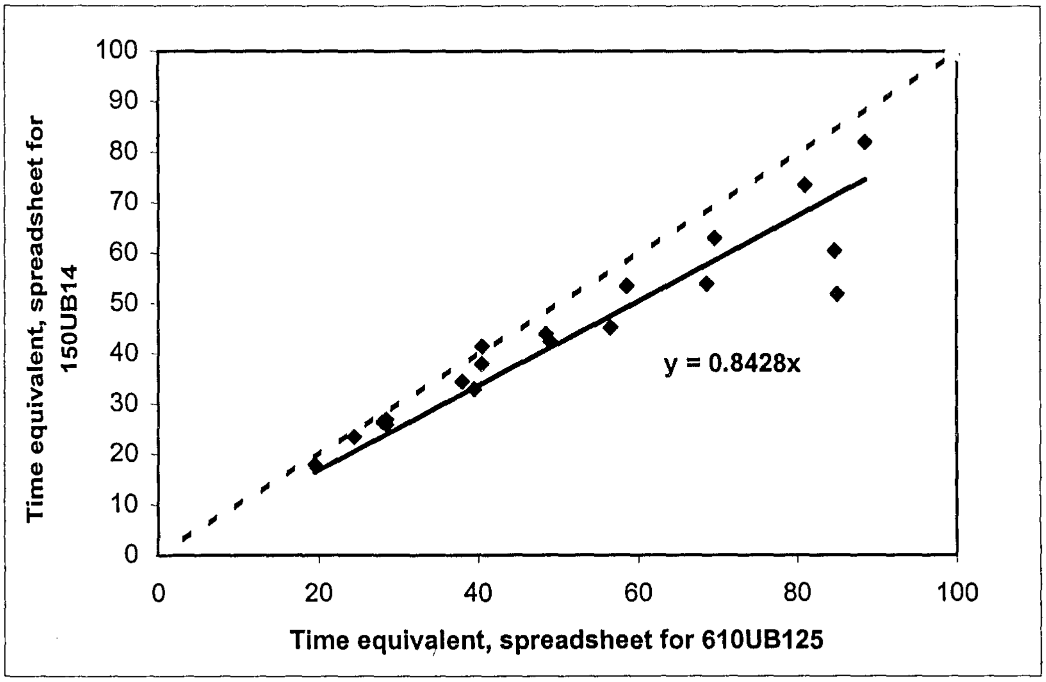

Figure 8.2(a): Comparison between 150UB14 and 610UB125

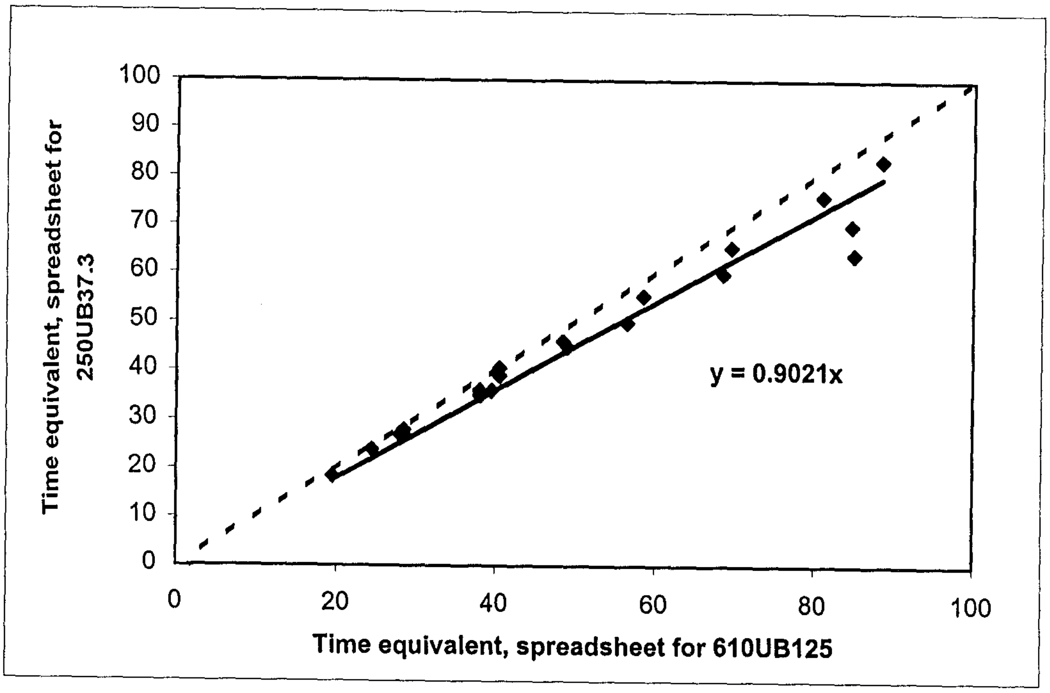

Figure 8.2 (b): Comparison between 250UB37.3 and 610UB125

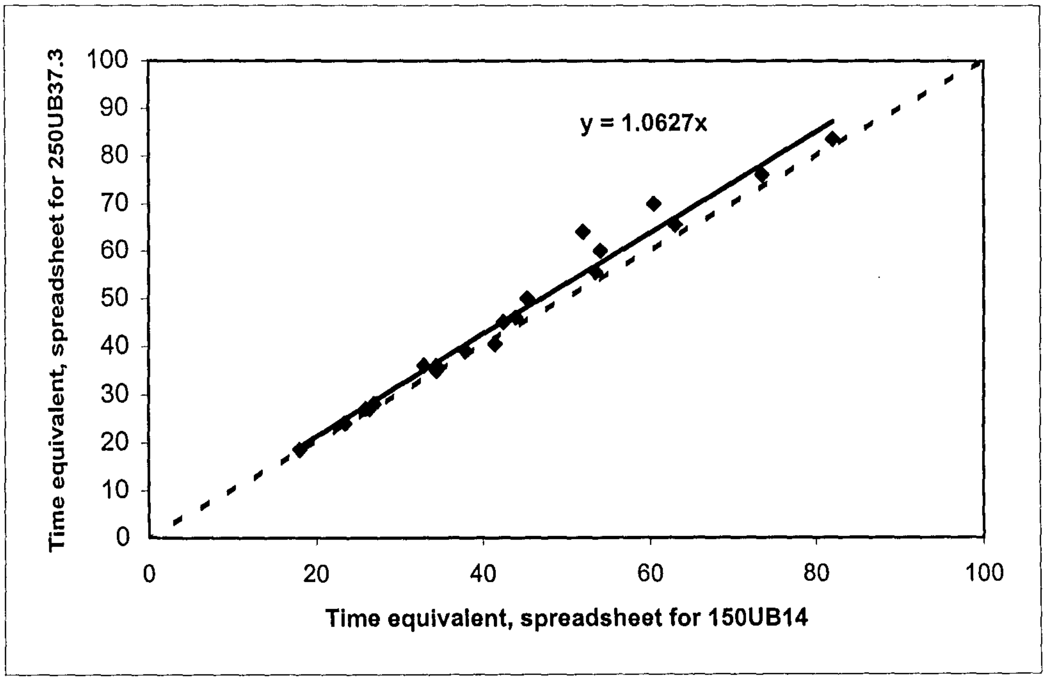

Figure 8.2 (c): Comparison between 250UB37.3 and 150UB14

Summary of Results	Spreadsheet Method	
	Slope of Regression line through origin	Correlation Coefficient, R^2
150UB14 vs 610UB125	0.84	0.94
250UB37.3 vs 610UB125	0.90	0.98
250UB37.3 vs 150UB14	1.06	0.98

Plotting the time equivalents for these three beam sizes together in figures 8.2(a) to 8.2(c) shows a relatively good agreement of the three data.

As shown by the result, the slope of regression of the graph for the extreme case, which is the comparison between the smallest, 150UB14 and the biggest beam, 610UB125 is as high as 0.843, which is reasonably close. This implies a little difference in the calculated time equivalent by the spreadsheet method caused by the different beam sizes used. In general, when the calculation of time equivalents is made for bigger beams, the time equivalents calculated by the spreadsheet method tend to be longer.

8.3.2 Different Insulation Thickness

Figures 8.3(a) to 8.3(c) are plots of the time equivalents from the spreadsheet method against those from Eurocode formula for the three insulation thicknesses.

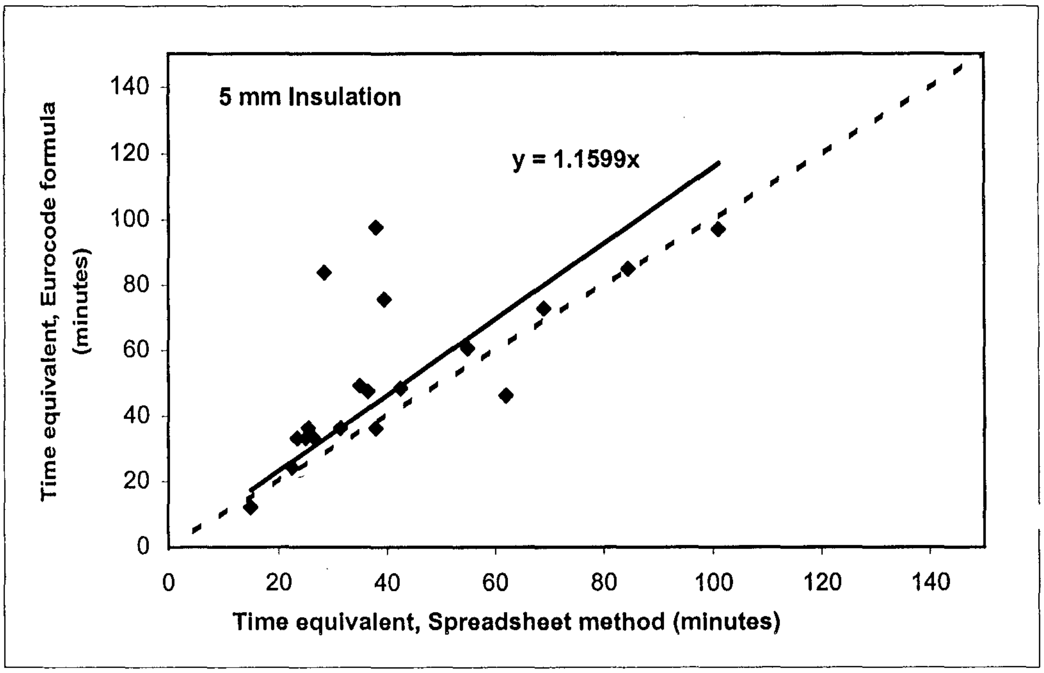

Figure 8.3(a): Comparison Eurocode formula and spreadsheet method: Insulation 5 mm

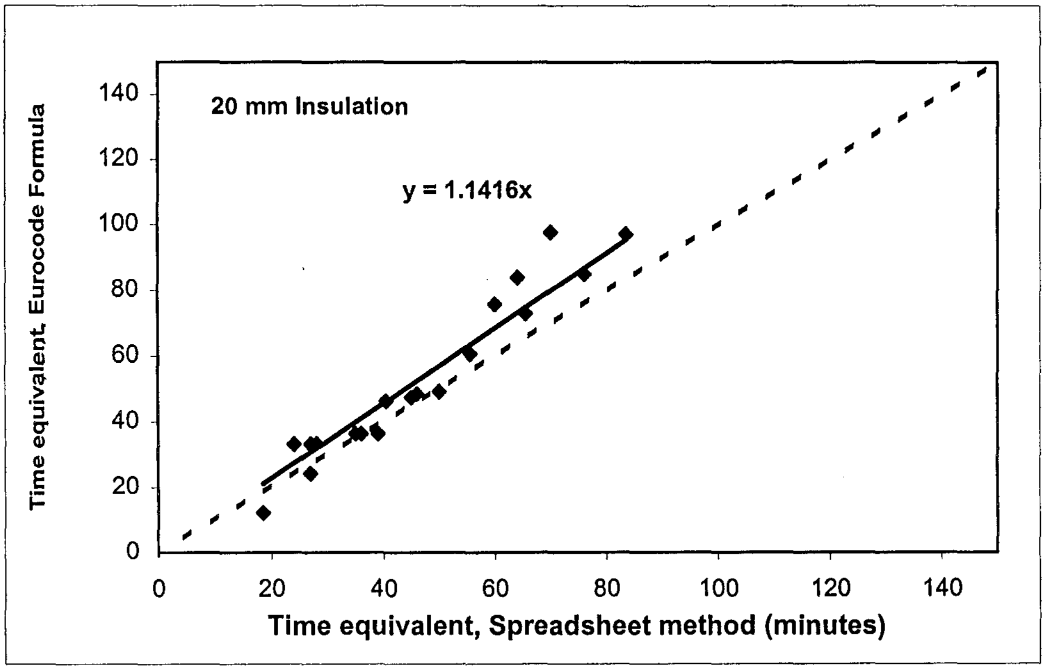

Figure 8.3(b): Comparison Eurocode formula and spreadsheet method: Insulation 20 mm

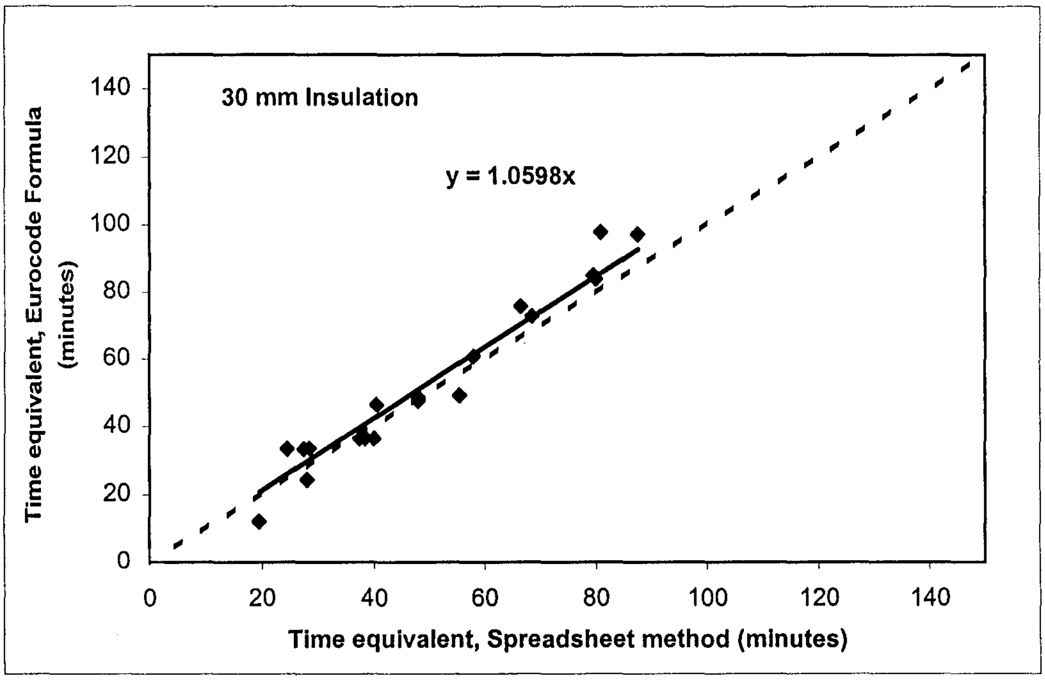

Figure 8.3(c): Comparison Eurocode formula and spreadsheet method: Insulation 30 mm

Summary of Results	Eurocode Formula vs Spreadsheet Method	
	Slope of Regression line through the origin	Correlation Coefficient, R^2
Insulation thickness 5 mm	1.16	0.70
Insulation 20 mm	1.14	0.97
Insulation 30 mm	1.06	0.98

The result shows that for thick insulation, the spreadsheet method tends to agree very well with the Eurocode formula. In fact as shown in the graphs, at insulation thickness of 30mm, both sets of data almost agree perfectly with one another with a slope of regression line of 1.06 and correlation factor of 0.98. In general, the slope of regression line and the correlation factor decreases as the insulation thickness decreases indicating that the time equivalents calculated by the spreadsheet method tend to be longer as the insulation gets thicker.

8.4 Conclusions

Theoretically, the fire severity of a compartment should be independent of the characteristics of element, that all elements in a post-flashover fire compartment should experience the same fire severity. However, it has been shown in this chapter that, the characteristics of the beam used do affect the time equivalent calculated by the spreadsheet method by certain degree. If the calculations are made for bigger beams or thicker insulation, the time equivalents tend to be longer and agree better with the Eurocode formula.

9 Evaluation of the k_c and k_b factors in Time Equivalent Formulae

9.1 Introduction

As discussed previously, besides fuel density and ventilation, another important factor in affecting the temperature profile of compartment fire is the thermal inertia of the boundary walls.

The Eurocode and CIB formulae each uses k_b and k_c factors to adjust for the different compartment lining used. The suggested k values to be used by formulae according to the compartment thermal inertia value, $(k\rho c)^{1/2}$ are as shown previously in table 1.1, extracted from the Structural Design for Fire (Buchanan 1999). The approved documents to New Zealand building code (BIA 1992), which uses Eurocode suggests a "general" k_b factor of 0.067 to be used in design calculations for compartment with unknown materials.

As expected, well insulated compartments or compartments with low $(k\rho c)^{1/2}$ are assigned a higher k factor compared to the poorly insulated compartment (high $(k\rho c)^{1/2}$ value). This is so since less heat is lost through conduction fire in a well-insulated compartment, thus resulting a higher maximum fire temperature and a higher time equivalent.

However, how well do these suggested k values conform to the real compartment fire situation is questionable. Therefore, the spreadsheet method, which has been confirmed in an earlier chapter to be an accurate way of simulating a compartment fire and calculate its resulting fire severity, is used here to revise these k factors.

9.2 Methodology

Equation 1.1 and 1.2 are the Eurocode and CIB time equivalent formulae discussed previously in chapter 1 and used to calculate time equivalent for various fire scenarios in chapter 5. Now, instead of calculating the time equivalent, those formulae are rearranged to calculate the 'ideal' k values that would give the exact same time equivalent as that calculated by the spreadsheet method. The rearrangement of these formulae are as shown below.

$$k_c = t_{eq} / w\, e_f \text{ (CIB)} \quad .....(9.1)$$

$$k_b = t_{eq} / w\, e_f \text{ (Eurocode)} \quad .....(9.2)$$

Where t_{eq} is the equivalent time calculated by the spreadsheet method for certain opening factor w and fuel load per floor area, e_f (MJ/m^2).

The 'ideal' k_c and k_b calculated by the formulae above are therefore the values that would give a formula-calculated time equivalent exactly the same as the spreadsheet-method-calculated time equivalent. The ideal k values are calculated for the following parameters:

- Floor area = 25m^2
- Height of compartment = 2.5m
- Ventilation = 1.5m (height) x 4m (width)
- Steel beam = 250UB37.3; density of steel, ρ_s = 7850 kg/m^3
- Insulation = 20mm; density, ρ_i = 300 kg/m^3; specific heat, c_i = 850 J/kgK; thermal conductivity, k =0.15 W/mK
- Fire = Eurocode parametric fire curve

For the following range of thermal inertia, $[k\rho c]^{1/2}$:

500, 720, 1000, 1160, 1500, 2000, 2500, 2800, 3000 Ws$^{1/2}$/m^{2}K

and fuel load per floor area, e_f (MJ/m^2):

500, 750 and 1000

The Alternative decay rate (ADR) has been introduced in chapter 7. Although the Eurocode decay rate (EDR) has been accepted in the approved document, Eurocode 1 part 2-2, and is widely used, the ADR is considered in this report to be a more reasonable decay rate. As mentioned before, it suggests a slower fire decay rate for a well-insulated fire compartment and a more rapid one for poorly insulated compartment, instead of the other way around, as suggested by the Eurocode Decay Rate. Therefore, the investigation of the k_b and k_c values is made using both decay rates.

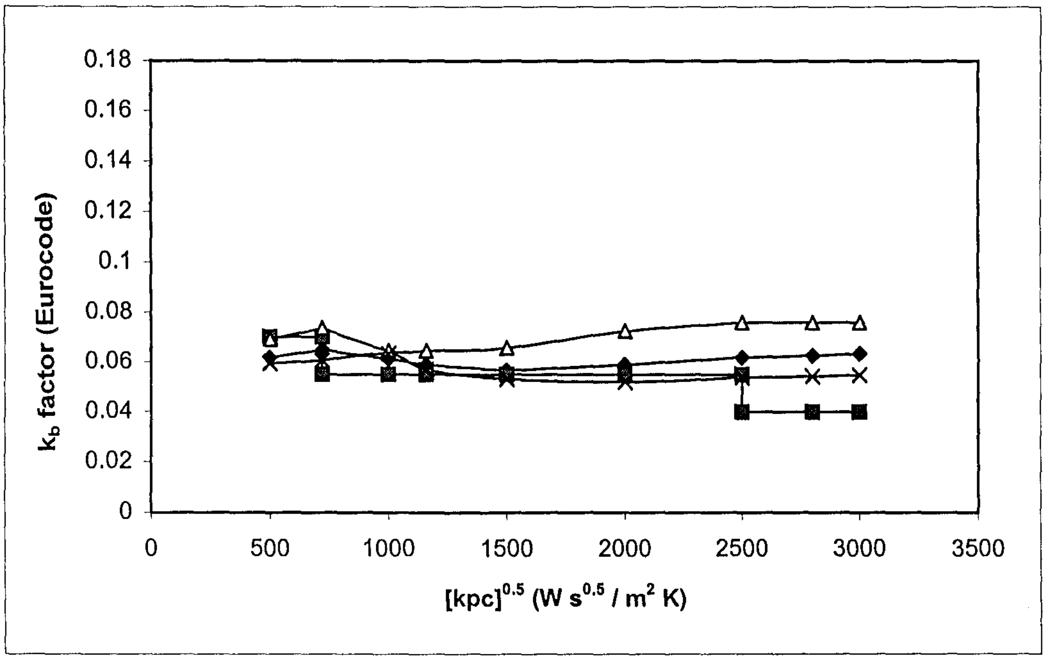

Figure 9.1: Ideal k_b values: EDR

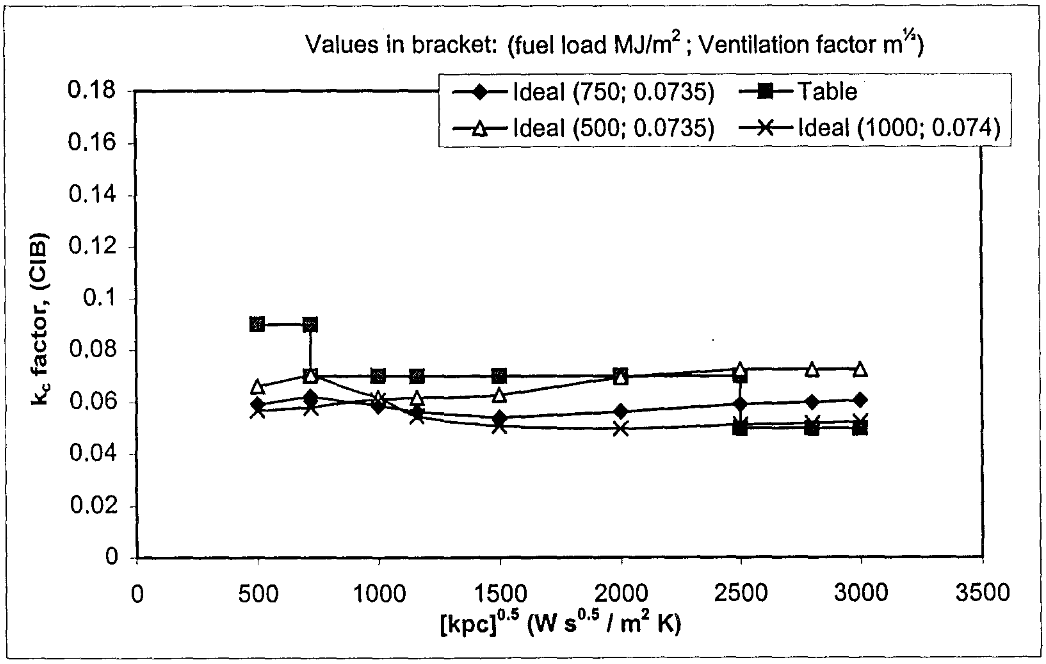

Figure 9.2: Ideal k_c values: EDR

9.3 Results and Comparison : EDR

The 'ideal' k_b and k_c values for different fuel load are plotted in figure 9.1 and figure 9.2 together with the values from the table for comparison:

Figure 9.1 and 9.2 show the 'ideal' k_b and k_c values calculated from equation 9.1 and 9.2 for various combinations of thermal inertia and fuel, plotted together with the standard values from table 1.1 of chapter 1. It can be seen that the ideal values calculated are different for different fuel load density while the standard values from table are independent of the fuel load. In general, the ideal values are smaller for higher fuel load and they have relatively similar values at both ends of the thermal inertia range but slightly lower values in the middle.

The graph shows a good agreement between the ideal and standard k_b and k_c values in certain regions but significant difference in another. For example, at thermal inertia of 1300 $Ws^{½}/m^2K$, the ideal k_b calculated for fuel load of 750 MJ/m^2 coincides with the standard k_b but for the same thermal inertia, the ideal k_b calculated for fuel load of 500 MJ/m^2 is significantly different from the standard one.

The ideal k_b value generally decreases as the fuel load increases, therefore it agrees better with the table value in the low thermal inertia region at low fuel load, in the intermediate region at intermediate fuel load and high thermal inertia region at high fuel load. This implies that Eurocode formula would give close results to the spreadsheet method when the thermal inertia and fuel load conform to above conditions and poor results when they do not.

As for the CIB formula, the ideal k_c is significantly different from the standard values. As shown in the figure 9.2, the calculated ideal values are generally far lower than those from the table. Except for the higher fuel load in the high-thermal inertia region, the ideal and table k_c values are almost totally different from each other. The difference is especially bigger for higher fuel load.

Thus, we would expect a major difference between the time equivalents calculated by the spreadsheet method and the CIB formula. In fact, this is already clearly shown by figure 6.4 of chapter 6 where the comparison between the CIB time equivalent formulae and the spreadsheet method yields a regression line of 1.46. This means that the CIB overestimates the time equivalent by 46% most of the time compared to the spreadsheet method while according to figure 6.3, Eurocode formula only overestimates the time equivalent by 14%.

9.4 Results and Comparison : ADR

The investigation is repeated using spreadsheet method with the Alternative decay rate (ADR). The 'ideal' k_b and k_c values for different fuel load are plotted in figure 9.3 and 9.4 together with the values from the table for comparison:

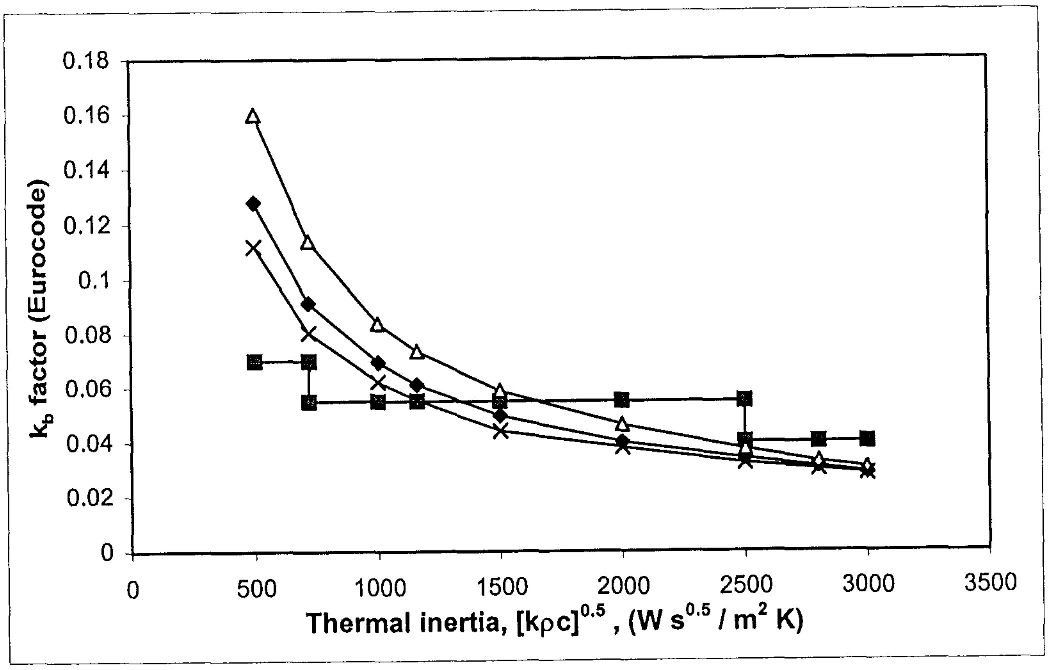

Figure 9.3: Ideal k_b values: ADR

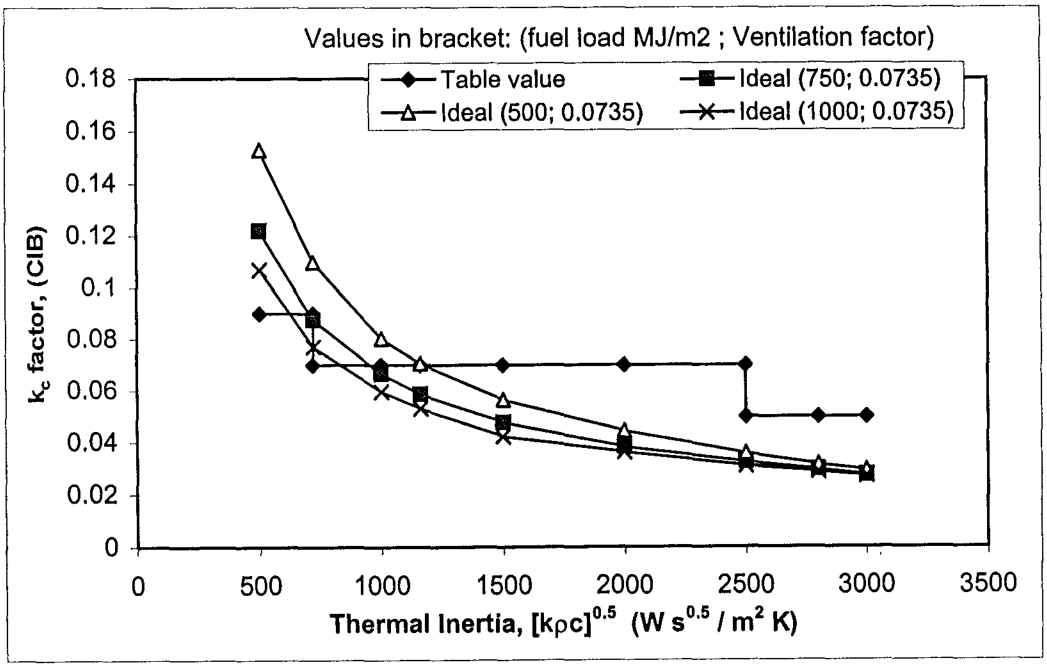

Figure 9.4: Ideal k_c values: ADR

Both figures 9.3 and 9.4 show that the ideal values calculated by spreadsheet method using the ADR follow a more similar trend as the values from the table. As shown by the diagram, both methods predict k_b and k_c values that decrease with the thermal inertia. However, the difference between the ideal values and the standard ones are significant for certain combination of fuel load and thermal inertia. For example, as shown in figure 9.3, a difference of more than 120% is found at thermal inertia of 500 $Ws^{½}/m^2K$ for fuel load of $500MJ/m^2$. For the combination of fuel load and thermal inertia in such case, we would expect to see a huge difference in the time equivalent calculated from the spreadsheet methods and Eurocode formula.

Apart from that, it can be observed from the figures that in contrary to the EDR, ADR predicts a much more dramatic change in k values with variation in thermal inertia. This is in coherent with the result shown by figure 7.7 of chapter 7. Also the difference in the k_b and k_c values for different fuel load calculated by ADR tend to be less compared to EDR.

9.5 Conclusion

In general, the k_b and k_c values from table do not agree well with the calculated ideal ones using either decay rate. The ideal values vary with the fuel density while the standard values from the table are independent of the fuel load. Both values tend to agree better for certain combination of fuel load and thermal inertia value than others.

If the calculation of time equivalents is done for such combination of fuel load and thermal inertia, good agreement between the spreadsheet method and time equivalent formula will be expected and vice versa. In general, the difference between the ideal and the standard k_c is larger most of the time compared to k_b.

The ideal k_b and k_c values calculated by spreadsheet using EDR are very different from that using ADR. While EDR gives k values that vary less than 20% with a 600% increase in thermal inertia values, ADR calculates k values that change dramatically up to 400% for the same range of thermal inertia values.

As the time equivalent formulae are empirical, based on experimental data produced from the exposure of certain protected steel beams to fire in compartment with certain geometry set up, their validity in the region beyond which the experimental data are produced are questionable. In fact, according to Buchanan (Buchanan, 1999) the derivation of both formulae are not well documented, thus the limitations of them are not known. It is therefore, more accurate to use the engineering calculation, that is, the spreadsheet method in the calculation of the time equivalent.

However, as the formulae have already been widely used in design calculations, it is therefore also desirable to improve their accuracy. One way of achieving this, is of course by modifying the standard values in the table. For example the standard k_b value in figure 9.3 should be significantly increased for the low thermal inertia region.

As the EDR and ADR each suggests different k_b and k_c behaviour with relative to the thermal inertia, more work would have to be done before deciding which decay rate should be used in the spreadsheet method for revising the k_b and k_c values.

10 Heat Transfer in Reinforced Concrete

10.1 Introduction

Reinforced concrete is heavily used in today's construction. It is recognised for its good fire resistance due to its low thermal conductivity and non-combustibility. Heat cannot penetrate easily through concrete, thus the reinforcement or the steel bars inside are protected during a fire. Therefore, concrete structures do not fail easily when exposed to fire.

As the time equivalent formulae are independent of the characteristics of the structural element, they assume that all members in a complete burnout fire experience the same fire severity or have same time equivalent. However, as the time equivalent formulae are based on experimental data obtained from the exposure of protected steel beam to fires, the applicability of them to concrete is questionable. An investigation is therefore carried out in this report to study how well do the time equivalent formulae estimate the fire severity for reinforced concrete structures.

In order to carry out this investigation, a one-dimensional finite element model for heat transfer has been developed on computer for this report. This model is able to simulate the exposure of a reinforced concrete member to fires and calculate the temperature of the reinforcement that is placed at certain depth below the concrete surface. By calculating the temperatures of the reinforcement exposed to the standard ISO 834 fire and parametric fire using this heat transfer model, one can determine the time equivalent for reinforced concrete structures, as explained in chapter 1. This model is then used to verify the validity of Eurocode time equivalent formula for a reinforced concrete structure in chapter 11.

10.2 One-dimensional Heat Transfer Model

The one-dimensional finite element model for heat transfer developed in this chapter follows the method described by Tucker (1998). According to the method, an element is divided into sections of equal thickness, Δx (m) with a node in the center. A finite difference representation of the Laplace's equation is then derived for each node:

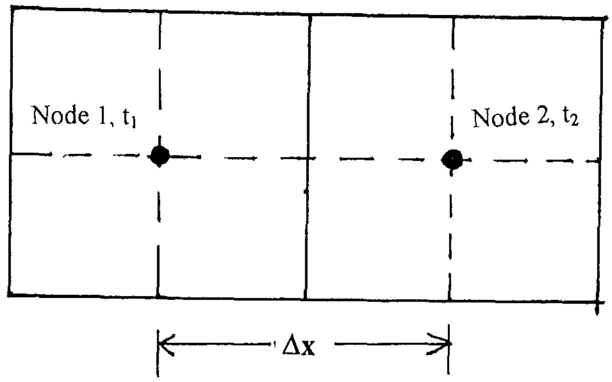

Figure 10.1: Division of an element into two sections of equal thickness: finite element method

Figure 10.1 shows a sample of element that has been divided into two sections of equal thickness. The temperature gradient half way between node 1 and 2 can be derived from the Laplace's equation as:

$$(\delta t / \delta x)_{1\sim2} \simeq (t_2 - t_1)/ \Delta x$$

where t and x are the temperature and thickness of the section respectively and δt, δx , Δx represent the small changes in those parameters.

10.2.1 Formulae Involved

Figure 10.2 illustrates the one-dimensional transfer of heat from one node to the next in an element. This transfer of heat is driven by the temperature difference between those two nodes, which in this report, is caused by exposure to fire. Formulae are used to calculate the heat flow into an element by the conduction or heat loss through convection at the surface. The formulae involved are:

a) Rate of heat conduction in and out of node

$= k\, A\, \Delta t / \Delta x$

where k = thermal conductivity (w/ m ^{o}C)
A = cross section area of the element respectively (m^2).
Δt = difference in temperature across two nodes (^{o}C)
and Δx = thickness between two nodes (m).

b) Rate of change of internal energy in node

$= \rho\ C_p\, A\, \Delta x\, \Delta t / \Delta \tau$

where ρ = density (kg/m^3)
C_p = specific heat of concrete (J/kg°C).
and $\Delta\tau$ = time step (s)

c) Rate of convection

$= h\, A\, (ts - t_\omega)$

where h = convective coefficient
t_s = steel temperature (°C)
t_ω = ambient temperature (°C)

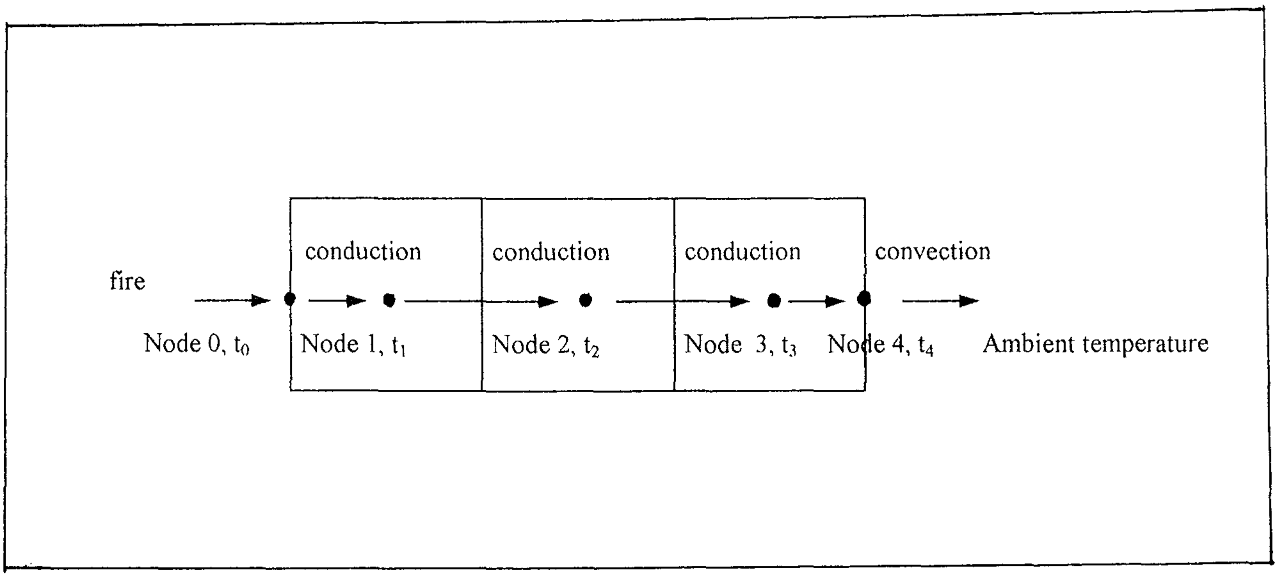

Figure 10.2: Illustration of one-dimensional heat transfer through an element

10.2.2 Setup of Model

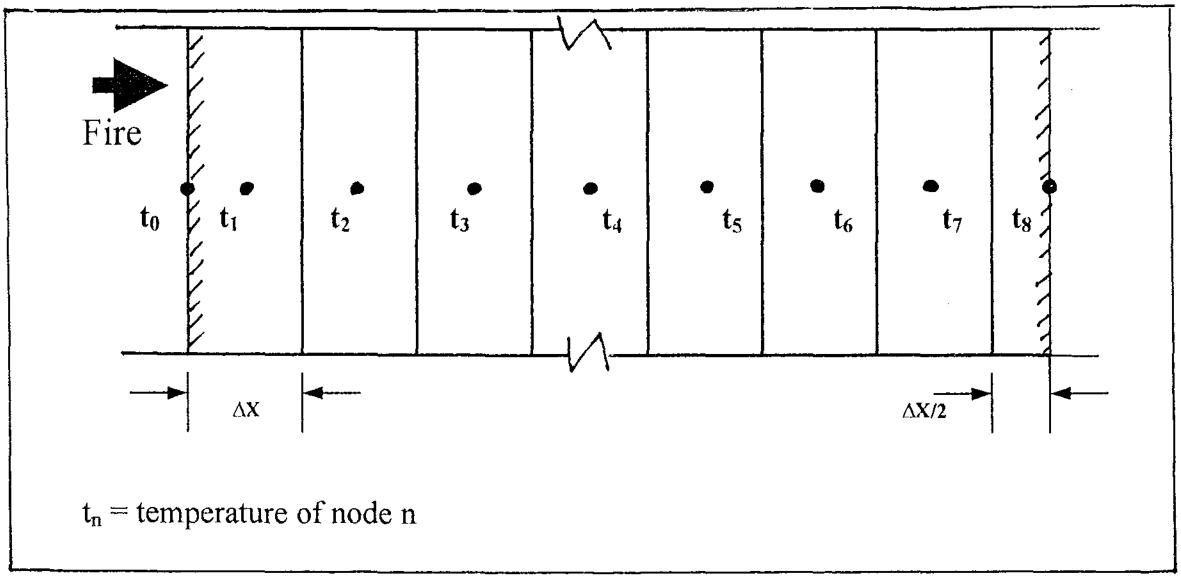

Figure 10.3: Division of element into 8 sections: finite element model

The concrete slab considered in this study is divided into 8 strips of section with a thickness of Δx (m) except for the last strip which thickness is only Δx / 2. A node namely node 0 to 8 is placed in the center of each strip, as shown in figure 10.3

For node 1 to 7, the heat balance equation is :

Rate of heat conduction into node	-	*Rate of heat conduction out of node*	=	*Rate of change of internal energy in node*

$$(k A \delta t / \delta x)_{n \sim n+1} - (k A \delta t / \delta x)_{n+1 \sim n+2} = 1/\alpha\ \delta E / \delta\tau$$

$$\Rightarrow k A (t^{P}_{n} - t^{P}_{n+1}) / \Delta x - k A (t^{P}_{n+1} - t^{P}_{n+2}) / \Delta x = \rho A \Delta x C_p (t^{P+1}_{n+1} - t^{P}_{n+1}) / \Delta\tau$$

where $\alpha = k / \rho C_p$

and
- k = thermal conductivity (w /m °C);
- ρ =density (kg / m^3)
- C_p =Specific heat (J / kg °C),
- δE = change in internal energy (J)
- $\delta\tau$ = change in time (seconds)
- P = time step , $0 < P <$ infinity
- n = number of the node , $0 < n < 7$ for figure 10.3
- t^{P+1}_{n+1}= temperature of node n+1 (node being calculated) (°C)
- t^{P}_{n+1}= previous temperature of node being calculated (°C)
- t^{P}_{n} = previous temperature of the node n (°C)
- t^{P}_{n+2} = previous temperature of node n+2 (°C)

By further rearrangement, the temperature for node 1 can be calculated using equation 10.1:

$$\mathbf{t^{P+1}_{1} = \Delta\tau / (\rho A \Delta x C_p) [k A / (\Delta x/2) (t^{P}_{0} - t^{P}_{1} - 2t^{P}_{1} + 2t^{P}_{2})] + t^{P}_{1}} \quad \ldots(10.1)$$

where t^{P}_{0} is the node exposed directly to fire and assumed to have the same temperature as the fire.

The temperature for node 2 to node 7 can be calculated using equation 10.2:

$$\mathbf{t^{P+1}_{n+1} = \Delta\tau / (\rho A \Delta x C_p) [k A / \Delta x (t^{P}_{n} - t^{P}_{n+1} - t^{P}_{n+1} + t^{P}_{n+2})] + t^{P}_{n+1}} \quad \ldots(10.2)$$

The difference between both formulae is due to the fact that the distance between node 0 and node 1 is only $\Delta x/2$ while the distance between any other two successive nodes is Δx.

The following example illustrates how the formula is used. Let's say the time step, $\Delta\tau$ = 30seconds. In order to calculate the temperature of node 1 (ie. n = 0) after 60 seconds (ie. P = 2 or 60 seconds/$\Delta\tau$) of exposure to fire, which temperature is 300°C, equation (10.1) would be written as:

$t^2_1 = \Delta\tau / (\rho\ A\ \Delta x\ C_p)\ [\ k\ A / (\Delta x/2)\ (300°C - t^1_1 - 2\ t^1_1 - 2t^1_2\ )] + t^1_1$

where node 0 which is directly exposed to fire is assumed to have the exact temperature as the fire calculated from previous time step.

As for node 8, which is exposed to the ambient temperature, the heat balance is :

Rate of heat Conduction Into node	-	*Rate of heat Convection out of node*	=	*Rate of change of internal energy in node*

$$\Rightarrow k\ A\ (t^p_7 - t^p_8\ ) / \Delta x - h\ A\ (\ t^p_8 - t_\omega) = \rho\ Cp\ A\ \Delta x / 2\ \ (t^{p+1}_8 - t^p_8) / \Delta\tau$$

$$\Rightarrow \mathbf{t^{p+1}_8 = \Delta\tau / (\rho\ A\ (\Delta x / 2)\ C_p)\ [k\ A\ (t^p_7 - t^p_8)/\Delta x - hA\ (\ t^p_8 - t_\omega)] + t^p_8} \ldots\mathbf{(10.3)}$$

where t_ω = ambient temperature (20 °C)

10.2.3 Stability Check of the Model

For finite element model, the time step $\Delta\tau$ used must not exceed the limit given by equation 10.4 in order to be numerically stable.

$$\Delta\tau \leq (\Delta x)^2 / \alpha\ [\ 2(\ 1 + h\ \Delta x / k)]\ \ \ldots\mathbf{(10.4)}$$

where $\alpha = k / \rho\ C_p$

10.2.4 Layout of Finite Element Model

Figure 10.4 is a sample of how the finite element model can be set up in order to link all the heat transfer equations 10.1 to 10.3. By entering the fire equation, which refers to the type of fire the element is exposed to, the spreadsheet will calculate the corresponding temperature rise in the element at various depth below the fire-exposed surface.

It can be seen that in the particular case shown in figure 10.4, an element with a thickness of 300 mm has been divided into eight strips and exposed to the standard fire ISO 834. As mentioned and shown in figure 10.3 before, the distance between node 0 and node 1 is only half of that between any other two successive nodes. Note that the variation of temperature occurs earlier for node nearer to the surface of exposure to fire. It can be seen that for node 7 and 8, no change in temperature has yet occur as these two nodes are located furthest away from the surface of exposure. Also note that the temperature of node 0 has been assumed to be the same as the fire's.

	Nodes :	0	1	2	3	4	....	7	8
	Distance (mm) =	0	20	60	100	140	....	260	300
Time		Directly exposed							
(minutes)	**ISO 834 Fire Curve**	to fire							
0.0	261.1446515	261.1447	20	20	20	20	....	20	20
1.0	404.3104565	404.3105	32.58146	20	20	20		20	20
2.0	476.1656567	476.1657	51.6478	20.32821	20	20	....	20	20
3.0	524.5273093	524.5273	72.97953	21.13668	20.00856	20		20	20
4.0	561.0295948	561.0296	95.18612	22.45968	20.03777	20.00022	....	20	20
5.0	590.3583173	590.3583	117.5938	24.29371	20.09997	20.0012		20	20
6.0	614.875175	614.8752	139.8258	26.61822	20.20679	20.00374		20	20
7.0	635.9387931	635.9388	161.6578	29.40421	20.36875	20.00894		20	20
8.0	654.4029363	654.4029	182.9528	32.61859	20.59507	20.0181		20	20
9.0	670.8393002	670.8393	203.6284	36.2267	20.89368	20.03269	....	20	20
10.0	685.6495294	685.6495	223.6376	40.19371	21.27121	20.05432		20	20
11.0	699.1266173	699.1266	242.9571	44.48557	21.73309	20.08469		20	20
12.0	711.490874	711.4909	261.5797	49.06955	22.28364	20.12556		20	20

Eqn for fire Eqn 10.1 for first node eqn 10.2 eqn 10.3 for last node

Figure 10.4 Sample layout of finite element model

10.3 Evaluation of the One Dimensional Heat Transfer model

10.3.1 Previous Work

Munukultla (1989) had developed a similar heat transfer model, 'Heat' to simulate the transfer of heat. Using 'Heat', he repeated an earlier work by Harmathy, who solved a one dimensional heat transfer into brick wall by numerical scheme. Munukutla then compared this results obtained from his 'Heat' computational program with Harmathy's results.

The details of the Harmathy's test which is repeated in this chapter is as described below:

- Thickness of brick : 200 mm
- Density of brick : 1760 kg/m^3
- Thermal conductivity, k = 0.954 W/m°C
- Specific Heat, Cp : 904.35 J/kg°C
- Surface Heat Transfer Coefficient, h = 16 W/m^2 °K
- Ambient temperature, t_ω = 23°C
- Fire Curve : Sudden increase in temperature to 997°C and maintained at that level

Figure 10.5(a) shows the temperature-time curves of the brick wall for various distance from the fire-exposed side, calculated by Munukutla using his HEAT program and by Harmathy's numerical scheme. The figure shows almost perfect agreement between both calculations.

Apart from Harmathy's test, Munuktla has also used his 'HEAT' program to simulate an experimental work by Woodside and Ruiter at BRANZ. Woodside and Ruiter's experiment involved the exposure of a concrete wall to the standard fire in a furnace. As shown in figure 10.5(b), Munukutla's 'HEAT' program was able to give close result to the experimental data from BRANZ. Both results shown in figure 10.5(a) and 10.5(b) confirmed the accuracy of Munukutla's 'HEAT' program.

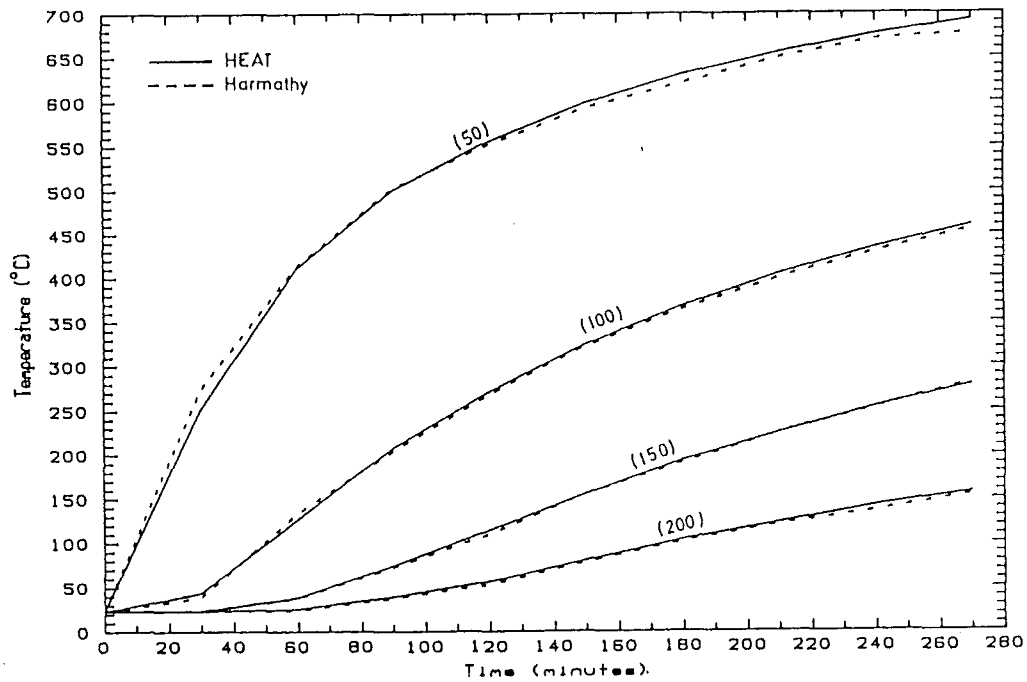

Figure 10.5(a): Comparison of Munukutla's results with Harmanthy's (Mununkutla 1989)

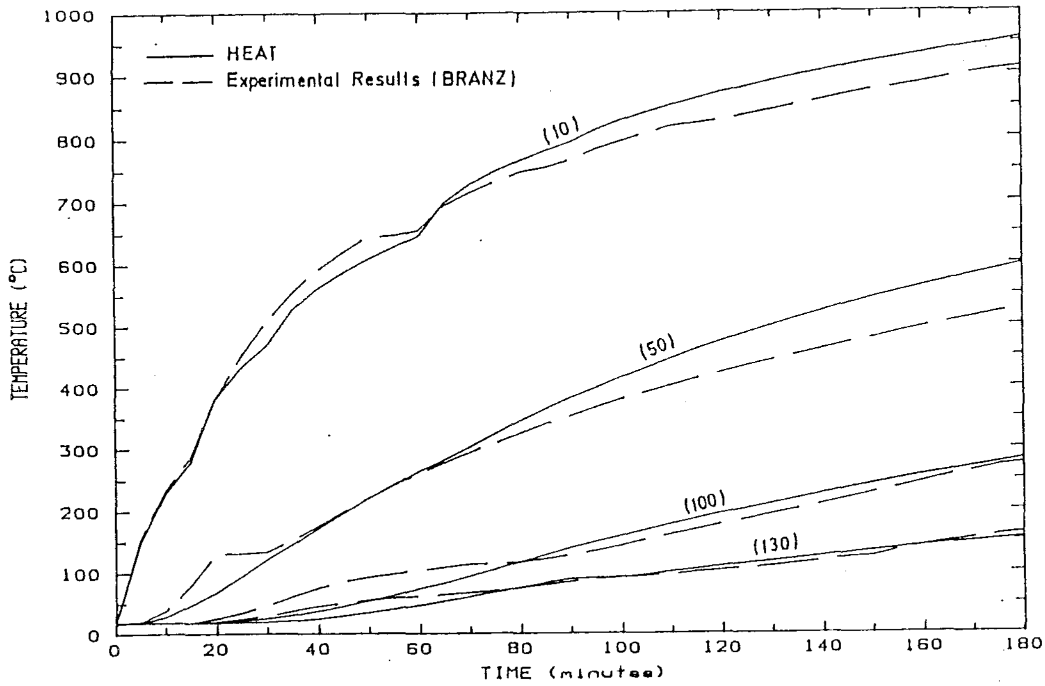

Figure 10.5(b): Comparison of Munukutla's results with Experimental result from BRANZ (Mununkutla 1989)

10.3.2 Calibrating the Finite Element Model

Due to the lack of sufficient information about the parameters of Woodside and Ruiter's test, only the Harmathy's test has been made use of to calibrate the finite element model developed for this report. The result from the repeated Harmathy's test is plotted in figure 10.6

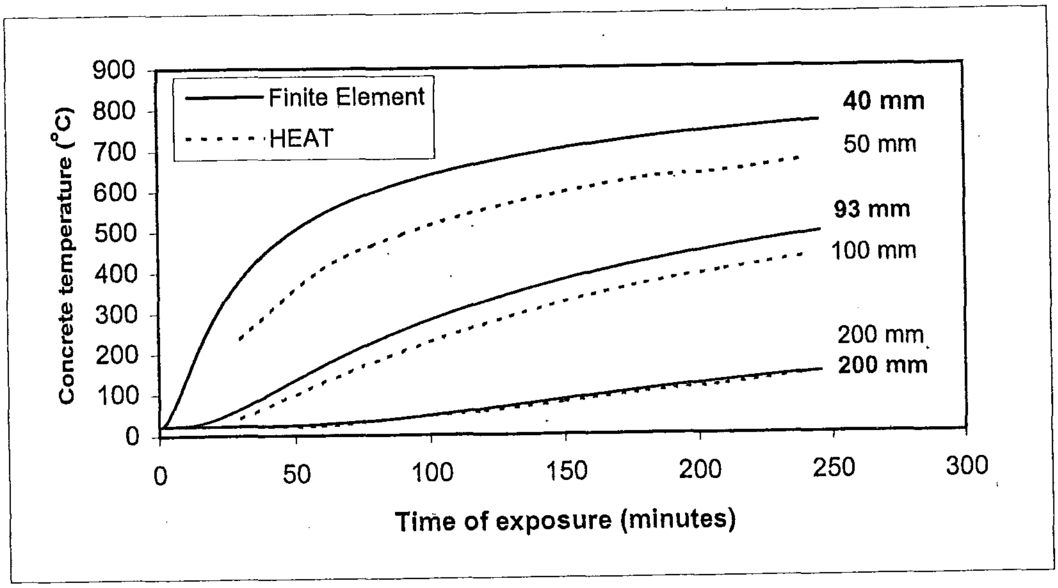

Figure 10.6 : Comparison between Munukutla's results and finite element model

Figure 10.7 shows the result obtained from the finite element model, plotted together with Munukutla's. Due to the way the thickness of the brick wall is divided in the finite element model, temperature of concrete at the depths of 50 mm and 100 mm (as shown in Munukutlas's result) are not readily obtainable. Instead, the temperatures at two of the nearest depths available from the finite element model (indicated by the values in bold letter) which are 40 mm and 93 mm are plotted in figure 10.7 for comparison, besides the temperature at 200 mm.

The repeated testing of Munukutla's concrete wall shows good agreement between the author and Munukutla's result. Temperature curves for node at 40 mm and 93 mm obtained from the finite element model seems to be following similar trend and close to the temperature of Munukutla's result at 50 mm and 100 mm respectively. Thus, a close agreement between both results would be expected if only the temperature curves at 50 mm and 100 mm are available from the finite element model. In fact, this is demonstrated by the temperature curves obtained at 200 mm where both results are almost identical.

10.4 Conclusion

The close agreement between the result obtained from the finite element model to Munukutlas's has demonstrated that this model is accurate and therefore is used in the following chapters for the investigation of the validity of time equivalent formulae and spreadsheet method for concrete structures.

11 Validity of Time Equivalent Formulae for Concrete Structures

11.1 Objective

As mentioned before, the time equivalent formulae are independent of the characteristics of structural element and assume a same fire severity for all members in a complete burnt out compartment. They have been developed empirically, based on experimental data obtained from the exposure of protected steel beams to fires.

However, the formulae are also commonly used to estimate the time equivalent for reinforced concrete structures. In fact, according to Buchanan(1999), Eurocode 1 part 2-2 allows the Eurocode time equivalent formula be used for all materials and the Swedish national application document only prohibits the use of the formula to be used for timber structures.

Several researches have been conducted to investigate the validity of the time equivalent formulae for reinforced concrete structures. Thomas(1996) concluded from his investigation that the time equivalent formulae tend to give poor and unsafe results for concrete, steel and timber structures while Franssen's (1996) results show that the Eurocode formula gives close results to his calculated time equivalents for reinforced concrete structures using the SAFIR program.

Therefore, this chapter also aims to investigate the accuracy of the Eurocode formula in estimating the time equivalent for reinforced concrete structure.

11.2 Previous Work

Franssen used the SAFIR fire simulation program discussed in chapter 1 to calculate the time equivalent for his reinforced concrete structure. He then compared the results to those obtained from the Eurocode formula. He concluded from the comparison that the Eurocode formula gives close results to SAFIR program in estimating time equivalents for reinforced concrete structures and also that the reinforced concrete structure behaves similarly to protected steel member when exposed to fires.

11.3 Methodology

Basically, the investigation in this chapter is to repeat Franssen's tests using the finite element model developed in the chapter 10. The one-dimensional finite element model developed for simulating the heat transfer has been proven to be successful and accurate.

11.3.1 Obtaining the Time Equivalent Using Finite Element Model

The finite element model developed in chapter 10 is used to simulate the exposure of concrete structure to the standard ISO 834 and Eurocode parametric fires. The steel bar is assumed to have the same temperature as the concrete at the depth which it is placed. Therefore, the time equivalent for the steel bar is assumed to be the same as that for the concrete at that depth. The time equivalent has been defined in chapter 1 and the method of formulating the finite element model in order to obtain the time equivalent is the same as the method for the spreadsheet method as discussed in details in section 3.1.3 of chapter 3.

11.3.2 Franssen's Test for Reinforced Concrete

Franssen's test has been discussed in detail and repeated for a protected steel beam in chapter 4. Six physical parameters, which are the floor area, fuel load, room height, opening height and width and thermal inertia of the compartment are varied one at a time within certain range to monitor the corresponding change in the calculated time equivalent.

These tests are repeated for the reinforced concrete slab that has the following properties:

- Penetration depth : 30 mm
- Density : 2300 kg / m^3 (concrete) , 7850 kg / m^3 (Steel)
- Specific Heat :1000 J / kg °C (concrete), 600 J/kg °C (Steel bar)
- Fire Curves : Standard and Eurocode Parametric fires
- Thermal conductivity, k = 1.6 W/mK (concrete)

The thermal properties of the concrete follow the values suggested by Buchanan (1999) for normal weight or siliceous concrete.

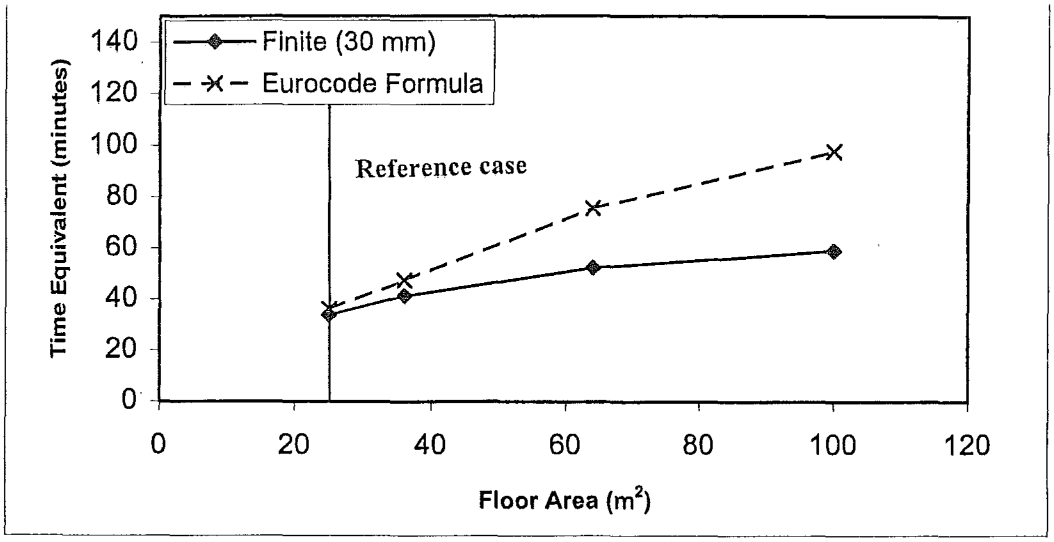

Figure 11.1: Time equivalent versus floor area: comparison of Eurocode formula and finite element model

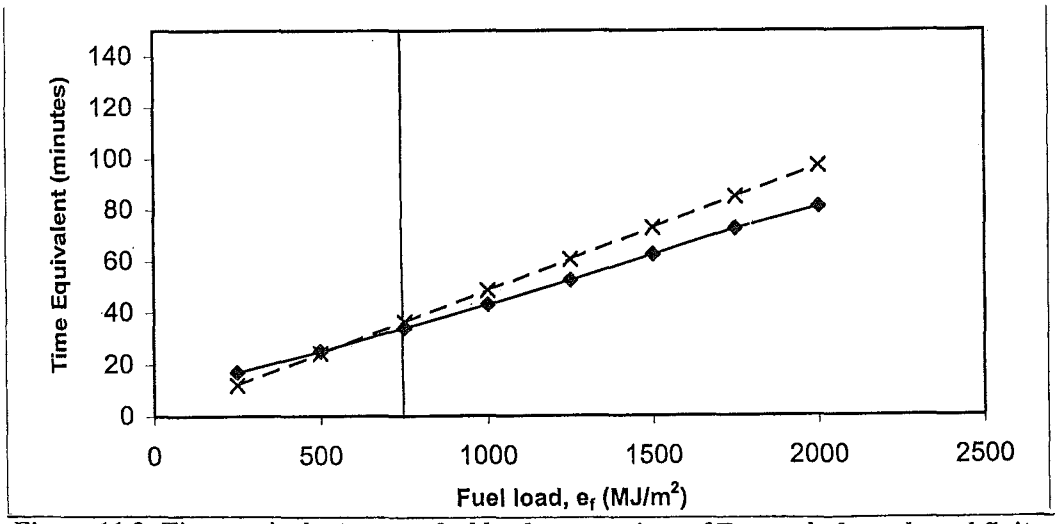

Figure 11.2: Time equivalent versus fuel load: comparison of Eurocode formula and finite element model

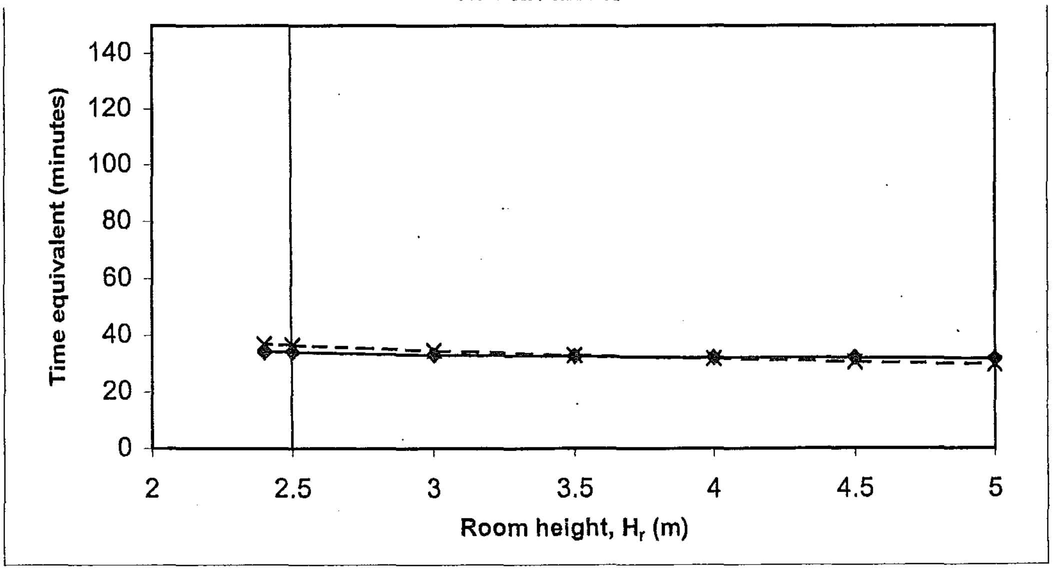

Figure 11.3: Time equivalent versus room height: comparison of Eurocode formula and finite element model

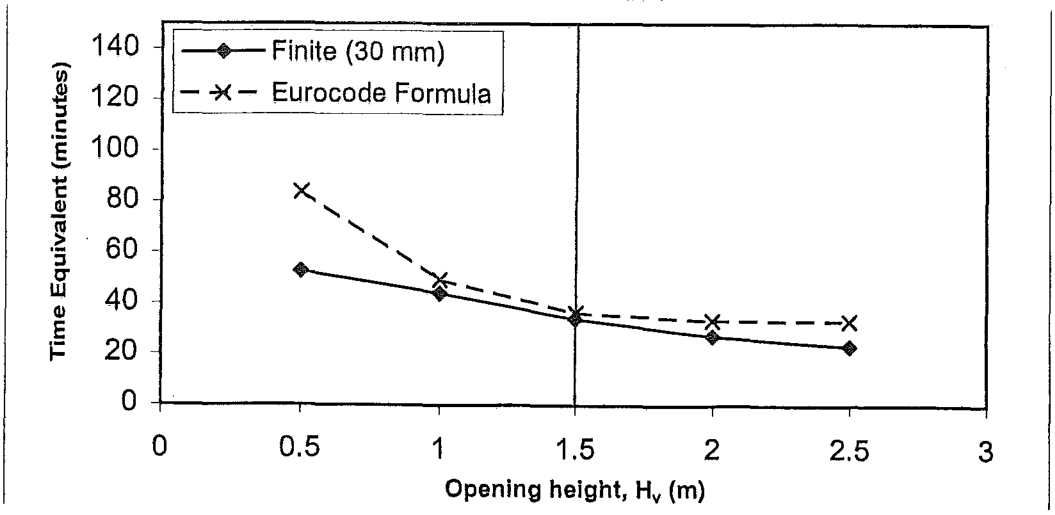

Figure 11.4: Time equivalent versus opening height: comparison of Eurocode formula and finite element model

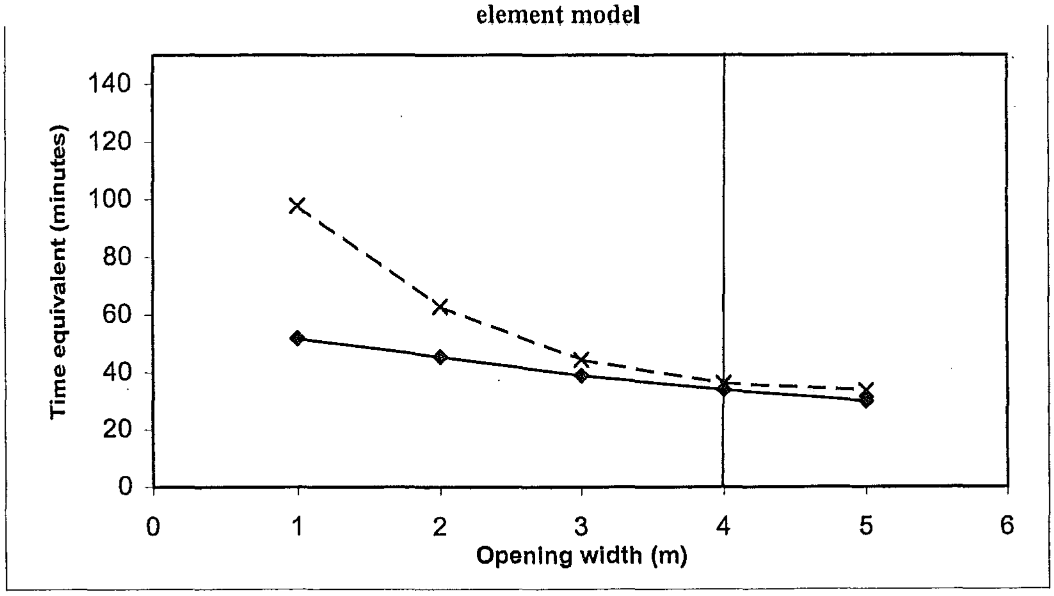

Figure 11.5: Time equivalent versus opening width: comparison of Eurocode formula and finite element model

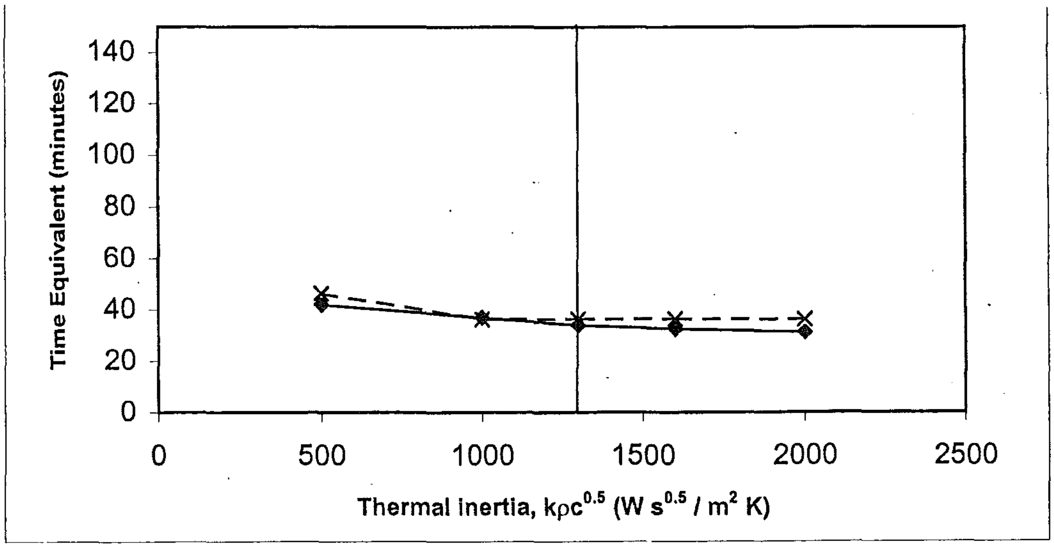

Figure 11.6: Time equivalent versus thermal inertia: comparison of Eurocode formula and finite element model

11.4 Results and Comparison

Figures 11.1 to 11.6 show the time equivalents calculated by the finite element model for the reinforced concrete structure at penetration depth of 30 mm plotted together with results from the Eurocode time equivalent formula. As shown in the graphs, the Eurocode formula has only been used to calculate the time equivalent within its limit as mentioned in chapter 1 equation 1.2.2.

As discussed before in chapter 4, the change of the time equivalent with the variation in the floor area in Franssen's study is actually a combined effect of the variation in the ventilation factor and fuel load density. It can be seen from the graphs that, the Eurocode formula tends to deviate significantly from the finite element model in region where the ventilation factor is low. For example, a difference as large as 40 minutes exists when the floor area increases up to 100 m^2 (which, as discussed in chapter 4 before, is due to the decrease in ventilation factor as the floor area increases). The same phenomenon occurs when the opening height and width decreases to 0.5 m and 1m respectively. This major difference in the behaviour between the spreadsheet method and time equivalent formula has been explained in detail in chapter 6.

Other than that, the results generally show good agreement between the Eurocode formula and finite element method. It can be seen that particularly for ventilation of 0.0735 which is the standard ventilation factor used in this study (opening height of 1.5 m and width of 4 m in a 5 m x 5m room), the results from both methods agree almost perfectly with one another. As most of the time the tests have been carried out at this ventilation factor, it is not surprising that good agreement between the finite element model and Eurocode formula are obtained. If a different ventilation factor has been used such as that at opening height of 1 m or width of 0.5 m, greater difference between both methods would have been expected.

Figure 11.7 shows the comparison of the time equivalents calculated from the finite element and Eurocode formula. In general, the Eurocode formula is conservative and overestimate the time equivalent by 23 %.

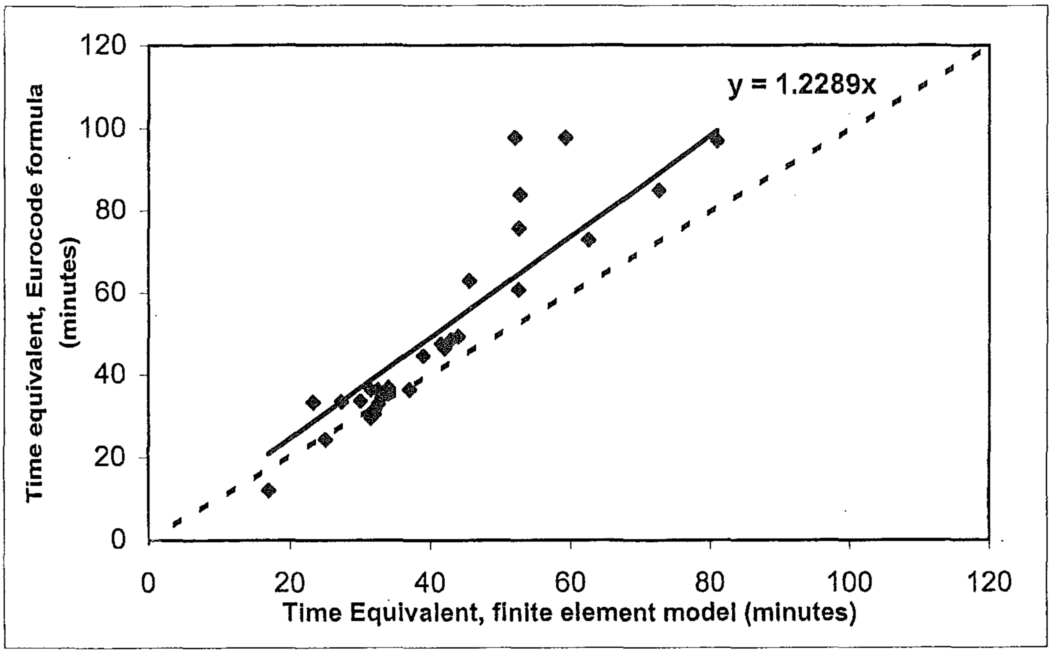

Figure 11.7: Comparison of Eurocode formula and finite element model

11.5 Conclusion

The Eurocode formula is found to be very accurate in estimating the time equivalent for reinforced concrete for certain range of ventilation factor. Results from the formula start to deviate quite significantly as the ventilation factor decreases to the value that is near to the lower limit of the validity of the formula. The formula is also found to give conservative results. Therefore, it can be concluded that the Eurocode formula is valid for reinforced concrete structures as long as the limit of its applicability is taken into consideration.

12 Validity of Spreadsheet method for Concrete Structures

12.1 Introduction

The spreadsheet method has been developed for calculating time equivalents for protected steel beam. The spreadsheet method as discussed in chapter 3 consists of equations that calculate the change in the temperature of the steel member as a result of the heat that penetrates through the insulation layer. Therefore, the spreadsheet method is basically also a heat transfer model which calculate the raise of temperature in steel protected by a layer of insulation. However, unlike the finite element model discussed in chapter 10, the spreadsheet method assumes uniform temperature in the steel member being heated.

This chapter aims to investigate the possibility of using the spreadsheet method for calculating time equivalent for the reinforcement of concrete structures. The reinforcement of concrete structures refers to the steel bars placed at certain depth under the concrete layer or the concrete cover. Similar to the insulation of a protected steel beam, the concrete cover of a reinforced concrete structure acts as a protection to the steel bars from direct exposure to fire. It is reasonable to assume that the spreadsheet method that is able to calculate the transfer of heat through the protective layer to the steel beam underneath should also work for the reinforced concrete structures.

12.2 Methodology in This Study

Franssen's test has been repeated for concrete structure in chapter 11 using the finite element model. The test is repeated here using the spreadsheet method. The results obtained are then compared to the finite element model. Details of the reinforced concrete structure is as described below.

- Structure: reinforced concrete structure
- Reinforcement: Steel bar with 15 mm diameter
- Concrete cover: 30 mm
- Properties of concrete: as described in chapter 10

The resultant time equivalent from the spreadsheet method is compared with that from the finite element model.

12.2.1 Using Spreadsheet Method for Reinforced Concrete Structure

The spreadsheet method used here was originally intended for protected steel beam. The author has modified the spreadsheet to use the insulation as the concrete layer and the protected steel beam as the steel reinforcement of the concrete.

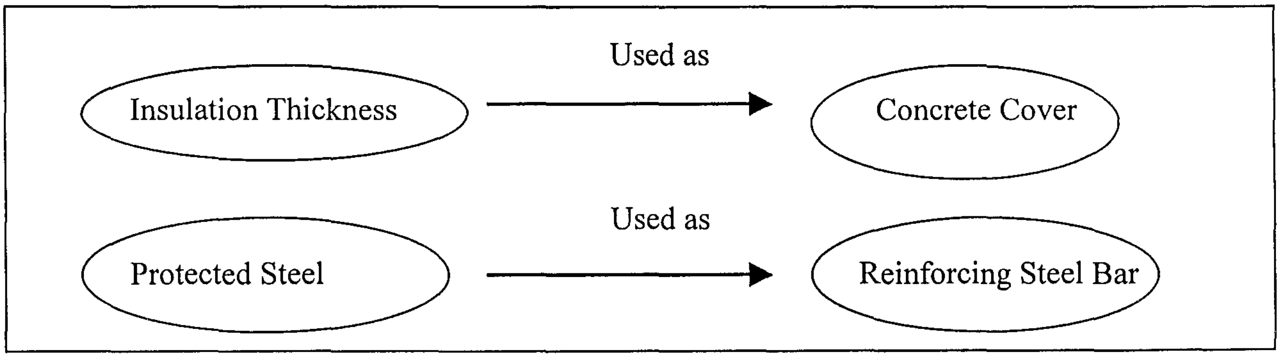

Figure 12.1: Illustration: using spreadsheet method for reinforced concrete structure

According to the analogy described in figure 12.1, the spreadsheet method is basically simulating the exposure of a protected steel bar to fires as illustrated in figure 12.2

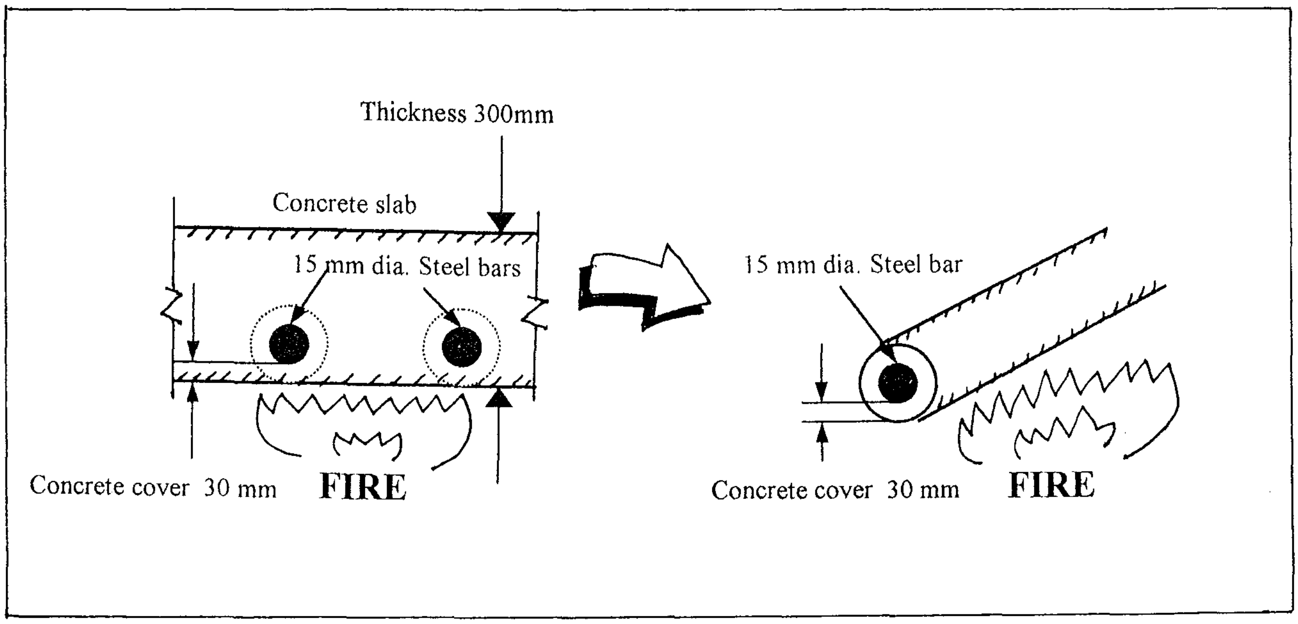

Figure 12.2: Exposure of protected steel bar to fire

Figure 12.2 shows the exposure of a concrete slab with a thickness of 300 mm to fire. The reinforcements are placed at 30 mm from the surface exposed to fire and assumed to have a diameter of 15 mm. The finite element model is used to simulate the exposure of this concrete slab to fires and the temperatures calculated for node that lies 30 mm from the face exposed fire is assume to the temperature of the reinforcement. The spreadsheet method on the other hand is used to simulate the heating of a steel bar 150 mm in diameter and insulated by a 30 mm thick concrete layer. Both methods are repeated for the standard and Eurocode fires.

Figure 12.3 shows the temperature-time curves for the concrete slab calculated by the spreadsheet method and finite element method respectively. It can be seen that the temperature-time behaviour of the concrete structure calculated by the spreadsheet method is very similar to that by the finite element model, indicating good agreement between both methods in modelling the exposure of concrete structure to fires. Spreadsheet method predicts slightly higher temperature rise in concrete reinforcement

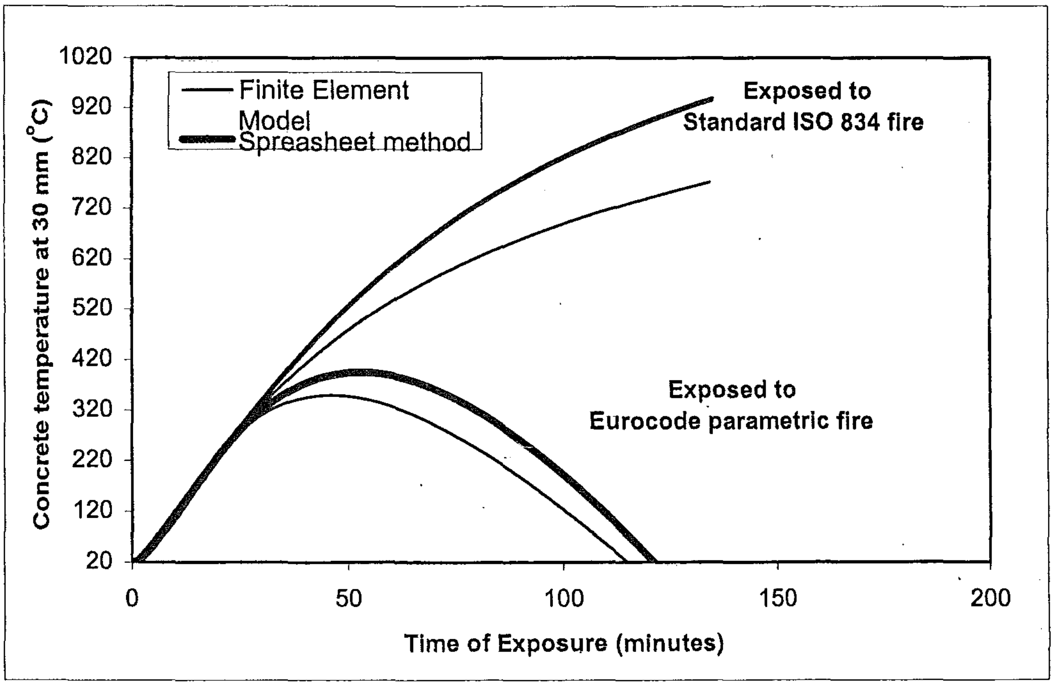

Figure 12.3: Temperature-time curves for concrete exposed to fires: comparison between spreadsheet method and finite element model

12.3 Result of Repeated Franssen's Tests for Reinforced Concrete

Figures 12.4(a) to 12.4(f) show the results of the repeated Franssen's study for reinforced concrete slab using the spreadsheet method. These figures are basically the same as figures 11.1 to 11.6 of chapter 11 but with the results from spreadsheet method included. It can be seen that the spreadsheet method agrees almost perfectly with finite element model with a difference of less than 7 minutes in all cases.

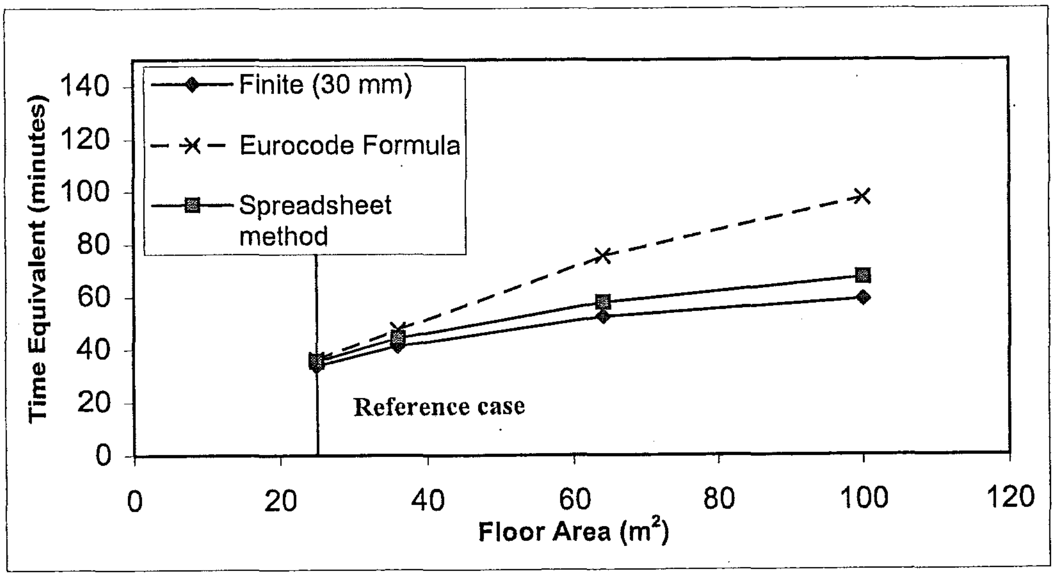

Figure 12.4(a): Time equivalent versus floor area: Comparison between the spreadsheet method and finite element model for reinforced concrete

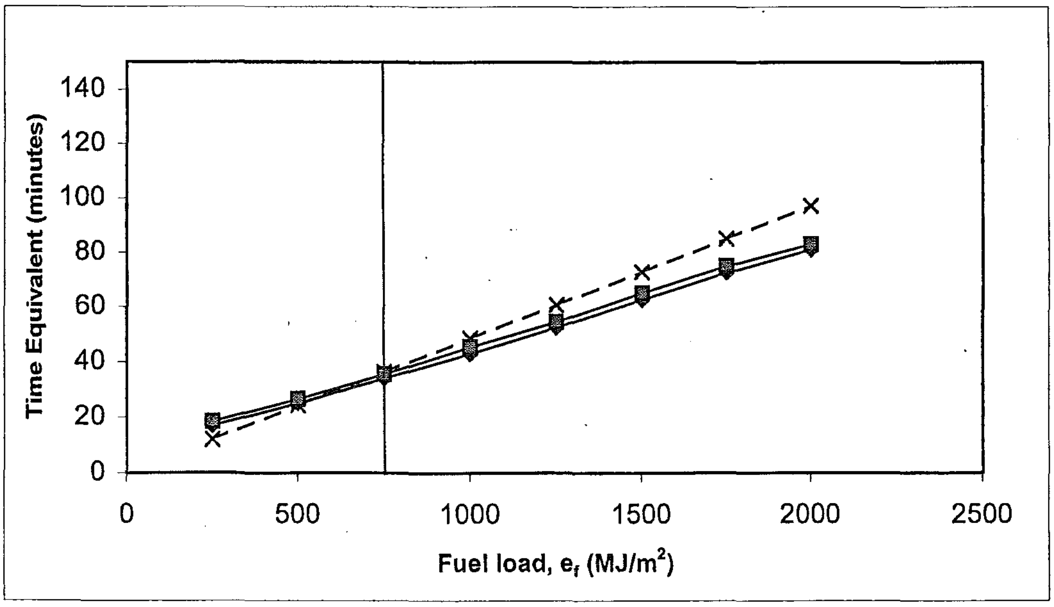

Figure 12.4(b): Time equivalent versus fuel load: Comparison between the spreadsheet method and finite element model for reinforced concrete

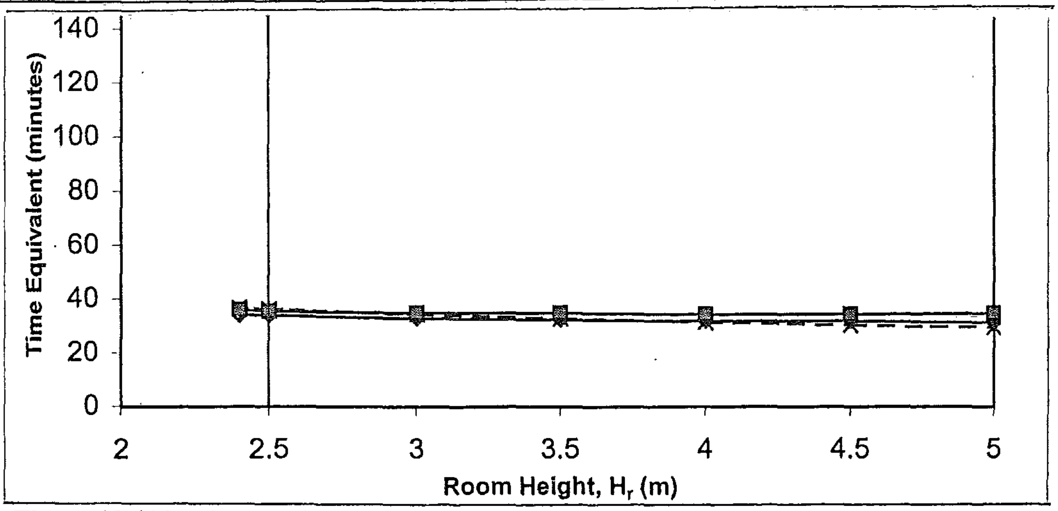

Figure 12.4(c): Time equivalent versus room height: Comparison between the spreadsheet method and finite element model for reinforced concrete

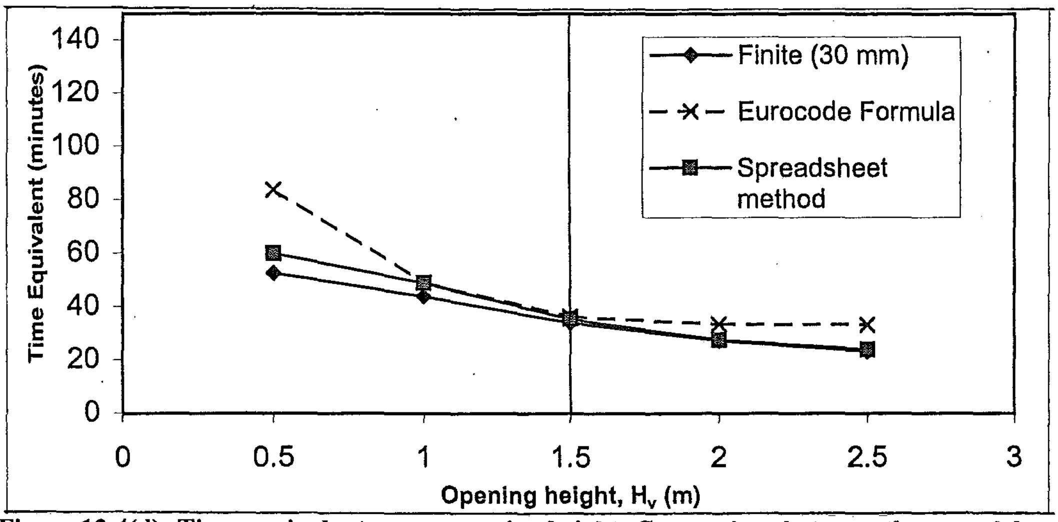

Figure 12.4(d): Time equivalent versus opening height: Comparison between the spreadsheet method and finite element model for reinforced concrete

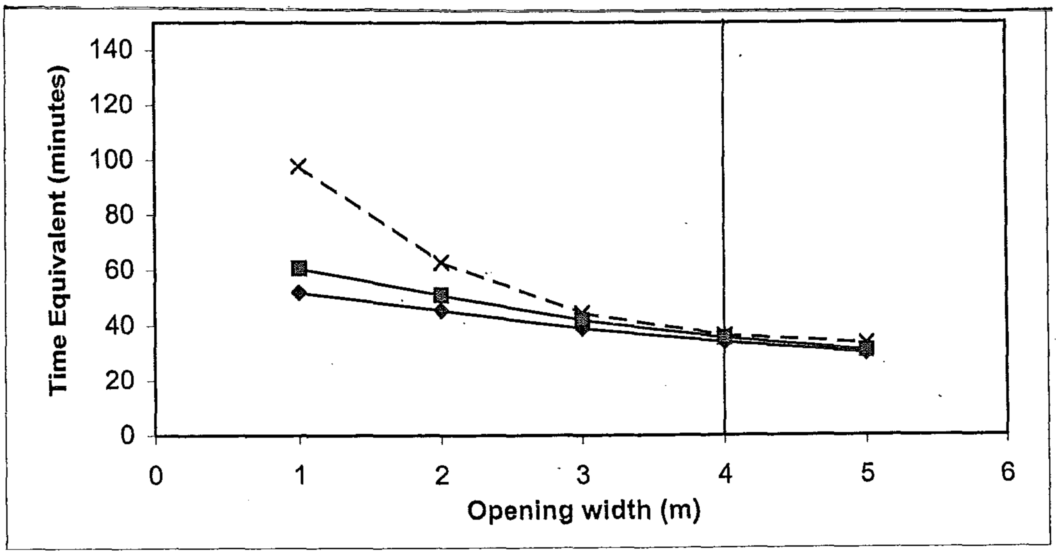

Figure 12.4(e): Time equivalent versus opening width: Comparison between the spreadsheet method and finite element model for reinforced concrete

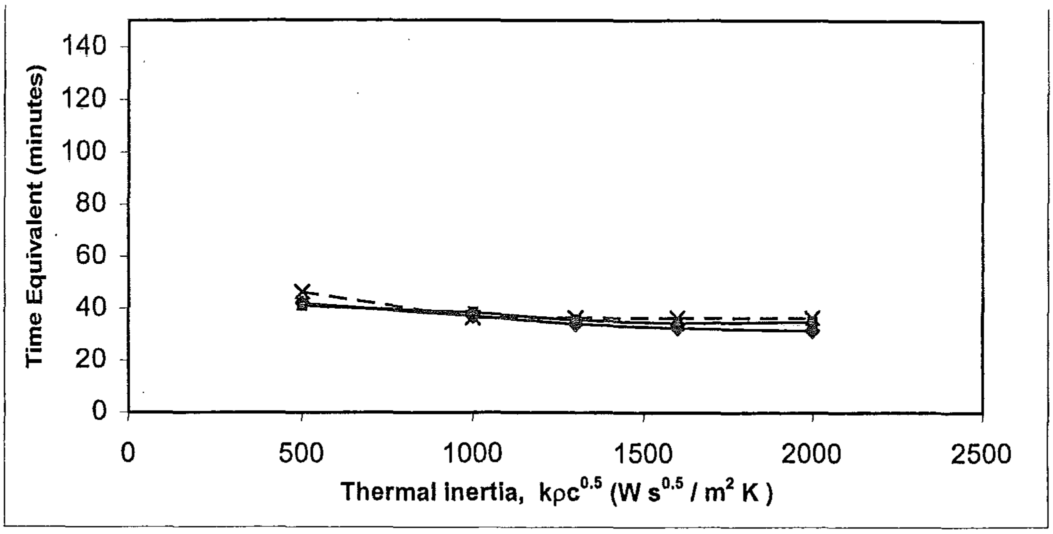

Figure 12.4(f): Time equivalent versus thermal inertia: Comparison between the spreadsheet method and finite element model for reinforced concrete

12.4 Conclusion

It can be concluded from the results that the proposed method of using the spreadsheet method for reinforced concrete has been successful. The spreadsheet method has been proven to give very close results to the finite element method, even though the equations used do not accurately model heat transfer through concrete structures.

13 Conclusions

13.1 The Spreadsheet Method

The spreadsheet method developed for simulating the exposure of structural member to fires has been studied and compared with the SAFIR program. It is shown that the spreadsheet method is very accurate in calculating the variation of protected steel temperature with time, especially for small to medium size steel members with thin insulation. It has also been shown that the spreadsheet method is able to repeat results of the study carried out by Franssen who used the SAFIR program to calculate the time equivalent for various fire situations. This indicates the success of the spreadsheet method developed for calculating time equivalents for protected steel member, especially for member with thin insulation.

The spreadsheet method is also found in this report to be accurate and good in predicting the behaviour and time equivalents of concrete structure exposed to fires. However, as the formulae used in the spreadsheet method do not accurately model the heat transfer process into concrete structures, more investigations would have to be done to confirm the validity of the spreadsheet method for reinforced concrete structures.

13.2 Validity of Time Equivalent Formulae for Steel Structures

The investigation carried out on the three time equivalent formulae, that is the Eurocode, CIB and Law formulae shows that the Law and Eurocode formulae are conservative and good in predicting the time equivalents for protected steel members. Both formulae are highly dependent on the time equivalent calculated from the spreadsheet method and found to overestimate the time equivalents by 21% and 14% respectively. The CIB formula on the other hand are found to consistently give significantly higher time equivalents. This study also shows that the time equivalent formulae are not valid for compartment fires with small ventilation and tend to deviate a great deal from the values calculated by the spreadsheet method.

The Eurocode formula is also found to give good estimate of time equivalents for reinforced concrete structures. The time equivalents calculated from the formula are conservative and highly dependent on the values calculated from the finite element model.

13.3 Suggested Further Research

The use of the spreadsheet method for calculating the time equivalents for concrete structures seems to be feasible but would require further research to verify this. The author hereby suggests further investigation to be carried out for commonly used commercially concrete structures such as reinforce concrete beams and columns and for different compartment fire set ups.

Apart from that, the k_c and k_b factors used in the CIB and Eurocode formulae are found to be significantly different from the 'ideal' values, which are calculated using the spreadsheet method. Revision of these factors is suggested.

The Alternative decay rate (ADR) has been compared to the Eurocode decay rate (EDR) which is the commonly used decay rate for engineering design. Both decay rates predict a very different behaviour in the time equivalent for certain range of compartment thermal properties. As the ADR is consider in this report to be a more logical decay rate, further research is suggested to study the difference between the two decay rates and possibly revise the EDR.

References

Buchanan, A.H. (Editor). 1994. Fire Engineering Design Guide, Center for Advanced Engineering, University of Canterbury, New Zealand.

Buchanan, A.H. 1999. Structural Design for Fire (Unpublished lecture notes). University of Canterbury

Cadorin, J.F & Cajot, L.G. 1999. Comparison of Equivalent Times from Eurocode 1 Part 2.2 Annex E and Experimental Tests. University of Liege Belgium.

Cooke, G. 1999. Time Equivalent – Is It a Good Measure of Compartment Fire Severity? Fire Safety Engineering. Vol 6, pp 26-31.

Drysdale, D. 1985. An Introduction to Fire Dynamics. John Wiley & Sons, Chichester, U.K.

EC1, 1994. EUROCODE 1: Basis of Design and Actions on Structures, Part 2-2 : Actions on Structures Exposed to Fire. ENV 1991 - 2-2. European Committee for Standardization, Brussels.

Feasey, R. 1999. Post Flashover Design Fires. Fire Engineering Research Report No. 99/6. Department of Civil Engineering, University of Canterbury.

Feeney, M.J. 1998. Design of Steel Framed Apartment and Hotel Buildings for Fire. Australasian Structural Engineering Conference, Auckland.

Franssen J.M, Cadorin J.F, Cajot L.G, Schleich J.B, Schweppe H and Kindmann R, 1996. Connection Between Parametric Temperature-Time Curves and Equivalent Time of Fire Exposure. Proceedings, IABSE Colloquium, Deft. Pp 407-417.

Gamble, W.L. 1989. Predicting Protected Steel Member Endurance Using Spreadsheet Programs. Fire Technology. Vol. 25, No.3, pp 256 – 273.

Gilvery, K.R. and Dexter, R.J. 1997. Evaluation of Alternative Methods for Fire Rating Structural Elements. National Institute of Standards and Technology (NIST-GCR-97-718).

Ingberg S.H, 1928. Tests of The Severity of Building Fires. National Fire Protection Quarterly, Vol. 22, No.1, pp 43 – 61.

Law, M. 1971. A Relationship Between Fire Grading and Building Design and Contents. Fire Research Note No. 877. Fire Research Station, U.K.

Law, M. 1997. A Review of Formulae for T-Equivalent. Proceedings of the 5th International Symposium on Fire Safety Science, Melbourne. Page 985-996.

Munukutla V.R. 1989. Modelling Fire Performance of Concrete Walls. Civil Engineering Research Report 89/5, University of Canterbury, New Zealand.

Pettersson, O. 1973. The Connection between a Real Fire Exposure and the Grating Conditions according to Standard Fire Resistance Tests – with Special Application to Steel Structures. Document CECM 3-73/73. European Commission for Constructional Steelwork.

Purkiss, J.A. 1996, Fire Safety Engineering: Design of Structures. Butterworth Heineman, Oxford, U.K.

Thomas G.C, Buchanan A.H and Fleischmann C.M, 1997. Structural Fire Design : The Role of Time Equivalence. Proceedings of the 5th International Symposium on Fire Safety Science, Melbourne. pp 607 – 618.

Thomas G.C, 1997. Fire Resistance of Light Timber Framed Walls and Floors. PhD thesis. Fire Engineering Research Report 97-7. University of Canterbury , New Zealand.

Tucker, A.S. 1998. Heat and Mass Transfer with H.V.A.C Applications (Unpublished lecture note for ENME 435/455). Department of Mechanical Engineering, University of Canterbury.

Appendix A

Time Equivalent for Protected Steel Member

Insert relevant data into yellow boxes

(A)

Steel beam dimension			
$F / V = H_p / A =$	211	m^{-1}	
Cross Sectional Area, $A_s =$		4.75E-03	m^2

(B)

Steel Properties		
Density	7850	kg/m^3

(C)

Insulation Properties		
Thickness	0.02	m
Density	300	kg/m^3
Specific heat	850	J kg/°C
Thermal Conductivity	0.15	W/m^2 °C
Cross Sectional Area , A_i (m^2)=	0.020045	

(D)

Compartment and Ventilation			
	Compartme	Ventilation	
Length	5	m	
Width	5	1.1	m
Height	2.5	1.5	m
Total area	100	m^2	
Floor area	25	m^2	
Ventilation area,	1.65	m^2	
Opening factor, F_v	0.020208	(for parametric fire)	
Thermal inertia, $(kpc_p)^{0.5}$ =	2000	$Ws^{0.5} / m^2 K$	
$\alpha v = Av / Af =$	0.066		
$\alpha h = Ah / Af=$	0		
$b_v =$	20.69555		

Appendix A

(E)

Fuel Load		
et (per total area)	187.5	MJ/m^2
ef (per floor area)	750	MJ/m^2
Duration of Heating, td	4342.277	seconds
Calorific Value ,	19	MJ/kg
Fuel load (kg / m^2)	39.47368	

Time Equivalent for Protected Steel Member

Choose modelling time step, δt =	40	seconds	OK!	$\rho_\sigma c_s A_s$	$2\rho_i c_i A_i$	$\rho_\sigma c_s A_s > 2\rho_i c_i A_i$? Yes
Choose initial temperature, T_o =	20	°C		2.24E+04	10222.95	

Duration of the heating phase of the Eurocode fire, t_d = 1.206188 hours

Γ = 0.085861 therefore, t_d^* = 0.103564 Hours

The decay rate for Eurocode parametric fire, dT / dt = 53.66303 °C per (real time)hour

= 0.596256 per time step

Result t_{eq}	Result t_{max}	Fictitious Time, t* (hours)	Time (minutes)	Time, t (seconds)	Fire Temperature, T_f ISO 834 (°C)	Fire Temperature, T_f Eurocode (°C)	Steel Temperature, Ts ISO 834 (°C)	Steel Temperature, Ts Eurocode (°C)	Difference $T_f - T_s$ ISO 834 (°C)	Difference $T_f - T_s$ Eurocode (°C)	Change in steel temp. ISO 834 (°C)	Change in steel temp. Eurocode (°C)	Load Capacity, r_f ISO 834	Load Capacity, r_f Eurocode
		0.000477005	0	0	214.6736	5.902502	20	20	194.6736	-14.0975	2.616315	-0.189463	1	1
		0.001431014	0.666667	40	349.2137	17.5547	22.61631	19.81054	326.5974	-2.255838	4.389302	-0.030317	1	1
		0.002385023	1.333333	80	418.9398	29.0062	27.00562	19.78022	391.9342	9.225977	5.267396	0.123992	1	1
		0.003339033	2	120	466.3371	40.26059	32.27301	19.90421	434.0641	20.35638	5.8336	0.273579	1	1
		0.004293042	2.666667	160	502.2893	51.3214	38.10661	20.17779	464.1827	31.14361	6.238379	0.418554	1	1
		0.005247052	3.333333	200	531.2624	62.19211	44.34499	20.59635	486.9175	41.59576	6.543923	0.559026	1	1
		0.006201061	4	240	555.5306	72.8761	50.88891	21.15537	504.6417	51.72073	6.782127	0.6951	1	1
		0.00715507	4.666667	280	576.4104	83.37673	57.67104	21.85047	518.7394	61.52626	6.971593	0.826882	1	1
		0.00810908	5.333333	320	594.7333	93.69727	64.64263	22.67735	530.0906	71.01992	7.124148	0.954472	1	1
		0.009063089	6	360	611.0576	103.841	71.76678	23.63182	539.2908	80.20913	7.247794	1.07797	1	1
		0.010017098	6.666667	400	625.7768	113.8109	79.01458	24.70979	546.7622	89.10115	7.348206	1.197474	1	1
		0.010971108	7.333333	440	639.1785	123.6103	86.36278	25.90727	552.8157	97.70307	7.429562	1.313079	1	1
		0.011925117	8	480	651.4793	133.2422	93.79234	27.22035	557.687	106.0219	7.495029	1.42488	1	1
		0.012879127	8.666667	520	662.8464	142.7095	101.2874	28.64523	561.559	114.0643	7.547067	1.532966	1	1
		0.013833136	9.333333	560	673.4116	152.0153	108.8344	30.17819	564.5771	121.8371	7.587629	1.637428	1	1
		0.014787145	10	600	683.2806	161.1623	116.4221	31.81562	566.8585	129.3467	7.61829	1.738353	1	1
		0.015741155	10.66667	640	692.5396	170.1535	124.0404	33.55398	568.4992	136.5995	7.640339	1.835827	1	1
		0.016695164	11.33333	680	701.2595	178.9915	131.6807	35.3898	569.5788	143.6017	7.654849	1.929934	1	1
		0.017649173	12	720	709.4997	187.6793	139.3355	37.31974	570.1642	150.3596	7.662716	2.020756	1	1
		0.018603183	12.66667	760	717.3103	196.2194	146.9983	39.34049	570.312	156.8789	7.664703	2.108373	1	1
		0.019557192	13.33333	800	724.7338	204.6145	154.663	41.44886	570.0709	163.1656	7.661462	2.192863	1	1
		0.020511202	14	840	731.8068	212.8672	162.3244	43.64173	569.4824	169.2254	7.653553	2.274304	1	1

Appendix C

Finite Element Method for Concrete Layer

Time Step	$\Delta T =$	55	Seconds	Stable		
Density	ρ =	1760	kg/m^3			
Area	A =	1	m^2			
Thickness	x =	200	mm		Convection	h =
	Δx =	0.026666667	m		Ambient temp. $t\omega$	=
		0.013333333				
$\alpha = k/\rho\ Cp =$		5.99376E-07				

Stability check :DT < 409.8905 seconds in order to be stable

Time Step x	Time (minutes)	Time (s)	FIRE	Nodes : 0 / Distance (mm) = 0 / Exposed to fire	1 / 13.3333333	2 / 40	3 / 66.6666667
0	0.0	0	997	997	23	23	23
1	0.9	55	997	997	113.305321	23	23
2	1.8	110	997	997	191.051529	27.1863712	23
3	2.8	165	997	997	258.17934	34.5887552	23.1940717
4	3.7	220	997	997	316.314583	44.4257259	23.7133093
5	4.6	275	997	997	366.820753	56.0697553	24.6408443
6	5.5	330	997	997	410.842627	69.0185596	26.0236699
7	6.4	385	997	997	449.342487	82.871673	27.8819157
8	7.3	440	997	997	483.130224	97.3113017	30.2160899
9	8.3	495	997	997	512.88836	112.086685	33.0127026
10	9.2	550	997	997	539.192872	127.001327	36.248605
11	10.1	605	997	997	562.530526	141.902578	39.8943119
12	11.0	660	997	997	583.313313	156.673139	43.9165206
13	11.9	715	997	997	601.89049	171.224142	48.2800003
14	12.8	770	997	997	618.558621	185.489518	52.948986
15	13.8	825	997	997	633.569964	199.421412	57.8881887
16	14.7	880	997	997	647.139475	212.986464	63.0635065
17	15.6	935	997	997	659.45067	226.162792	68.4425065
18	16.5	990	997	997	670.660526	238.937545	73.9947322
19	17.4	1045	997	997	680.903596	251.304932	79.6918778
20	18.3	1100	997	997	690.295449	263.26462	85.5078648
21	19.3	1155	997	997	698.935567	274.82046	91.4188458
22	20.2	1210	997	997	706.909775	285.979448	97.4031566
23	21.1	1265	997	997	714.292287	296.750909	103.441233
24	22.0	1320	997	997	721.147427	307.145835	109.515501
25	22.9	1375	997	997	727.531084	317.176367	115.610258
26	23.8	1430	997	997	733.491936	326.855382	121.711538
27	24.8	1485	997	997	739.072488	336.196175	127.806982
28	25.7	1540	997	997	744.309952	345.212203	133.885705
29	26.6	1595	997	997	749.236985	353.916896	139.938165
30	27.5	1650	997	997	753.882329	362.323513	145.956046
31	28.4	1705	997	997	758.271341	370.445028	151.932137
32	29.3	1760	997	997	762.426452	378.294054	157.860225
33	30.3	1815	997	997	766.36756	385.882787	163.734995
34	31.2	1870	997	997	770.112362	393.222968	169.551935
35	32.1	1925	997	997	773.676635	400.32586	175.30725

Appendix C

16	W/m^2.K
23	^{0} C

4	5	6	7	8			
93.3333333	120	146.6666667	173.333333	200	Specific Heat , Cp J/ kg.K	Thermal Conductivit W/m.K	Averaged temperature of concrete
23	23	23	23	23	904.35	0.954	23
23	23	23	23	23	904.35	0.954	34.28817
23	23	23	23	23	904.35	0.954	44.52974
23	23	23	23	23	904.35	0.954	53.87027
23.0089968	23	23	23	23	904.35	0.954	62.43283
23.0412302	23.00041707	23	23	23	904.35	0.954	70.32163
23.113493	23.00228975	23.00001933	23	23	904.35	0.954	77.62508
23.2432478	23.00733966	23.00012369	23.0000009	23	904.35	0.954	84.41835
23.4473508	23.01794136	23.00045252	23.0000065	23.0000001	904.35	0.954	90.76542
23.7412292	23.03703716	23.00124259	23.0000269	23.0000007	904.35	0.954	96.72091
24.138391	23.06802271	23.0028456	23.0000821	23.0000031	904.35	0.954	102.3315
24.6501758	23.11462133	23.00573896	23.0002065	23.0000103	904.35	0.954	107.6373
25.2856778	23.18075895	23.01053005	23.0004539	23.000028	904.35	0.954	112.6726
26.051786	23.27044724	23.01795441	23.0009013	23.0000664	904.35	0.954	117.467
26.9533036	23.3876794	23.02886891	23.0016531	23.000141	904.35	0.954	122.0461
27.9931156	23.53634077	23.04424097	23.0028447	23.0002754	904.35	0.954	126.432
29.1723834	23.72013504	23.06513467	23.0046446	23.0005022	904.35	0.954	130.644
30.4907518	23.94252571	23.09269496	23.0072568	23.0008654	904.35	0.954	134.6988
31.9465556	24.20669173	23.12813064	23.0109212	23.0014221	904.35	0.954	138.6108
33.5370192	24.51549619	23.17269695	23.0159145	23.0022439	904.35	0.954	142.393
35.2584452	24.87146622	23.22767828	23.0225488	23.0034183	904.35	0.954	146.0564
37.1063869	25.27678279	23.29437156	23.0311714	23.0050503	904.35	0.954	149.6111
39.0758057	25.73327864	23.37407069	23.0421619	23.0072627	904.35	0.954	153.0656
41.1612108	26.242443	23.46805216	23.0559306	23.0101972	904.35	0.954	156.4278
43.3567823	26.80543163	23.57756217	23.0729156	23.0140146	904.35	0.954	159.7044
45.656479	27.42308114	23.70380525	23.0935795	23.0188945	904.35	0.954	162.9017
48.0541308	28.09592634	23.84793449	23.1184061	23.0250355	904.35	0.954	166.025
50.5435167	28.82421987	24.01104331	23.1478971	23.0326544	904.35	0.954	169.0794
53.1184315	29.60795325	24.19415869	23.1825684	23.0419851	904.35	0.954	172.0691
55.7727402	30.44687873	24.39823593	23.2229465	23.0532785	904.35	0.954	174.9983
58.5004227	31.34053141	24.62415468	23.269565	23.0668001	904.35	0.954	177.8704
61.2956103	32.2882512	24.87271624	23.3229613	23.0828297	904.35	0.954	180.6889
64.1526133	33.28920429	25.14464188	23.3836728	23.1016591	904.35	0.954	183.4566
67.0659428	34.34240384	25.44057229	23.4522341	23.1235909	904.35	0.954	186.1763
70.0303269	35.44672979	25.76106779	23.5291742	23.1489365	904.35	0.954	188.8504
73.0407211	36.60094746	26.10660935	23.6150132	23.1780147	904.35	0.954	191.4814

Appendix D

Results from repeated test of Franssen's study (Steel).

(With E-C decay rate)

Variation :	Floor Area m^2	Fire Load MJ / m^2	Room Height m	Opening Height m	Opening Width m	Thermal Properties	Time Equivalent (Minutes)	Franssen's Results (minutes)
Floor area	16	750	2.5	1.5	4	1300	27	28
Floor area	25	750	2.5	1.5	4	1300	35.5	38
Floor area	36	750	2.5	1.5	4	1300	44.5	46
Floor area	64	750	2.5	1.5	4	1300	58.5	60
Floor area	100	750	2.5	1.5	4	1300	68	76
Floor area	144	750	2.5	1.5	4	1300	72	116
Floor area	256	750	2.5	1.5	4	1300	71	200
Floor area	324	750	2.5	1.5	4	1300	68	
Floor area	400	750	2.5	1.5	4	1300	65	

Variation :	Floor Area m^2	Fire Load MJ / m^2	Room Height m	Opening Height m	Opening Width m	Thermal Properties	Time Equivalent (Minutes)	Franssen's Results (minutes)
Fire Load	25	250	2.5	1.5	4	1300	18.5	16
Fire Load	25	500	2.5	1.5	4	1300	27	26
Fire Load	25	750	2.5	1.5	4	1300	35.5	35
Fire Load	25	1000	2.5	1.5	4	1300	45.5	45
Fire Load	25	1250	2.5	1.5	4	1300	55	56
Fire Load	25	1500	2.5	1.5	4	1300	65	64
Fire Load	25	1750	2.5	1.5	4	1300	75	75
Fire Load	25	2000	2.5	1.5	4	1300	83	85

Variation :	Floor Area m^2	Fire Load MJ / m^2	Room Height m	Opening Height m	Opening Width m	Thermal Properties	Time Equivalent (Minutes)	Franssen's Results (minutes)
Room Hr	25	750	2.4	1.5	4	1300	36	39
Room Hr	25	750	2.5	1.5	4	1300	35.5	38
Room Hr	25	750	3	1.5	4	1300	35	36
Room Hr	25	750	3.5	1.5	4	1300	35	36
Room Hr	25	750	4	1.5	4	1300	34.5	35
Room Hr	25	750	4.5	1.5	4	1300	35	34
Room Hr	25	750	5	1.5	4	1300	35	37

Variation :	Floor Area m^2	Fire Load MJ / m^2	Room Height m	Opening Height m	Opening Width m	Thermal Properties	Time Equivalent (Minutes)	Franssen's Results (minutes)
Vent. Hv	25	750	2.5	0.2	4	1300	32	31
Vent. Hv	25	750	2.5	0.5	4	1300	61	80
Vent. Hv	25	750	2.5	1	4	1300	49	51
Vent. Hv	25	750	2.5	1.5	4	1300	35	37
Vent. Hv	25	750	2.5	2	4	1300	28	30
Vent. Hv	25	750	2.5	2.5	4	1300	23	26

Variation :	Floor Area m^2	Fire Load MJ / m^2	Room Height m	Opening Height m	Opening Width m	Thermal Properties	Time Equivalent (Minutes)	Franssen's Results (minutes)

Appendix D

Vent. W	25	750	2.5	1.5	0.5	1300	55	55
Vent. W	25	750	2.5	1.5	1	1300	61	76
Vent. W	25	750	2.5	1.5	2	1300	51	52
Vent. W	25	750	2.5	1.5	3	1300	42.5	44
Vent. W	25	750	2.5	1.5	4	1300	35.5	36
Vent. W	25	750	2.5	1.5	5	1300	31.5	31

Variation :	Floor Area m^2	Fire Load MJ / m^2	Room Height m	Opening Height m	Opening Width m	Thermal Properties	Time Equivalent (Minutes)	Franssen's Results (minutes)
$(k \rho C)^{0.5}$	25	750	2.5	1.5	4	500	41	43
$(k \rho C)^{0.5}$	25	750	2.5	1.5	4	1000	38.5	39
$(k \rho C)^{0.5}$	25	750	2.5	1.5	4	1300	35.5	38
$(k \rho C)^{0.5}$	25	750	2.5	1.5	4	1600	35	37.5
$(k \rho C)^{0.5}$	25	750	2.5	1.5	4	2000	35	37

Results from repeated test of Franssen's study (Concrete).

(With E-C decay rate)

Variation :	Floor Area m^2	Fire Load MJ / m^2	Room Height m	Opening Height m	Opening Width m	Thermal Properties	Finite Element (Minutes)	Spread sheet (minutes)	Franssen's Results (minutes)
Floor area	16	750	2.5	1.5	4	1300	27.5	27	24.5
Floor area	25	750	2.5	1.5	4	1300	34.5	35.5	41
Floor area	36	750	2.5	1.5	4	1300	41.5	44.5	45
Floor area	64	750	2.5	1.5	4	1300	51.5	58	56
Floor area	100	750	2.5	1.5	4	1300	58.5	67.5	65
Floor area	144	750	2.5	1.5	4	1300	63.3	71.3	69.5
Floor area	256	750	2.5	1.5	4	1300	66	70	77.7
Floor area	324	750	2.5	1.5	4	1300	65.3	66.7	81.8
Floor area	400	750	2.5	1.5	4	1300	61.7	63.3	83.9

Variation :	Floor Area m^2	Fire Load MJ / m^2	Room Height m	Opening Height m	Opening Width m	Thermal Properties	Finite Element (Minutes)	Spread sheet (minutes)	Franssen's Results (minutes)
Fire Load	25	250	2.5	1.5	4	1300	18.5	18.5	25
Fire Load	25	500	2.5	1.5	4	1300	26	26.5	33.3
Fire Load	25	750	2.5	1.5	4	1300	34.5	35.5	41
Fire Load	25	1000	2.5	1.5	4	1300	44	45.5	50
Fire Load	25	1250	2.5	1.5	4	1300	53.5	54.5	59.2
Fire Load	25	1500	2.5	1.5	4	1300	63	65	70.8
Fire Load	25	1750	2.5	1.5	4	1300	73	75	79.2
Fire Load	25	2000	2.5	1.5	4	1300	82	83	87.5

Variation :	Floor Area m^2	Fire Load MJ / m^2	Room Height m	Opening Height m	Opening Width m	Thermal Properties	Finite Element (Minutes)	Spread sheet (minutes)	Franssen's Results (minutes)
Room Hr	25	750	2.4	1.5	4	1300	35	36	41.3
Room Hr	25	750	2.5	1.5	4	1300	34.5	35.5	41
Room Hr	25	750	3	1.5	4	1300	33.5	35	40.9

Variation :	Floor Area m^2	Fire Load MJ / m^2	Room Height m	Opening Height m	Opening Width m	Thermal Properties	Finite Element (Minutes)	Spread sheet (minutes)	Franssen's Results (minutes)
Room Hr	25	750	3.5	1.5	4	1300	33	35	40.9
Room Hr	25	750	4	1.5	4	1300	32	34.5	37.6
Room Hr	25	750	4.5	1.5	4	1300	31.5	34.5	36.8
Room Hr	25	750	5	1.5	4	1300	31.5	35	36.8

Variation :	Floor Area m^2	Fire Load MJ / m^2	Room Height m	Opening Height m	Opening Width m	Thermal Properties	Finite Element (Minutes)	Spread sheet (minutes)	Franssen's Results (minutes)
Vent. Hv	25	750	2.5	0.2	4	1300	26	30	40.1
Vent. Hv	25	750	2.5	0.5	4	1300	52	60	61
Vent. Hv	25	750	2.5	1	4	1300	43.5	49	49.1
Vent. Hv	25	750	2.5	1.5	4	1300	34.5	35.5	41
Vent. Hv	25	750	2.5	2	4	1300	28.5	27.5	36.8
Vent. Hv	25	750	2.5	2.5	4	1300	25.5	24	32.7

Variation :	Floor Area m^2	Fire Load MJ / m^2	Room Height m	Opening Height m	Opening Width m	Thermal Properties	Finite Element (Minutes)	Spread sheet (minutes)	Franssen's Results (minutes)
Vent. W	25	750	2.5	1.5	0.5	1300	48	55	61.4
Vent. W	25	750	2.5	1.5	1	1300	51.7	60.7	59.3
Vent. W	25	750	2.5	1.5	2	1300	44.5	51	53.2
Vent. W	25	750	2.5	1.5	3	1300	39	42	45
Vent. W	25	750	2.5	1.5	4	1300	34.5	35.5	41
Vent. W	25	750	2.5	1.5	5	1300	31.5	31	32.7

Variation :	Floor Area m^2	Fire Load MJ / m^2	Room Height m	Opening Height m	Opening Width m	Thermal Properties	Finite Element (Minutes)	Spread sheet (minutes)	Franssen's Results (minutes)
$(k \rho C)^{0.5}$	25	750	2.5	1.5	4	500	46.5	41	57.3
$(k \rho C)^{0.5}$	25	750	2.5	1.5	4	1000	38.5	38.5	47
$(k \rho C)^{0.5}$	25	750	2.5	1.5	4	1300	34.5	35.5	41
$(k \rho C)^{0.5}$	25	750	2.5	1.5	4	1600	32.5	34.5	40.9
$(k \rho C)^{0.5}$	25	750	2.5	1.5	4	2000	31.5	35	36.8